THE ASTROPHYSICAL JOURNAL SUPPLEMENT SERIES, 98:69–101, 1995 May


# EVOLUTIONARY POPULATION SYNTHESIS IN STELLAR SYSTEMS. II. EARLY-TYPE GALAXIES

ALBERTO BUZZONI[1]
Osservatorio Astronomico di Brera; and Instituto Nacional de Astrofísica, Optica y Electrónica, Mexico
*Received 1993 August 18; accepted 1994 August 17*

## ABSTRACT

In this work we present an articulated analysis addressing the general problem of the present evolutionary status of early-type galaxies (ETGs). This relies on the original approach to stellar evolutionary population synthesis developed in Buzzoni (1989).

Optical and infrared synthetic colors and spectral indices are analyzed in some detail exploring their selective sensitivity to the distinctive parameters of the stellar populations. We demonstrate that, among broadband colors, $B - V$ is the best tracer of age while $V - K$ is the most effective tracer of metallicity. Also the infrared indices of the CO and $H_2O$ features are implemented supplying a grid of 78 theoretical models for simple stellar populations (SSPs). It is shown that they have a direct impact both on the study of the stellar mass loss modulating post–main-sequence evolution and internal reddening, as well as on the determination of the initial mass function (IMF) and the $M/L$ ratio of galaxy stellar populations through the study of the dwarf star contribution.

The relevant case of the template galaxy M32 is discussed in detail, dealing with the well-known "age-metallicity dilemma" for a confident discrimination of the combined effects on the galaxy spectral energy distribution. ETGs are found to be fully consistent with old (15 Gyr) stellar populations, confirming that metallicity is the main parameter governing the observed color distribution. The typical value of [Fe/H] is about or slightly higher than the solar value ([Fe/H] = $+0.10 \pm 0.35$).

Cluster ellipticals are found to be coeval within a ±20% uncertainty, while a larger spread in age is found for field ETGs with a mean age of 11.5 Gyr. About three-fourths of the ETG population in the field should be older than 10 Gyr, and only 2% younger than 5 Gyr.

Stellar populations in ETGs seem consistent with a Salpeter or with a slightly flatter IMF ($s \leq 2.35$) with a spread in the power-law index $\Delta s \leq \pm 1$. Dwarf-dominated populations are definitely ruled out, at least in the core of the galaxies.

The case of composite stellar populations to fit real galaxies is accounted for, deriving a contribution from the metal-poor stellar component to the galactic spectral energy distribution of typically 5%.

Luminosity evolution of ETGs follows a power law such as $\partial M_v / \partial \ln t = 1.30 - 0.27\ (s - 1)$ which exactly matches Tinsley & Gunn's (1976) former results. Evolutionary $(e + k)$-corrections are given in the Johnson $B$, $V$, and $K$ bands and in the Gunn $g$, $r$, and $i$ system, allowing us to track the expected apparent evolution in magnitude and color for six different cosmological models.

*Subject headings:* galaxies: evolution — galaxies: photometry — galaxies: stellar content

## 1. INTRODUCTION

A better understanding of the overall properties of stellar populations in early-type galaxies (ETGs; meaning essentially bulge-dominated systems like elliptical galaxies and S0) is of paramount importance when attempting to embody in a global interpretative framework the genesis of galaxies and the subsequent evolution leading to the different morphological types. There are reasons to believe that evolution may have proceeded in ETGs in a more simplified way, for instance, with respect to spiral galaxies.

A common scenario that results from the standard dynamical models is that ETGs might likely have formed under dissipative gravitational collapse from primeval low-momentum gas clouds (e.g., Arimoto & Yoshii 1987). Early evolution should, therefore, have been accomplished over a short free-fall time such as $\dot{R} \sim GM_{\rm TOT}/R^2$.

This implies $t_{\rm ff} \sim 1.5 (R_{100}^{3/2}/M_{11}^{1/2})$ Gyr—expressing the typical dimension of the cloud, $R_{100}$, in units of 100 kpc and the total mass, $M_{11}$, in units of $10^{11} M_\odot$.

Most of the gas should have been converted into stars during the first gigayear, and the early generations of massive stars dying as type II SNs supplied a formidable amount of energy, able to strip the residual gas, inhibiting or strongly reducing any subsequent star formation (this is the so-called galactic-wind phase; see Arimoto 1988; Matteucci & Brocato 1990; Ferrini & Poggianti 1993).

A balance is achieved between the SN disruptive action (modulated by the star formation rate [SFR] and by the initial mass function [IMF] of the stellar population) and the gravitational potential of the parent galaxy (that derives from its total mass). The more massive the galaxy, the larger its binding energy per unit mass ($\Omega_G \propto M_{\rm TOT}^{0.45}$ ergs g$^{-1}$; Saito 1979) and the more easily the SN wind will be neutralized, avoiding the galaxy's losing a larger fraction of its residual gas. As a consequence, we should expect star formation to proceed further in this case, allowing SN-enriched matter to be locked into new

[1] Postal address: Osservatorio Astronomico di Brera, Via Bianchi, 46, 22055 Merate (Como), Italy.

more metal-rich stars. Only low-mass systems (namely, the dwarf spheroidals and, to some extent, the globular clusters) would not escape a more dramatic gas stripping due to a slower collapse, and star formation in these systems would be abruptly interrupted in the early stages leaving only metal-poor stellar populations.

A major point of this unified scenario is that a sort of continuity can be envisaged between ETGs, dwarf ellipticals, and globular clusters, indeed a result extensively supported by the observational evidence (Frogel, Persson, & Cohen 1980; Burstein et al. 1984; Buzzoni, Gariboldi, & Mantegazza 1992). One important conclusion of the standard theory on dynamical collapse is that the present age of stellar populations in ETGs should be comparable with the Hubble time. We should conclude therefore that ETGs basically consist of old coeval stellar populations displaying a spread in metallicity among and within the single galaxies induced by differentiated histories of SN metal enrichment (Frogel et al. 1978).

On the other hand, an alternative outlook to the problem stems from the recent results of theoretical *N*-body simulations. The main issue in this regard is that bulge-dominated systems might naturally derive from interaction processes like merging or cannibalism involving disk galaxies (Barnes 1989; Governato, Bhatia, & Chincarini 1991). If this is the case, and the majority of ETGs are really generated by this kind of mechanism, then one should expect that a large spread in the intrinsic properties of the galaxies would exist. In particular, the basic hypothesis of coevality could no longer be valid, as ETGs could form at different epochs, assembling more heterogeneous stellar populations.

These arguments indirectly came to support similar conclusions suggested by a certain class of models for population synthesis (O'Connell 1980; Pickles 1985). In particular, discussing the case of M32, O'Connell (1980) concluded that "major star formation in M32 continued until only $\sim$5 Gyr ago, or 10 Gyr after the formation of the oldest globular clusters in our Galaxy" fueling, therefore, a not yet fully settled controversy about the determination of the absolute age of the ETGs (cf., e.g., Gunn, Stryker, & Tinsley 1981 and Renzini 1986 for an opposing point of view).

In this work we try a more articulated analysis, addressing the general problem of the evolutionary status of ETGs at the present time. This will be accomplished by building on the original approach to stellar evolutionary population synthesis (EPS) developed in Buzzoni (1989, hereafter Paper I). As we discussed there, EPS can provide a powerful tool to probe the distinctive properties of real stellar populations, once secured on solid interpretative bases, paying attention to a complete and self-consistent description of the astrophysical constraints.

Synthetic colors or spectral indices behave like selective tools, able to explore in a quite specific way the different features marking a stellar population. It is from such a combined framework that we hope to retrieve the right piece of information.

This important aspect will be the starting point in the present analysis and will be reviewed in some detail in § 2. A discussion on broad- and narrowband indices in § 3 will include the synthesis of IR indices like the CO and $H_2O$ features.

In § 4 we assess more extensively the problem of dating ETGs through a critical comparison of some of the current models for population synthesis. The problem of a fair estimate of the age of ETGs is intimately related to the problem of the age of the template M32, and to that of the reliable discrimination between age and metallicity effects on the spectral energy distribution of the galaxies.

Section 5 is devoted to a study of the IMF in the stellar populations of ETGs. This deals directly with the estimate of the total mass of the galaxies, and with their $M/L$ ratio.

The case of internal reddening in ETGs will be addressed in § 6, considering the ISM enrichment via the stellar wind. Only to a first-order approximation can ETGs really be described by simple stellar populations (SSPs), as defined in Paper I. Indeed, the case of composite stellar populations must be taken into account in § 7 in order to give a quantitative hint of the expected differences once a more complex and realistic scenario is considered.

Finally, as a direct result of our analysis of the present status of ETGs, back-in-time evolution will be explored in § 8 in order to study what primeval galaxies would look like.

## 2. RATING TOOLS FOR EPS

The basic aim of EPS models when matching the integrated colors or spectral energy distribution (SED) of a stellar aggregate is to single out the contribution from homogeneous groups of stars within the whole population. Obviously, this is not a straightforward task, especially for external galaxies where we cannot recognize stars individually.

From a formal point of view, "resolving" a stellar population would mean restoring the density distribution of its stars in a *C-M* diagram. However, starting from the integrated SED of a galaxy alone, many different solutions can be envisaged in principle, as one could imagine populating the *C-M* plane in a virtually infinite number of combinations all giving the same integrated spectrum. This is a well-recognized feature in automatic computational algorithms (the classic ones are those for linear programming; Faber 1972; O'Connell 1976), and one needs then to complement the analysis by supplying more astrophysical constraints in order to restrict the field of solutions to plausible cases only.

A merit of EPS is that a constraint is naturally given by the adopted grid of theoretical isochrones describing the expected evolution of an SSP at different ages. In particular, evolutionary lifetimes will directly provide a link with the expected number distribution of the stars along the different branches in a *C-M* diagram, as widely discussed in Paper I.

However, two questions remain open in this case. First, different isochrones can in principle give similar integrated SEDs. Second, it is clear that, in any case, the reliability of our solution is strictly related to the reliability of the theoretical framework adopted, as incomplete isochrones would produce biased results.

While at this stage of the application one can only rely on optimizing the latter point a priori by means of a wise choice of the theoretical set of isochrones; on the other hand, an effort can be made to refine the match between models and observations via broadband colors and spectral indices. It is worth briefly discussing, therefore, which link we expect between (spectro)photometric indices and intrinsic properties of SSPs,

and how effectively one can rely on achieving a univocal fitting model.

### 2.1. *Broadband Colors*

The obvious advantage of using broadband photometry with respect to spectrophotometry is that a huge amount of data can be collected in a shorter time and for fainter galaxies. Moreover, performing multicolor photometry is more or less like performing (very) low-resolution spectroscopy, still preserving the overall shape of the continuum emission of the SED.

In an SSP every star emits at every wavelength, but the weight of the different homogeneous groups (binned in temperature or luminosity) is different with varying $\lambda$. The relative contribution to the total luminosity is therefore a combination of three parameters: (1) the relative number size of a group of stars with respect to the total population, (2) their typical absolute luminosity, and (3) their typical temperature, modulating the absolute luminosity at the different wavelengths.

An instructive example of how the different quantities work is given in Figure 1, referring to the models of Paper I. Here we give the relative partition of the contribution to the total luminosity in bolometric and in the Johnson $B$ and $K$ bands for a 15 Gyr SSP with solar metallicity and canonical Salpeter IMF (in addition, a red–horizontal-branch [R-HB] morphology is assumed, and a mass-loss rate coefficient $\eta = 0.3$; cf. Paper I, Table 5K).

Two groups of stars dominate for opposite reasons in bolometric, that is, the upper main-sequence (MS) stars about the turnoff (TO) point (due to their huge number; cf. point 1 above) and the red stars (both dwarfs and giants; cf. point 2) cooler than 4000 K. The two groups split once considering the partition of the total luminosity at the different wavelengths. In the $B$ band, most of the light (about two-thirds) comes from the upper MS and the subgiant branch (SGB). In particular, the TO bin alone counts for over one-third of the total, making clear why integrated colors like $U - B$ or $B - V$ are such effective estimators of the TO color in SSPs (cf. Fig. 2).

The partition in the $K$ band in Figure 1 is almost complementary to $B$, and now over two-thirds of the IR light is supplied by cool stars in the red and asymptotic giant branches (RGB and AGB, respectively) and by the red dwarfs in the lower MS. The different trends appear even more clearly in Figure 3 when considering stellar gravity instead of tempera-

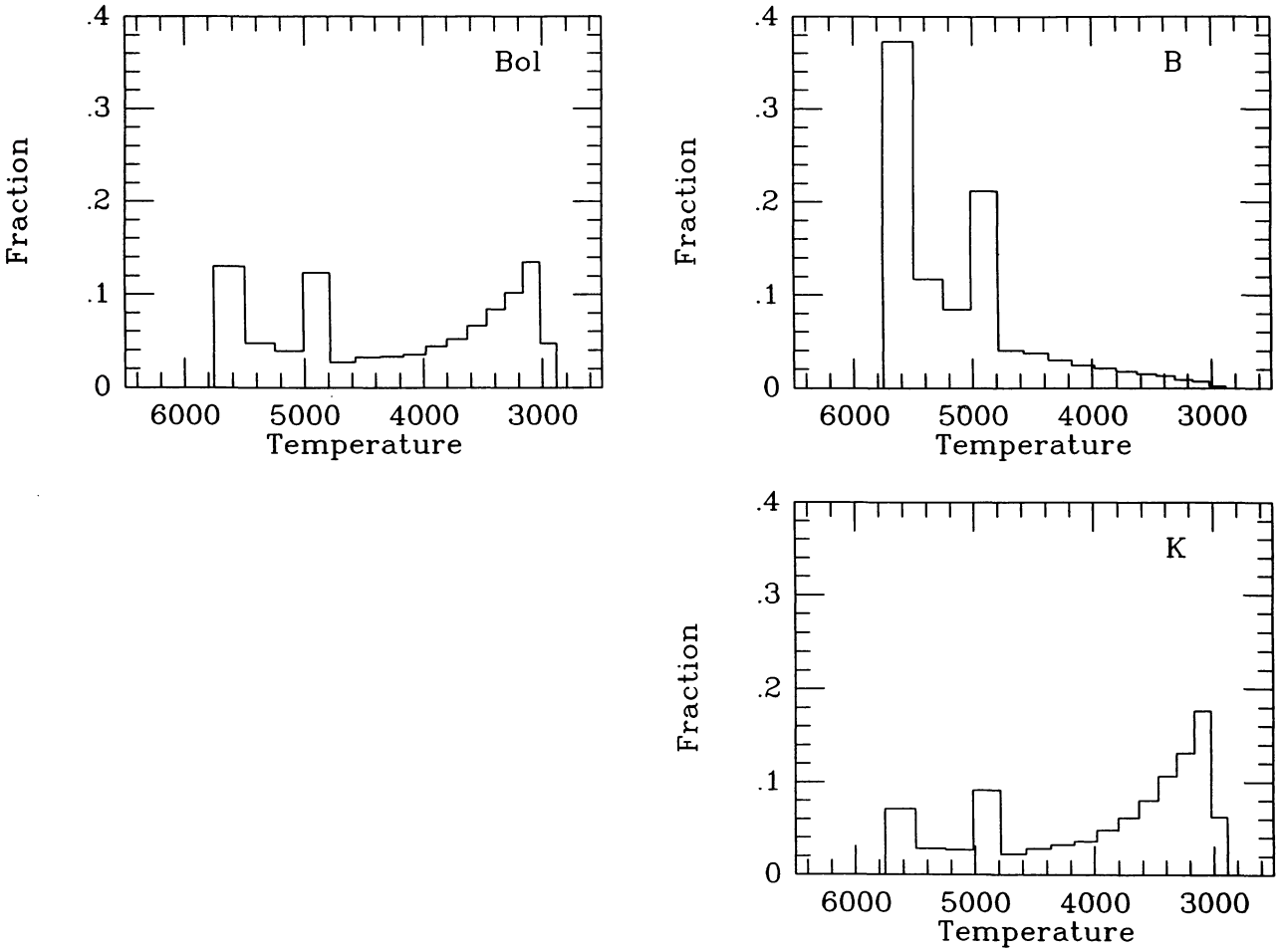


FIG. 1.—Percentage contribution to bolometric, $B$, and $K$ light vs. temperature from stars in a 15 Gyr SSP with [Fe/H] = 0 and Salpeter IMF. An R-HB morphology is assumed (it is the clump of stars about 5200 K). Bins are for equal steps $\Delta \log T = 0.02$.

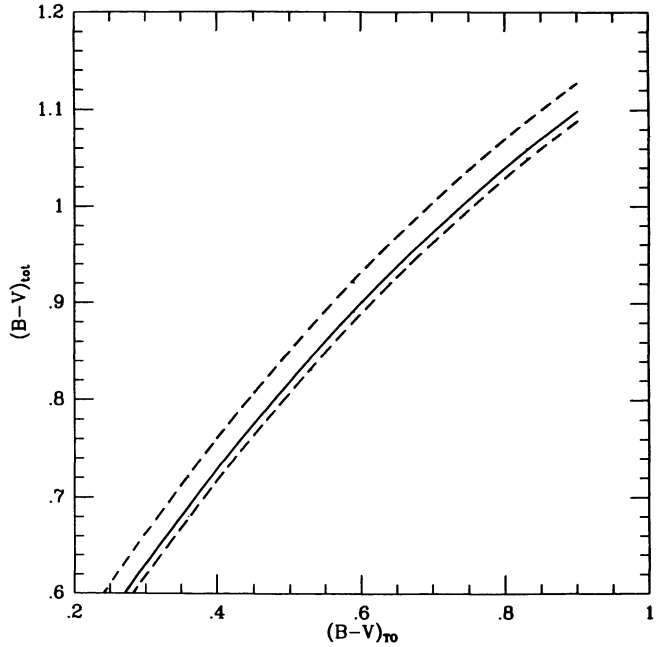


FIG. 2.—Relationship between integrated $B - V$ of an SSP and $B - V$ of its TO point. Solid line is for a Salpeter IMF ($s = 2.35$), while dashed lines are for dwarf-dominated SSPs ($s = 3.35$; *upper line*) and giant-dominated SSPs ($s = 1.35$; *lower line*).

ture as the leading parameter in the histograms (the advantage of using log $g$ is that it runs more or less monotonically along the isochrone, decreasing from dwarfs to giants).

It is interesting to compare these results following the same SSP back to an age of 5 Gyr (cf. Fig. 4). No drastic changes seem to occur, with only the MS and AGB groups slightly broadening in the $B$ and $K$ histograms, respectively (the former because the MS is now a bit more extended to higher temperature, the latter due to a full development of the AGB to brighter luminosity).

Taking as reference the 15 Gyr SSP model, we computed the luminosity-weighted mean gravity and temperature along different isochrones and for different photometric bands in order to summarize the intervening changes made by changing age from 15 to 5 Gyr, and by changing metallicity from solar ([Fe/H] = 0) to supersolar ([Fe/H] = +0.22). The results are reported in Figure 5.

A change in age from 15 to 5 Gyr mainly reflects on the isochrone by increasing the $B$ mean temperature (thanks to a bluer TO) and decreasing the $K$ mean gravity (due to a more extended AGB). The converse happens by increasing metallicity from solar to supersolar. We now find that effective stellar contributors to the $B$ band have on average higher gravity (increasing by 15% in our example), while mean temperature decreases by 1%. On the other hand, in the IR, $K$ light is supplied by slightly cooler stars (3% cooler in average) with no relevant changes in the mean gravity. Therefore, in attempting to discriminate between age and metallicity effects in a comparative study of SEDs of different SSPs, one should conclude that age acts by decreasing $\langle \log T \rangle_B$ and increasing $\langle \log g \rangle_K$, while metal enhancement acts by increasing $\langle \log g \rangle_B$ and decreasing $\langle \log T \rangle_K$.

The sensitivity of broadband colors to age or metallicity variations can be tested by fitting the grid of models of Paper I and computing the partial derivatives with respect to $t$ and $Z$. Restricting to the range of parameters more suitable for galaxies (i.e., $t = 5 \rightarrow 15$ Gyr and $Z = \frac{2}{3} \rightarrow \frac{3}{2} Z_\odot$), the results are summarized in Table 1 and Figure 6. It appears that $V - K$ is the color maximizing the dependence on [Fe/H], while $B - V$ is the most suitable to track absolute age.

A word of caution is necessary when considering the UV colors from the models of Paper I. A well-recognized feature of the Kurucz (1979) model atmospheres is that blanketing effects could have been systematically underestimated, especially at low temperatures. This resulted in a flux excess shortward of 4000 Å, inducing bluer colors. In Paper I we discussed this question in some detail, showing that the effect should have been implicitly recovered in the code, at least in stars warmer than 6000 K (i.e., earlier than spectral type G0 or with $B - V \leq 0.6$). The reason is that the model of Vega adopted for the $U$ calibration suffered from the same effect, thus compensating for the UV excess.

However, some complications can arise when considering cooler stars beyond the range of the Kurucz models, for which we had to extrapolate the Bell & Gustaffson (1978) atmospheres shortward of 3000 Å (see Paper I for details of the adopted procedure). Figure 7 quantifies the effect in the ($U - V$, $B - V$)-plane, comparing the star colors from Paper I with the standard relation of Johnson (1966) for solar dwarfs. An increasing UV excess affecting the $U$ magnitude starts appearing about spectral type G5 V, growing to later types up to $\Delta U \sim 0.3$ mag for M0 stars.

Of course, the consequences for the integrated SEDs of the models are much reduced, given that cool stars usually contribute a small fraction (~20% or less) of the integrated light at 3000 Å. Quite notably, this would only negligibly affect the partial derivatives in Table 1 because the UV contribution from cool stars does not vary so much when the distinctive parameters of the SSPs are varied, at least for solar or subsolar metallicity, and moreover we verified that, apart from the zero point, model atmospheres still correctly tracked a differential change in metallicity in a ($U - B$, $B - V$)-diagram (see Golay 1974).

Direct tests on standard stars (Malagnini et al. 1992) seem to demonstrate that problems with the proper handling of the line blanketing also remain unsolved in Kurucz's (1992) new generation of model atmospheres, which now appear to overestimate the effect. Instead of attempting any correction accounting for these new model atmospheres, we devised a more straightforward and immediate procedure to correct the $U - V$ colors of Paper I by slightly dimming the $U$ magnitudes of stars along the isochrones by an additional term $\Delta U$, such as $\Delta U = 0.5[(B - V)_{\rm star} - 0.6]$ (if $(B - V)_{\rm star} \geq 0.6$) and $\Delta U = 0$ (otherwise), in order to match the Johnson (1966) locus in Figure 7. By running a selected grid of models we then derived in graphic form the correction to be added to integrated old colors to account properly for stellar blanketing. The residuals (in the sense $\Delta(U - V) = (U - V)_{\rm new} - (U - V)_{\rm Paper\ I}$) are plotted in Figure 8. Henceforth, it is in-

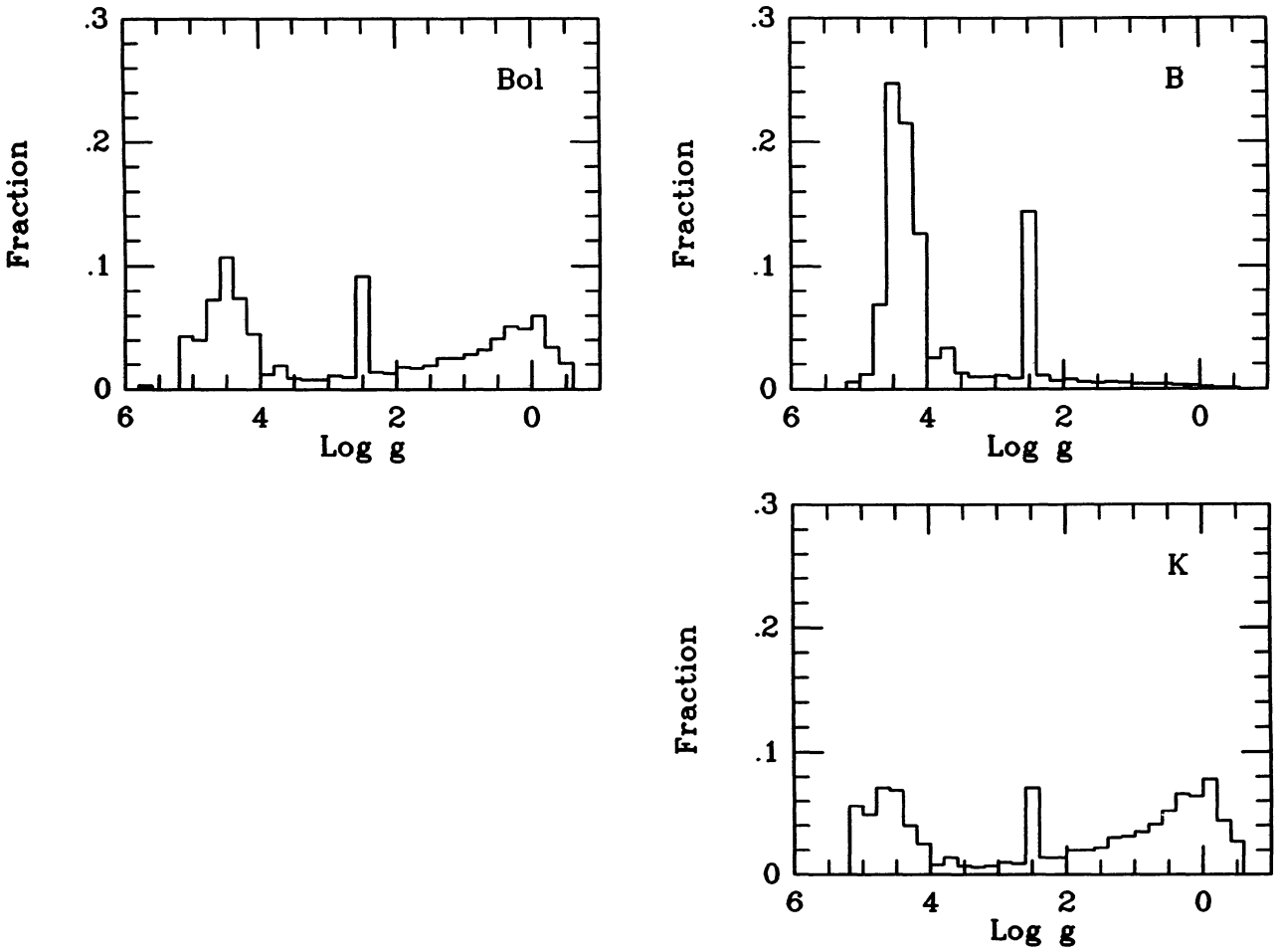


FIG. 3.—Percentage contribution to bolometric, $B$, and $K$ light vs. gravity for stars in a 15 Gyr SSP with [Fe/H] = 0 and Salpeter IMF. An R-HB is assumed (the clump of stars about $\log g = 2.5$). Bins are for equal steps $\Delta \log g = 0.2$.

tended that all colors in the models involving $U$ magnitudes are given in the new corrected form.

### 2.2. *Spectral Indices*

Narrowband indices can be easily derived for single stars and galaxies from middispersion spectroscopy. A pioneering study in this sense involving spectral features in the visual range was first undertaken by Spinrad & Taylor (1969, 1971), and systemized by Faber (1973), Burstein et al. (1984), and Faber et al. (1985). In addition to the work of previous authors, a large set of observations has been collected for stars of different spectral types by Worthey (1992), Gorgas et al. (1993), Buzzoni et al. (1992), and Buzzoni, Mantegazza, & Gariboldi (1994) allowing us to derive the composite relationship of the indices with respect to the stellar leading parameters. The definition of these empirical fitting functions has been an important step in coping with population synthesis and deriving the integrated values expected for SSPs.

Observations of narrowband indices in ETGs have been supplied by Davies et al. (1987), Gorgas, Efstathiou, & Aragon Salamanca (1990), and Worthey, Faber, & Gonzalez (1992), with special care to the H$\beta$ and the $Mg_2$ indices that are among the most prominent features in the spectra of ETGs. An extension of the database to globular clusters in the Galaxy and in M31 has been carried out by Burstein et al. (1984) and Brodie & Huchra (1990). A synthesis of the 4000 Å break in stellar populations of giant ellipticals has been attempted by Hamilton (1985) exploring the cosmological implications of the problem.

In the UV, an extensive study of the spectral features of stars and a consequent application to modeling ETGs has been carried out by Rose (1984, 1985a, b, c), Rose & Tripicco (1984), Boulade, Rose, & Vigroux (1988), and Tripicco & Bell (1990), while on the opposite range in wavelength, the two most outstanding indices of CO and $H_2O$ in the IR about 2 $\mu$m have been calibrated on stars by Baldwin, Frogel, & Persson (1973b) and supplied for a number of ETGs by Frogel et al. (1975, 1980) and Aaronson, Frogel, & Persson (1978).

There is no doubt that by means of the narrowband indices one can perform the most in-depth "endoscopy" in an unresolved stellar population, thanks to a selective dependence of the spectral features on specific ranges in stellar temperature, gravity, and metallicity. Therefore, through an appropriate

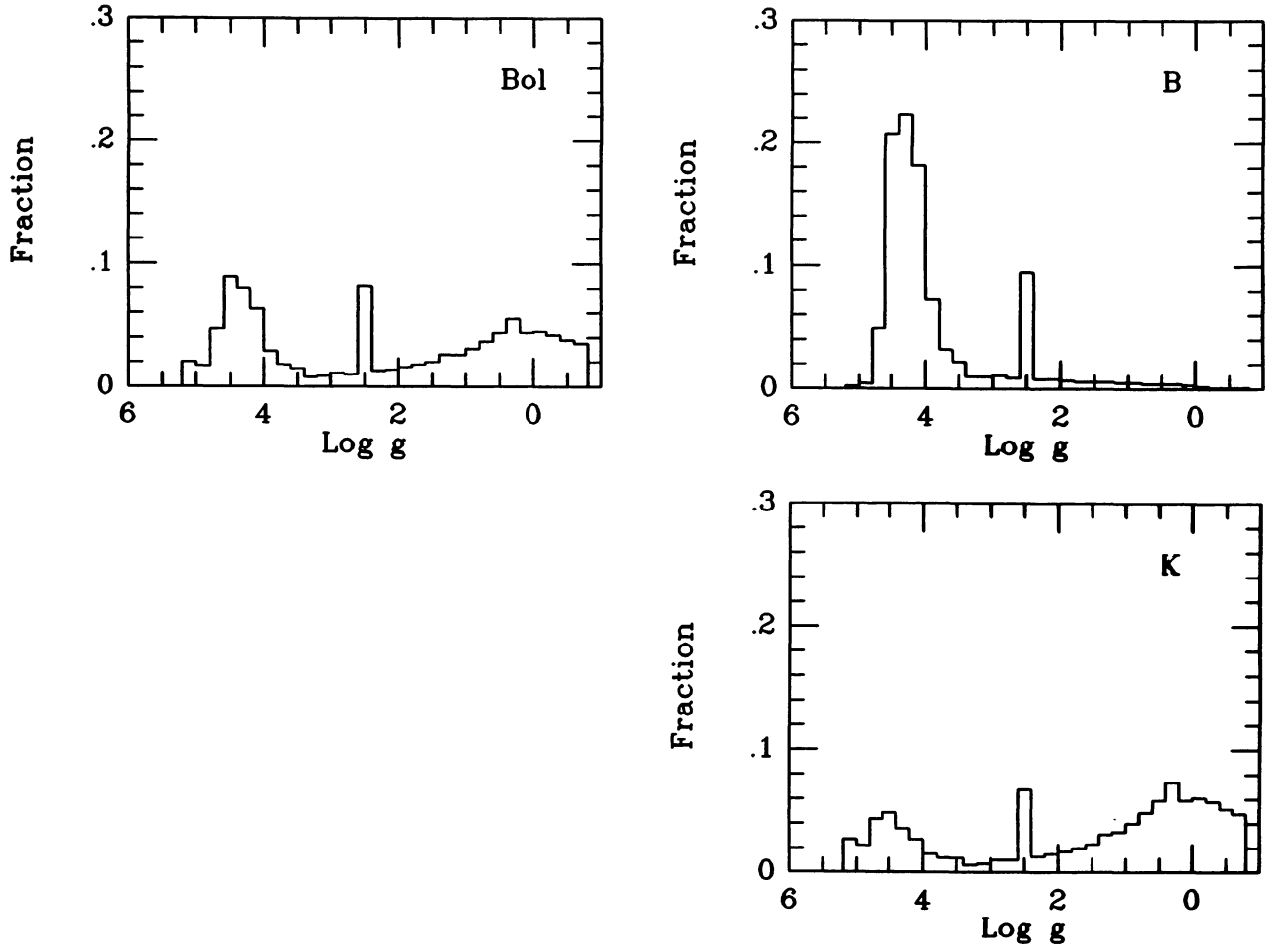


FIG. 4.—Same as Fig. 3, but for a 5 Gyr SSP

match with synthesis models we can single out different parts of the *C-M* diagram of stellar populations, investigating in fine detail the distribution of stars in temperature and luminosity.

This approach has been systematically carried on by Buzzoni et al. (1992, 1994) by supplying synthetic indices like $Mg_2$, H$\beta$, Fe52, and Fe53 for a wide grid of SSP models. In this regard, it is worth recalling here, in Figure 9, some of those results showing the way the H$\beta$ and Fe52 indices are contributed by the different evolutionary branches in a *C-M* diagram of an SSP. In addition, we computed also the expected distribution for $Mg_2$, referring to Buzzoni et al. (1992), and for the CO and $H_2O$ indices as well, which we will discuss in more detail in the next section.

By comparing the different histograms for the same SSP, one can very neatly realize how effectively a combined analysis of the indices allows us to restore the different features in the *C-M* diagram. According to the discussion in Buzzoni et al. (1992, 1994) we find that H$\beta$ is mainly sensitive to TO stars, while the base of the RGB mainly contributes to the Fe52 and Fe53 features. The $Mg_2$ index carries information mainly on the upper part of the RGB and AGB, while CO and $H_2O$ indices are useful indicators for the AGB extension and for the fraction of red dwarfs in the lower MS, as we will see in more detail in the next section. In Figure 10 we summarized these concepts giving a more immediate sketch of the different behavior of the relevant indices in an SSP.

## 3. IR SYNTHESIS FOR ETGs

In addition to the discussion in the previous section about the synthesis of indices in the visual range, it is worth expanding our analysis to also include IR synthesis for a direct application to ETGs.

In this regard, the two indices of CO and $H_2O$ are potentially ideal tools to explore the evolutionary status of the cooler stellar component in ETGs below 4000 K. According to Frogel et al. (1978), it is evident from the relevant panels in Figure 9 that CO and $H_2O$ work in opposite and complementary ways, tracking the intrinsic properties of an SSP. While CO almost exclusively tracks low-gravity stars along the red giant branches, $H_2O$ displays a bimodal dependence, collecting especially the contribution from the high-gravity red dwarfs in the lower MS.

The reasons for their different behavior reside in the physical conditions of the cool stars contributing the features. An illuminating discussion of the mechanisms modulating the CO

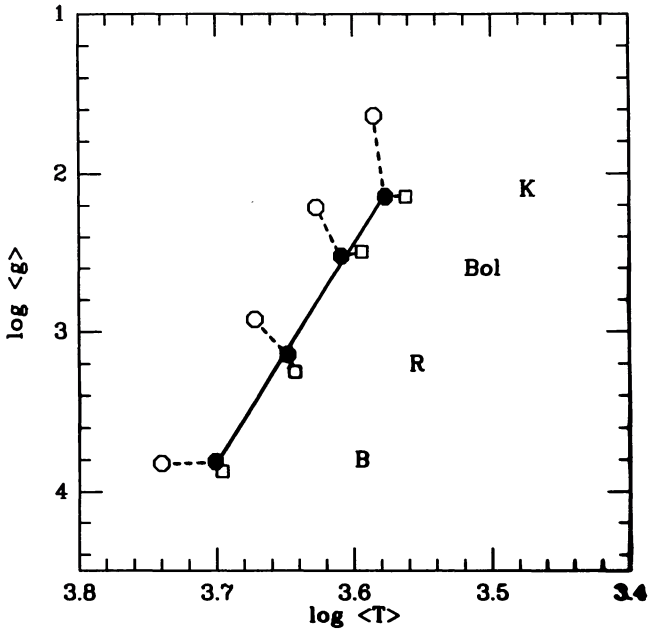


FIG. 5.—Mean light-weighted log $T$ and log $g$ in different photometric bands for a 15 Gyr SSP of solar metallicity and Salpeter IMF (*filled dots*). The variation resulting from a selective change in age from 15 Gyr to 5 Gyr (*open dots*) and in metallicity from [Fe/H] = 0 to +0.22 (*open squares*) is displayed. Note the opposite trend in the changes of $\langle \log g \rangle$ and $\langle \log T \rangle$. A younger age causes $\langle \log g \rangle$ in the IR to decrease (due to larger radii for giant stars) and $\langle \log T \rangle$ in the blue to increase (due to a bluer TO), while a more metal-rich stellar population causes $\langle \log g \rangle$ in the blue to increase (due to slightly more massive TO stars for a fixed age) and $\langle \log T \rangle$ in the IR to decrease (due to a redder RGB + AGB).

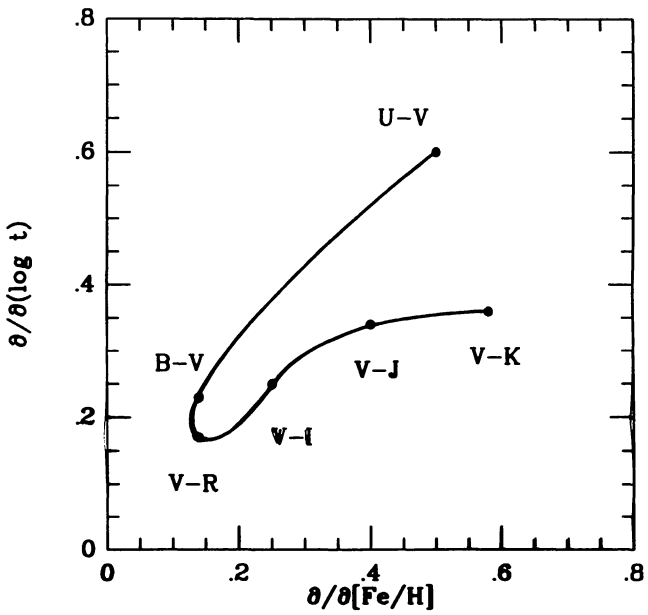


FIG. 6.—SSP color sensitivity to a change in age or metallicity. Plotted are the partial derivatives listed in Table 1. Colors such as $U-V$ and $V-K$ have larger dependence on $t$ or [Fe/H]. However, $B-V$ is more suitable for tracing age due to its weaker dependence on metallicity, while $V-K$ would better respond to [Fe/H] (minimizing age dependence).

feature in the atmospheres of G and K stars has been provided by Bell & Tripicco (1991) and could also help in understanding $H_2O$. Basically, the relative strength of a molecular band in a stellar atmosphere depends on a balance between line and continuum absorption coefficients. For the case of CO, Bell & Tripicco (1991) conclude that the inverse dependence on the stellar gravity (with the feature reinforced in the spectra of giants) mainly derives from the fact that giants are more transparent than dwarfs in the continuum at 2.2 $\mu$m, as free-free absorption from $H^-$ is decreased by lower electron pressure.

The same conditions hold for $H_2O$, but now the feature strength directly depends on the $H_2$ molecular abundance, which is favored by the lower energetics induced in high electron pressure (i.e., high stellar gravity) regimes. As a consequence, in this case the mechanisms contributing to the continuum and line opacity are in synergy, and thus the $H_2O$ band is expected to be reinforced in the spectra of the dwarf stars.

TABLE 1

COLOR SENSITIVITY TO METALLICITY AND AGE

| | ∂/∂[Fe/H] | ∂/∂(log $t$) |
|---|---|---|
| $U-V$ ..... | 0.5 | 0.6 |
| $B-V$ ..... | 0.14 | 0.23 |
| $V-R$ ..... | 0.14 | 0.17 |
| $V-I$ ..... | 0.25 | 0.25 |
| $V-J$ ..... | 0.40 | 0.34 |
| $V-K$ ..... | 0.58 | 0.36 |

A wide set of theoretical model atmospheres allowing us to explore the dependence of the CO index on the leading parameters of stars has been computed by Bell & Briley (1991). The comparison with the observational database for Population I stars performed by Baldwin et al. (1973b) and Cohen, Frogel, & Persson (1978) resulted in a pretty good agreement once little adjustments in the zero point of the theoretical calibration were introduced. In particular, Bell & Briley's models are successful in reproducing the observed slope of the index versus temperature (or $V-K$), accounting in great detail for C depletion channels in giants and for the other intervening effects in the stellar structure.

One main point in their discussion, however, is that, contrary to what was assumed by Baldwin et al. (1973a) and Frogel et al. (1978), the CO index is not free from a direct dependence on metallicity through C and O abundance. A similar conclusion should hold also for $H_2O$ (but no precise calculations are available to date), although in this case one might expect a much weaker trend with metallicity because of the less critical constraint posed by the abundance of atomic oxygen alone.

Although this might apparently weaken the effectiveness of these IR indices for population synthesis purposes, nevertheless they can still play an important role once the direct dependence on [Fe/H] can be confidently accounted for by theory and be included in the empirical fitting functions describing the trends versus stellar temperature and gravity.

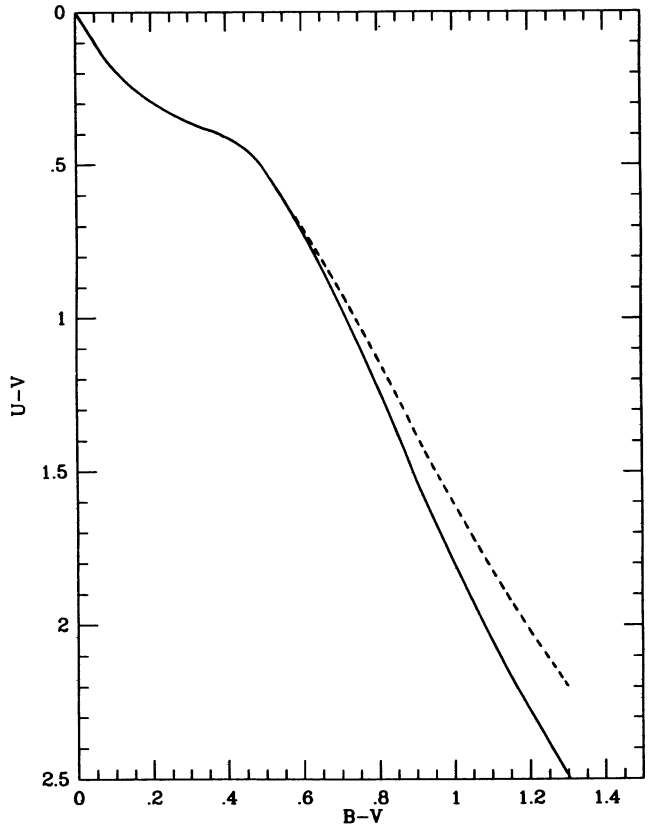


FIG. 7.—Comparison between the Johnson (1966) locus for dwarf stars (*solid line*) and that adopted in Paper I (*dashed line*). The difference at redder colors entirely derives from a partial lack of blanketing in the models of Paper I, causing a $U$ excess.

The CO and $H_2O$ indices have been implemented in the synthesis code of Paper I in a way similar to that performed in Buzzoni et al. (1992, 1994) for $Mg_2$ and $H\beta$. An empirical calibration of CO versus $V-K$ from the stellar database of Cohen et al. (1978) has been provided by Frogel et al. (1978, Table 12), while a calibration for $H_2O$ has been proposed by Aaronson et al. (1978, Table 2). Both can be transformed homogeneously by means of the Johnson (1966) temperature scale for giants and dwarfs.

The results, suitable for Population I stars with bona fide solar metallicity, are summarized in the two panels of Figure 11. One can clearly appreciate the different trends in the indices with an inverse dependence on the luminosity class. As discussed by Aaronson et al. (1978), a larger uncertainty affects the behavior of Mira and carbon stars cooler than ~2800 K. While Mira variables seem to greatly enhance both the CO and $H_2O$ indices, though with a large spread (see Aaronson et al. 1978, Table 1), quite curiously carbon stars display a much weaker CO index in spite of a strong absorption feature. This is due to exceedingly red continua that cause the measured indices to indicate the opposite (Aaronson et al. 1978). In order to also give a reference value for these extremely cool stars, we adopted in our synthesis CO = 0.40 and $H_2O$ = 0.45 for giants below 2800 K.

Metallicity effects have been accounted for by using the partial derivatives from the models of Bell & Briley (1991). Restricting to the case of intermediate and metal-rich populations ([Fe/H] > −1.5), from their data we derive these relations of transformation for stars, giving the new indices pertinent to a different [Fe/H] starting from the corresponding values for [Fe/H] = 0:

$$\mathrm{CO} = \mathrm{CO}_\odot + 0.06[\mathrm{Fe/H}] \quad (\text{if } \mathrm{CO}_\odot \geq 0.10), \qquad (1)$$

$$\mathrm{CO} = \mathrm{CO}_\odot + 0.06\mathrm{CO}_\odot[\mathrm{Fe/H}] \quad (\text{if } \mathrm{CO}_\odot < 0.10). \qquad (2)$$

Unfortunately, no quantitative corrections can be made for $H_2O$ accounting for nonsolar $Z$, but as we pointed out above these might be negligible, and in any case our conclusions would not be strongly affected in the relevant range of metallicity for ETGs.

We explored synthetic CO and $H_2O$ in a grid of 78 models for SSPs spanning a range for $Z$ between 0.0001 and 0.03. As in Paper I, age runs from 4 to 18 Gyr, while two supplementary IMFs have been accounted for in addition to the Salpeter case ($s$ = 2.35), testing giant- and dwarf-dominated SSPs (with $s$ = 1.35 and 3.35, respectively). Mass loss via stellar wind has been introduced via the coefficient $\eta$ in the Reimers (1975) notation (cf. Paper I for details). Concerning the horizontal-branch (HB) morphology, there is no dependence of the indices on it, and we consider here only the case of a red clump (R-HB morphology in the notation of Paper I). The results are summarized in the series of Tables 2, 3, and 4.

## 4. WHICH AGE FOR ETGs?

By combining the present results on IR synthesis with those obtained in Paper I and in Buzzoni et al. (1992, 1994), we are now in a position to perform a full analysis of the evolutionary status of ETGs in their different aspects. A first basic question arises dealing with the problem of a confident discrimination between age and metallicity effects in order to achieve an unbiased measure of the age of ETGs.

### 4.1. *Age Dating and Energetics in SSPs*

In Buzzoni et al. (1992) we addressed the problem of the absolute age of ETGs on the basis of a calibration for the $Mg_2$

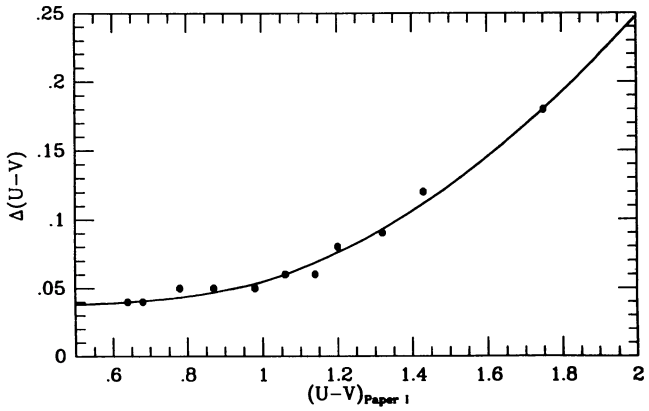


FIG. 8.—Correction to be applied to integrated $U-V$ colors of models of Paper I to account for stellar blanketing. New $U-V$ colors can be obtained by adding the $\Delta(U-V)$ offset to the old ones. This correction has already been applied throughout in the models of this paper.

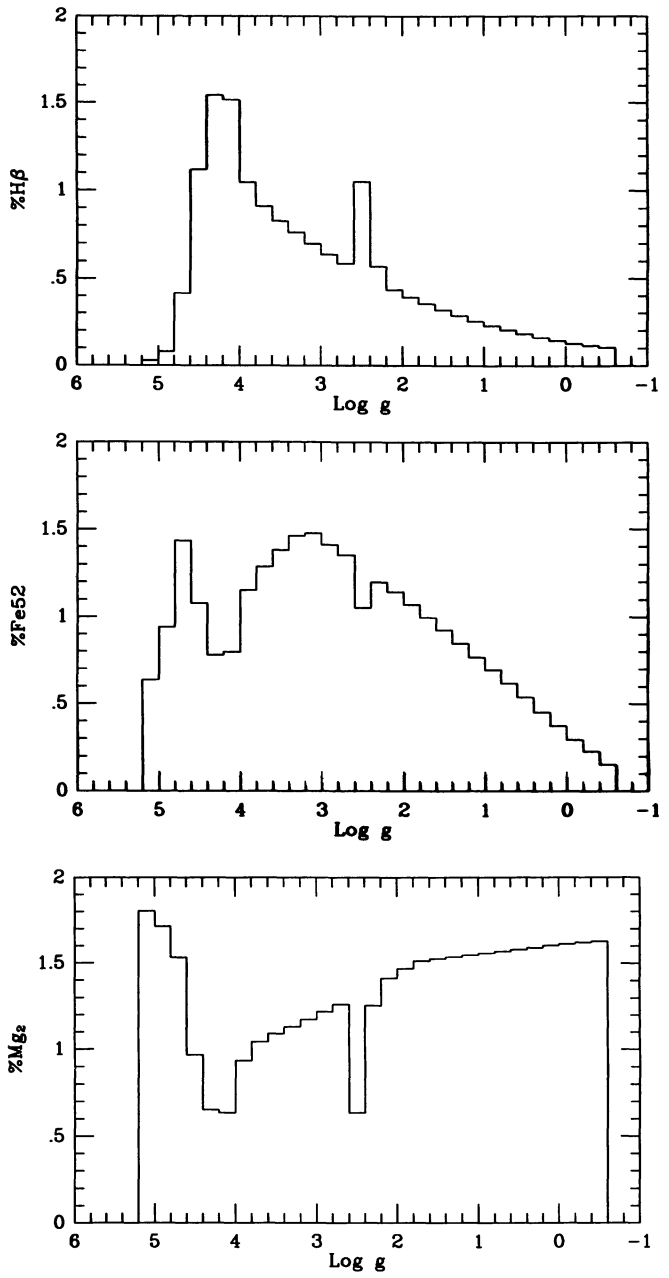


FIG. 9.—Disaggregated contributions to the integrated Hβ, Fe52, $Mg_2$, CO, and $H_2O$ features from stars of different gravity in a 15 Gyr Salpeter SSP with solar metallicity and R-HB morphology.

The quantity displayed is the ratio of the relative contribution of each stellar bin to the continuum and to the residual light in the absorption feature. A value of ~1.0 indicates that stars contribute with the same weight both to the continuum and to the line, while values in excess of unity mean that those stars mainly contribute to the absorption feature.

It appears that TO stars are the main contributors to the integrated Hβ of the SSP, while Fe52 is mainly contributed by stars at the base of the RGB. The AGB and RGB stars supply $Mg_2$ and CO, while the $H_2O$ index also responds to low-MS red dwarfs.

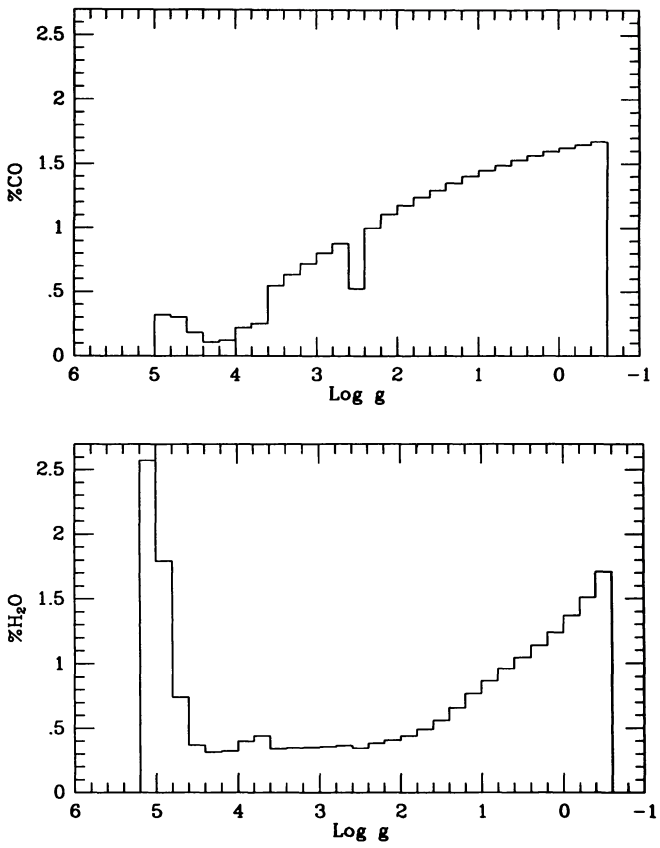


FIG. 9—*Continued*

index. The main conclusion was that ETGs should be consistent with old stellar populations moderately metal rich ([Fe/H] = +0.15) and with an age of 15 Gyr. Independent support in this sense also came from the analysis of the Hβ feature that better traces the TO temperature (Buzzoni et al. 1994). In the controversy about dating ETGs this leads us therefore to favor the "old-stars" solution instead of requiring any supplementary episode of star formation that should have occurred at more recent epochs.

Nonetheless, because the arguments in favor of the alternative scenario are relevant, it is important, we believe, to make a special effort to clarify the situation and better explore whether and how the apparent dichotomy can be disentangled.

In a series of papers, O'Connell (1976, 1980, 1982, 1983, 1986) widely discussed the problem of dating galaxies by means of "optimized synthesis" (to recall his own terminology) using linear programming algorithms applied to empirical stellar libraries to match broadband colors and selected spectral features in the spectra of ETGs and in the nuclei of spiral galaxies.

His optimum fitting models for giant ellipticals indicated metal-rich populations with a TO about the spectral type G5 V, while comparing with the relevant case of M32 a nearly solar stellar population with a TO at ~F8 V seemed more appropriate (O'Connell 1980).

Translated to absolute age via calibration through the Yale isochrones (Ciardullo & Demarque 1977), this led him to conclude that a spread in age with a substantial contribution from stars as young as 5 Gyr was consistent with both M32 and the giant ellipticals, once taking account of the different metallicities.

Accordingly, Pickles (1985) achieved the same results by performing synthesis of ETGs in the Fornax cluster, confirm-

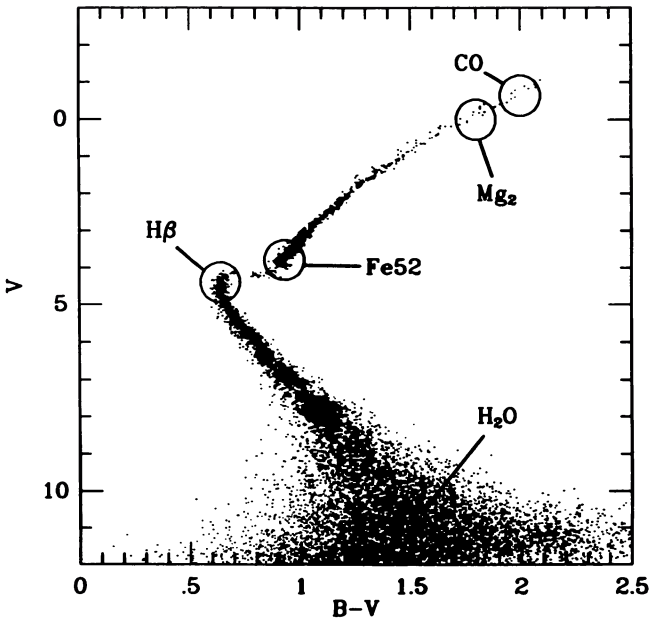


FIG. 10.—A simplified sketch of the selective index dependence in a synthetic *C-M* diagram of a 15 Gyr Salpeter SSP with [Fe/H] = 0 (it is model S throughout in the paper). The synthetic *C-M* diagram is a simulation of a total of 11,000 stars brighter than $M_v = +12$. For a better sampling in the diagram the RGB + HB + AGB sample has been enhanced by a factor of 10. A Poissonian error has been applied to the magnitudes ($\sigma$[mag] $\propto 10^{0.2\text{mag}}$) with $\sigma(V) = 0.01$ mag at $M_v = +4.0$.

ing again that stars about spectral type G5–8 should be the leading group dominating the TO region in the galaxies and supporting the presence of a stellar population of intermediate age of ~6–10 Gyr based on the revised Yale isochrones of Green, Demarque, & King (1987). Apparently, therefore, ETGs should have experienced a rather complex history after the epoch of globular cluster formation ~15 Gyr ago.

Under more detailed analysis, however, one could realize that the approach to population synthesis in O'Connell's and Pickles's models is basically different from EPS. The pros and cons of performing optimized synthesis are well known (cf. O'Connell 1986 and Renzini 1988 for a discussion). The main advantage is that one could test independently the correctness of the theory of stellar evolution in the sense that the "right" isochrone and stellar luminosity function could in principle be retrieved empirically from the observations and not adopted a priori. The weak point is that any *formally* realistic solution might not also be a *physically* realistic one due to spurious or improper constraints induced, for example, by an incomplete stellar library or by the criteria adopted to single out the best fit.

A recurrent point in the age dating of unresolved stellar populations is that age and metallicity should be dealt with at once. As is well known, the "age-metallicity dilemma" originates from the fact that by enhancing the chemical composition in the stars we also increase the mean opacity in their interiors (without sensibly affecting the nuclear energetics). This means that a larger radius is needed for a star to release the same amount of energy, and its temperature should decrease accordingly, as $L_{\text{TOT}} \propto R^2T^4$. As far as the integrated SED of an SSP is concerned, the net effect of increasing either [Fe/H] or age works, in any case, in the direction of making the SED redder. As a result, most of the current disagreement about the age of ETGs, in fact, derives from a disagreement in the metallicity scale (Renzini & Buzzoni 1986).

From this point of view, EPS models might have a major advantage over optimized synthesis. As the latter somehow relaxes the theoretical constraints on evolutionary lifetimes coming from stellar evolution, any reliability in the dating process crucially depends on a successful fit of the 4000 Å region in the integrated SED thus determining the spectral type of the warmest MS stars in the mix. Moreover, to infer age, this then requires a double supplementary step, relying first on a confident calibration of spectral type versus temperature, and eventually on a calibration of the TO temperature versus age. As a consequence, the whole procedure is not completely free from any assumptions about stellar evolution, and *it ultimately relies on a comparison with theoretical isochrones, which is the first and more immediate step for EPS.*

In addition to the available models for optimized synthesis of O'Connell (1976) (OC model) and Pickles (1985) (PK model; we will assume his model for NGC 1404 as a reference in the following discussion), it is of some relevance here to also attempt a comparative review and discussion of the current EPS models for ETGs. We, therefore, wish to consider with special care the original work of Tinsley & Gunn (1976) (TG model), the models of Guiderdoni & Rocca-Volmerange

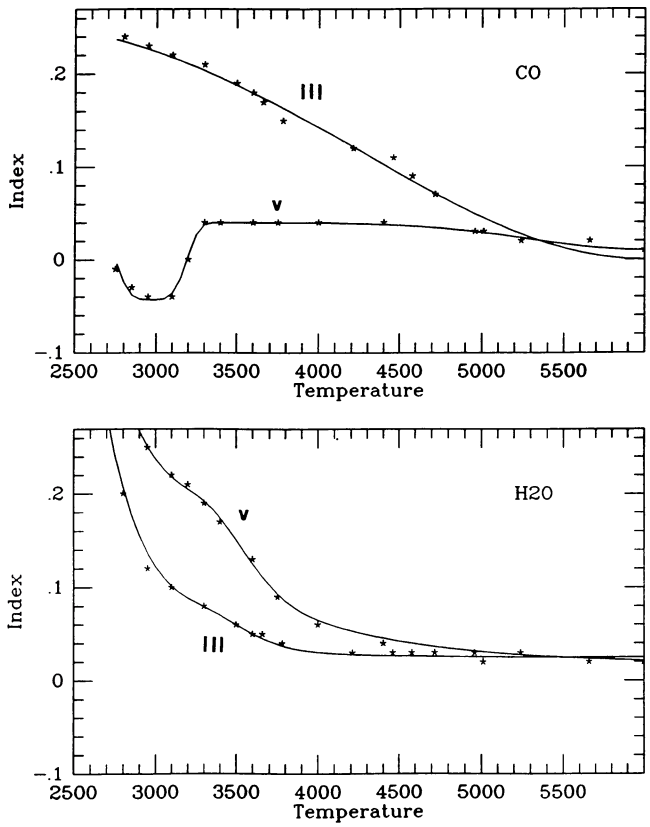


FIG. 11.—Frogel et al. (1978) and Aaronson et al. (1978) index calibration of CO and $H_2O$ for dwarf and giant stars.

TABLE 2

SSP MODELS FOR $s = 1.35$

| log $Z$ | [Fe/H] | AGE (Gyr) | $\eta = 0.3$ | | | $\eta = 0.5$ | | |
|---|---|---|---|---|---|---|---|---|
| | | | $V-K$ | CO | $H_2O$ | $V-K$ | CO | $H_2O$ |
| −3.00 ..... | −1.27 | 8.0 | 2.46 | 0.012 | 0.027 | 2.39 | 0.011 | 0.027 |
| | | 10.0 | 2.50 | 0.012 | 0.028 | 2.42 | 0.011 | 0.027 |
| | | 12.5 | 2.51 | 0.012 | 0.028 | 2.43 | 0.011 | 0.028 |
| | | 15.0 | 2.52 | 0.012 | 0.029 | 2.44 | 0.011 | 0.028 |
| | | 18.0 | 2.54 | 0.012 | 0.029 | 2.45 | 0.011 | 0.029 |
| −2.00 ..... | −0.25 | 4.0 | 2.91 | 0.129 | 0.050 | 2.81 | 0.122 | 0.046 |
| | | 5.0 | 2.93 | 0.128 | 0.050 | 2.84 | 0.120 | 0.046 |
| | | 6.0 | 2.95 | 0.127 | 0.051 | 2.85 | 0.119 | 0.046 |
| | | 8.0 | 2.97 | 0.125 | 0.052 | 2.87 | 0.117 | 0.047 |
| | | 10.0 | 3.00 | 0.125 | 0.054 | 2.89 | 0.116 | 0.049 |
| | | 12.5 | 3.02 | 0.123 | 0.055 | 2.92 | 0.115 | 0.051 |
| | | 15.0 | 3.04 | 0.123 | 0.056 | 2.92 | 0.113 | 0.052 |
| −1.77 ..... | −0.02 | 4.0 | 3.05 | 0.151 | 0.062 | 2.95 | 0.143 | 0.056 |
| | | 5.0 | 3.07 | 0.151 | 0.063 | 2.96 | 0.142 | 0.056 |
| | | 6.0 | 3.08 | 0.149 | 0.063 | 2.97 | 0.140 | 0.057 |
| | | 8.0 | 3.10 | 0.148 | 0.065 | 3.00 | 0.139 | 0.059 |
| | | 10.0 | 3.13 | 0.147 | 0.066 | 3.03 | 0.138 | 0.060 |
| | | 12.5 | 3.17 | 0.146 | 0.068 | 3.05 | 0.136 | 0.061 |
| | | 15.0 | 3.19 | 0.144 | 0.070 | 3.07 | 0.133 | 0.063 |
| −1.54 ..... | 0.22 | 4.0 | 3.18 | 0.186 | 0.100 | 3.08 | 0.165 | 0.069 |
| | | 5.0 | 3.20 | 0.187 | 0.105 | 3.08 | 0.163 | 0.069 |
| | | 6.0 | 3.21 | 0.185 | 0.104 | 3.11 | 0.163 | 0.071 |
| | | 8.0 | 3.24 | 0.185 | 0.109 | 3.14 | 0.161 | 0.073 |
| | | 10.0 | 3.27 | 0.183 | 0.111 | 3.16 | 0.158 | 0.074 |
| | | 12.5 | 3.29 | 0.180 | 0.112 | 3.19 | 0.155 | 0.076 |
| | | 15.0 | 3.33 | 0.185 | 0.127 | 3.21 | 0.159 | 0.089 |

TABLE 3

SSP MODELS FOR $s = 2.35$

| log $Z$ | [Fe/H] | AGE (Gyr) | $\eta = 0.3$ | | | $\eta = 0.5$ | | |
|---|---|---|---|---|---|---|---|---|
| | | | $V-K$ | CO | $H_2O$ | $V-K$ | CO | $H_2O$ |
| −3.00 ..... | −1.27 | 8.0 | 2.48 | 0.011 | 0.032 | 2.42 | 0.011 | 0.032 |
| | | 10.0 | 2.52 | 0.012 | 0.032 | 2.45 | 0.011 | 0.032 |
| | | 12.5 | 2.54 | 0.012 | 0.034 | 2.47 | 0.011 | 0.033 |
| | | 15.0 | 2.56 | 0.011 | 0.035 | 2.49 | 0.011 | 0.035 |
| | | 18.0 | 2.59 | 0.011 | 0.036 | 2.51 | 0.011 | 0.036 |
| −2.00 ..... | −0.25 | 4.0 | 2.88 | 0.122 | 0.053 | 2.78 | 0.114 | 0.049 |
| | | 5.0 | 2.90 | 0.120 | 0.054 | 2.82 | 0.112 | 0.050 |
| | | 6.0 | 2.93 | 0.119 | 0.054 | 2.83 | 0.111 | 0.051 |
| | | 8.0 | 2.96 | 0.117 | 0.056 | 2.87 | 0.108 | 0.053 |
| | | 10.0 | 3.00 | 0.116 | 0.059 | 2.91 | 0.106 | 0.055 |
| | | 12.5 | 3.03 | 0.113 | 0.062 | 2.95 | 0.104 | 0.059 |
| | | 15.0 | 3.07 | 0.112 | 0.063 | 2.96 | 0.102 | 0.060 |
| −1.77 ..... | −0.02 | 4.0 | 3.01 | 0.142 | 0.065 | 2.92 | 0.133 | 0.059 |
| | | 5.0 | 3.05 | 0.141 | 0.067 | 2.94 | 0.131 | 0.060 |
| | | 6.0 | 3.06 | 0.139 | 0.067 | 2.96 | 0.130 | 0.061 |
| | | 8.0 | 3.09 | 0.137 | 0.070 | 3.00 | 0.128 | 0.064 |
| | | 10.0 | 3.14 | 0.134 | 0.072 | 3.04 | 0.125 | 0.067 |
| | | 12.5 | 3.18 | 0.132 | 0.075 | 3.08 | 0.122 | 0.069 |
| | | 15.0 | 3.22 | 0.129 | 0.078 | 3.12 | 0.118 | 0.073 |
| −1.54 ..... | 0.22 | 4.0 | 3.13 | 0.175 | 0.101 | 3.03 | 0.154 | 0.071 |
| | | 5.0 | 3.16 | 0.175 | 0.106 | 3.05 | 0.152 | 0.073 |
| | | 6.0 | 3.18 | 0.172 | 0.106 | 3.08 | 0.151 | 0.075 |
| | | 8.0 | 3.23 | 0.170 | 0.111 | 3.13 | 0.147 | 0.078 |
| | | 10.0 | 3.27 | 0.168 | 0.113 | 3.17 | 0.144 | 0.080 |
| | | 12.5 | 3.31 | 0.162 | 0.116 | 3.21 | 0.139 | 0.085 |
| | | 15.0 | 3.35 | 0.165 | 0.130 | 3.25 | 0.140 | 0.098 |

TABLE 4

SSP MODELS FOR $s = 3.35$

| log $Z$ | [Fe/H] | AGE (Gyr) | $\eta = 0.3$ $V-K$ | $\eta = 0.3$ CO | $\eta = 0.3$ $H_2O$ | $\eta = 0.5$ $V-K$ | $\eta = 0.5$ CO | $\eta = 0.5$ $H_2O$ |
|---|---|---|---|---|---|---|---|---|
| −3.00 ..... | −1.27 | 8.0 | 2.64 | 0.010 | 0.053 | 2.60 | 0.010 | 0.055 |
| | | 10.0 | 2.66 | 0.011 | 0.050 | 2.61 | 0.010 | 0.052 |
| | | 12.5 | 2.69 | 0.011 | 0.052 | 2.64 | 0.010 | 0.053 |
| | | 15.0 | 2.73 | 0.010 | 0.056 | 2.68 | 0.010 | 0.057 |
| | | 18.0 | 2.76 | 0.010 | 0.057 | 2.70 | 0.010 | 0.059 |
| −2.00 ..... | −0.25 | 4.0 | 2.94 | 0.100 | 0.070 | 2.86 | 0.092 | 0.069 |
| | | 5.0 | 2.97 | 0.098 | 0.072 | 2.91 | 0.090 | 0.070 |
| | | 6.0 | 3.01 | 0.096 | 0.074 | 2.94 | 0.088 | 0.072 |
| | | 8.0 | 3.07 | 0.092 | 0.078 | 3.01 | 0.084 | 0.077 |
| | | 10.0 | 3.14 | 0.090 | 0.083 | 3.07 | 0.081 | 0.082 |
| | | 12.5 | 3.20 | 0.084 | 0.089 | 3.13 | 0.076 | 0.089 |
| | | 15.0 | 3.23 | 0.084 | 0.090 | 3.16 | 0.074 | 0.090 |
| −1.77 ..... | −0.02 | 4.0 | 3.09 | 0.111 | 0.086 | 3.02 | 0.102 | 0.083 |
| | | 5.0 | 3.14 | 0.109 | 0.089 | 3.06 | 0.099 | 0.086 |
| | | 6.0 | 3.15 | 0.109 | 0.088 | 3.07 | 0.099 | 0.086 |
| | | 8.0 | 3.22 | 0.104 | 0.094 | 3.15 | 0.095 | 0.092 |
| | | 10.0 | 3.28 | 0.100 | 0.098 | 3.21 | 0.091 | 0.096 |
| | | 12.5 | 3.35 | 0.096 | 0.103 | 3.28 | 0.086 | 0.101 |
| | | 15.0 | 3.42 | 0.090 | 0.109 | 3.35 | 0.079 | 0.108 |
| −1.54 ..... | 0.22 | 4.0 | 3.18 | 0.142 | 0.115 | 3.10 | 0.123 | 0.093 |
| | | 5.0 | 3.23 | 0.139 | 0.123 | 3.15 | 0.117 | 0.099 |
| | | 6.0 | 3.27 | 0.135 | 0.124 | 3.18 | 0.115 | 0.102 |
| | | 8.0 | 3.34 | 0.130 | 0.129 | 3.26 | 0.110 | 0.106 |
| | | 10.0 | 3.41 | 0.125 | 0.134 | 3.33 | 0.104 | 0.111 |
| | | 12.5 | 3.49 | 0.115 | 0.144 | 3.42 | 0.096 | 0.124 |
| | | 15.0 | 3.54 | 0.115 | 0.154 | 3.47 | 0.095 | 0.132 |

(1987) (GR model), and the recent ones by Bruzual & Charlot (1993) (BC model). A synoptic sketch can be found in Table 5, comparing these models with two original models for 15 Gyr SSPs with solar (S) and supersolar (SS) metallicity (i.e., [Fe/H] = 0 and +0.22, respectively) taken from Paper I, which, in our opinion, better match the ETG population at the present time. A number of interesting remarks stem from an accurate analysis of the table and are worth further comment:

1. There is general agreement among the different sources in attributing to ETGs a dominant stellar population at the TO typically about the spectral type G5 V, the residual uncertainty being only plus or minus three spectral subclasses.

2. This implies that $B - V$ at the TO is identified with a notably high accuracy, spanning just a 0.09 mag interval from 0.63 to 0.72 with a preferred value of about $(B - V)_{TO} = 0.67$.

3. All the models, but Pickles (1985), adopt a lower mass for MS stars of $M_l = 0.1\ M_\odot$. This makes the different estimates of the $M/L$ ratio homogeneous. Only Tinsley & Gunn (1976) obtain an exceedingly low ratio, all the others range from 6 to 14 (in the $V$ light and in solar units). The value of Tinsley & Gunn is easily explained by considering their giant-dominated stellar population (note that this model assumes a flat IMF with an exponent $s = 1.0$ instead of the Salpeter value). This makes the population brighter for fixed total mass and therefore gives a lower $M/L$. To a lesser extent, this is also the case for Guiderdoni & Rocca Volmerange, who use a composite IMF from Scalo (1986).

4. A striking point appears in Table 5 when we compare the $V$ light partitions among the different stellar evolutionary phases for the set of models. All the models, except that of O'Connell, display an abnormally enhanced contribution (up to a factor of 2 or more) from the giant branches relative to our S or SS reference models, for which MS:post-MS = 0.88 and 1.02, respectively.

This is particularly evident for both the TG and the GR models (MS:post-MS = 0.45 and 0.37, respectively). We are inclined to attribute most of this discrepancy to an artificial excess in the post-MS evolutionary phases rather than to a deficiency in the MS contribution, as the latter should derive much more confidently from the adopted reference isochrones and should not be expected to change so drastically (see Table 5 for the sources adopted by the different authors).

Again, the case of Tinsley & Gunn (1976) is readily explained, as they adopted in their models an age-independent RGB derived empirically from old disk giants. Clearly, this induced a discontinuity in the luminosity function when grafting on the SGB, with a brighter RGB while the rest of the population fades and reddens with increasing age (see their Fig. 1). In addition, although authors correctly applied the prescription of the "fuel consumption theorem" (Renzini & Buzzoni 1986), preserving the physical self-consistency in their code, they probably failed by overestimating the RGB lifetime from the empirical luminosity function adopted.

By reference, in the S model of Table 5, the RGB extends in bolometric from $\log L = 0.49$ up to $3.38\ L_\odot$ at the onset of the helium flash, lasting 510 Myr in total. This has to be compared in Tinsley & Gunn with a giant branch starting at $\log L = 0.89$, and rising up to 4.19 in about 900 Myr. By a fortunate coinci-

TABLE 5

SYNOPTIC TABLE OF CURRENT MODELS FOR ETGs

A. BASIC PARAMETERS

| | TG | OC | PK | GR | BC | S | SS |
|---|---|---|---|---|---|---|---|
| Age (Gyr) | 15 | 5 | 6.8 | 13.2 | 13.5 | 15 | 15 |
| [Fe/H] | 0.0 | >0.0 | 0.33 | 0.0 | 0.0 | 0.0 | 0.22 |
| $s$ | 1.0 | ... | ... | 1.25[a] | 2.35 | 2.35 | 2.35 |
| $M_l$ | 0.09 | 0.10 | 0.20 | 0.10 | 0.10 | 0.10 | 0.10 |
| TO group | G6–7 V | G0–5 V | G5–8 V | G6 V | G5 V | G3 V | G6 V |
| $(B-V)_{TO}$ | 0.70 | 0.63 | 0.70 | 0.72 | 0.66 | 0.64 | 0.69 |
| Reference for MS | 1 | 2 | 2 | 3 | 4 | 5 | 6 |

B. PREDICTED COLORS AND $M/L$

| | TG | OC | PK | GR | BC | S | SS | Mean Observed[b] |
|---|---|---|---|---|---|---|---|---|
| $B-V$ | 0.98 | ... | ... | 0.97 | 0.93 | 0.93 | 0.96 | $0.95 \pm 0.06$ |
| $V-K$ | 2.97 | 3.29 | ... | ... | 3.16 | 3.22 | 3.35 | $3.27 \pm 0.16$ |
| CO | 0.14 | 0.16 | ... | ... | ... | 0.13 | 0.16 | $0.16 \pm 0.02$ |
| $H_2O$ | 0.08 | 0.12 | ... | ... | ... | 0.08 | 0.13 | $0.12 \pm 0.02$ |
| $Mg_2$ | ... | ... | ... | ... | 0.23 | 0.28 | 0.31 | $0.29 \pm 0.03$ |
| $M/L_v$ | >3.0 | 14.3 | <10.7 | 6.2 | 10.1 | 13.4 | 15.8 | $>6 \pm 3$ |

C. PERCENTAGE OF $V$ LIGHT

| | TG | OC | PK | GR | BC | S | SS |
|---|---|---|---|---|---|---|---|
| MS | 31.1 | 45.0[c] | 32.7 | 27.2 | 37.0 | 36.9 | 50.6 |
| SGB | 10.3 | 11.0[c] | 20.1 | ... | 11.5 | 14.4 | 13.7 |
| RGB + HB + AGB | 58.6 | 40.1[c] | 45.0 | 72.8 | 51.5 | 38.7 | 35.7 |
| Metal-poor or hot stars | ... | 3.9[c] | 2.2 | ... | ... | ... | ... |
| MS:SGB:GB | 100:33:188 | 100:24:89 | 100:61:138 | ... | 100:31:139 | 100:31:83 | 100:27:71 |
| MS:post-MS | 100:221 | 100:113 | 100:199 | 100:268 | 100:170 | 100:114 | 100:98 |

[a] A composite IMF is assumed. The power index refers to the relevant range of mass for old SSPs.

[b] $B-V$ and $V-K$ from Persson et al. 1979; CO from Frogel et al. 1978; $H_2O$ from Aaronson et al. 1978; $Mg_2$ from Davies et al. 1987; $M/L_v$ in solar units from Faber & Jackson 1976.

[c] Taken at 5015 Å.

REFERENCES FOR MS.—(1) Hejlesen et al. 1972; (2) Green et al. 1987; (3) Mengel et al. 1979; (4) Schaller et al. 1992; (5) Vandenberg 1985; (6) Vandenberg & Laskarides 1987.

dence, the RGB excess partially compensates for the rough or missing treatment of the HB + AGB phases in those models (see also Paper I on this point).

Most intriguing is the case of Guiderdoni & Rocca-Volmerange (1987), given the same theoretical reference framework as in the S model for the post-MS modeling. Despite any difference in the MS stellar tracks (they adopted the Yale isochrones instead of Vandenberg's), we have reason to believe that more serious problems should arise in consistently matching the post-MS evolution.

Again, the fuel consumption theorem provides an immediate argument to check the physical self-consistency of that model. From equations (6)–(8) of Paper I, the fuel consumption in hydrogen-equivalent $M_\odot$ for stars in post-MS evolutionary phases that contribute a fraction $L_{PMS}/L_{TOT}$ of the total bolometric luminosity of an SSP is

$$\text{Fuel} = \frac{L_{PMS}}{L_{TOT}} B_{11}^{-1} \sim 0.6 \frac{L_{PMS}}{L_{TOT}} (M_\odot), \qquad (3)$$

where $B_{11}$ is the "specific evolutionary flux" of the SSP (Renzini & Buzzoni 1986) in units of $10^{-11}\ L_\odot^{-1}\ \text{yr}^{-1}$. Its value does not change much with time, becoming $\sim B_{11} = 1.7 \pm 0.3$ (Paper I). According to equation (3), and also considering Figure 3 in Renzini & Buzzoni (1986), we derive that $\sim 0.37\ M_\odot$ is burnt during post-MS evolution by stars in a 15 Gyr SSP of solar metallicity. This is $\sim 50\%$ of the actual mass ($\sim 0.8\ M_\odot$) for stars along the giant branches. On the other hand, as the GR model burns a factor of $268/114 = 2.35$ more fuel than predicted by the fuel consumption theorem for fixed MS performance, this would require the quite unlikely situation that its post-MS stars burn virtually the totality of their mass.

To show how shifty the effect can be, and how hardly detectable just on the basis of the colors or the spectral analysis, we report in Table 6 the results of an experiment giving the changes in the integrated colors and spectral indices for the S model by artificially doubling the whole post-MS lifetime. One can see that no striking variations are apparently induced on the SED, as we are acting on stars with individual colors similar on average to those of the original SSP. Of course, this will be magnified when tracking evolution back in time, inducing drastically different behavior of the stellar population. Figure 12 demonstrates that major revisions might also be required

TABLE 6

EFFECT OF DOUBLING THE POST-MS LIFETIME

| Model | S | S′ (post-MS ×2) |
|---|---|---|
| $B-V$ | 0.93 | 0.97 |
| $V-K$ | 3.22 | 3.35 |
| CO | 0.13 | 0.15 |
| $H_2O$ | 0.08 | 0.08 |
| $Mg_2$[a] | 0.28 | 0.28 |
| Fe52[b] | 3.03 | 3.00 |
| Fe53[b] | 2.45 | 2.42 |
| Hβ[b] | 1.62 | 1.57 |
| $M/L_v$ | 13.4 | 8.7 |
| Percentage of $V$ Light | | |
| MS | 46.9 | 30.6 |
| SGB | 14.4 | 18.8 |
| RGB | 20.6 | 26.9 |
| HB | 13.7 | 17.9 |
| AGB | 4.4 | 5.8 |
| MS:SGB:GB | 100:31:83 | 100:62:166 |
| MS:post-MS | 100:114 | 100:228 |

[a] In magnitudes according to Buzzoni et al. 1992.
[b] In angstroms according to Buzzoni et al. 1993.

for the models of Bruzual & Charlot (1993) and Pickles (1985).

Due to their different synthesis approach, both the PK and OC models are less stringent in deriving the $M/L$ ratio, it being in fact a free parameter poorly constrained by the spectral fit (~95% of the total mass in those models is locked into faint M6–8 V red dwarfs). Though with this important caveat, it is relevant to note that, among the different models considered, that of O'Connell seems the most similar to the S and SS models, fulfilling the precepts of the fuel consumption theorem.

Once again, the theorem further emphasizes the importance of a reliable treatment of the post-MS evolution in the synthesis models, not only assuring continuity in the $C$-$M$ plane but also in the overall luminosity function of the synthetic stellar population.

### 4.2. *M32 and the "Fair-Template" Problem*

On the basis of the previous discussion we come back to the big question: What derives then from a discrepancy of nearly a factor of 3 in the age estimate of ETGs? As is well known, the case of M32 is the real key to the current controversy.

In this respect we are in a delicate position, as we are, in fact, assessing the general problem of the age of ETGs by resting on this ostensibly "fair" local template. Unfortunately, to a large extent, M32 might be a somewhat peculiar galaxy. It is hard to think that the vicinity of M31 could not have influenced its early evolution leaving a tidally stripped remnant of a once larger system as its high surface brightness seems to indicate. Space observations in the far-UV (O'Connell et al. 1992) show that M32 displays drastically different behavior with respect to other ellipticals or to the bulge of M31. In any case, despite any possible complications, M32 is clearly the unavoidable ETG template which refer to, and the only elliptical galaxy for which we have some direct hints by partially resolving its stellar population.

The inference of a blue TO about F8 V coupled with a claimed solar metallicity were the two strong points leading O'Connell (1980) to first attribute a young age of ~4–5 Gyr to this galaxy. Since that work, major contributions attempting to resolve the M32 stellar population in different photometric bands came from Freedman (1989, 1992), Davidge & Nieto (1992), Davidge & Jones (1992), and Elston & Da Silva (1992). In addition, Rose (1984, 1994) and Boulade et al. (1988) extensively reassessed the case of M32 on the basis of a combined synthesis of UV spectral features, while Davidge (1990) discussed its IR properties, and Hardy et al. (1994) searched for spectral surface gradients in the optical range.

Despite any more or less direct and unambiguous argument raised by the different authors in favor of a large spread in age (and therefore in favor of the presence of a young stellar population in the galaxy), we still believe that none of the observational evidence can be considered as conclusive in this sense and free from any possible weighty bias. Let us try to excerpt, on the contrary, some of the relevant issues that do emerge in our opinion from a combined analysis of the current data in favor of an "old-stars" solution consistent with a canonical age of ~15 Gyr for the galaxy.

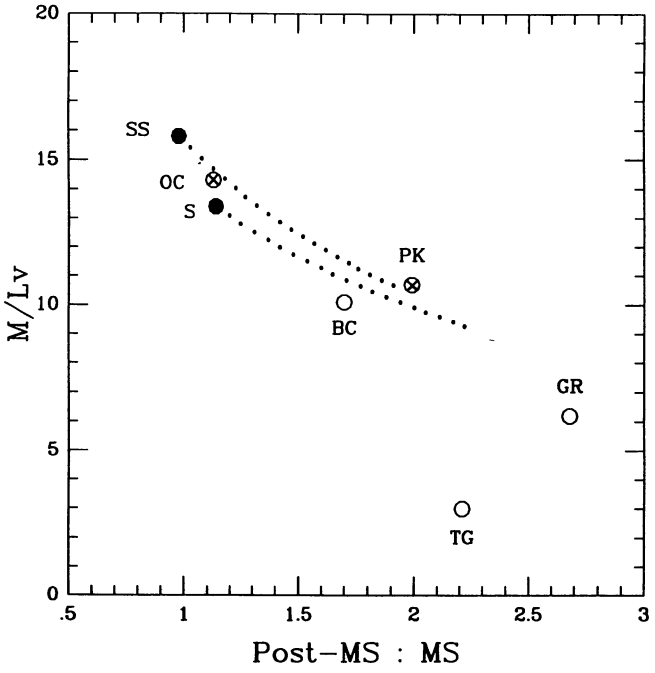


FIG. 12.—Comparison of current models for ETGs in Table 5. Plotted is the ratio of contribution to $V$ light from post-MS/MS evolutionary phases vs. mass-to-light ratio. The TG model is from Tinsley & Gunn (1976), OC from O'Connell (1976), PK from Pickles (1985), GR from Guiderdoni & Rocca-Volmerange (1987), BC from Bruzual & Charlot (1993), and S and SS from Paper I assuming [Fe/H] = 0 and +0.22, respectively. Crosses mark models obtained via optimized linear synthesis (OC and PK). Dotted lines show the change induced in the two reference models (*filled dots*) by relaxing the fuel consumption theorem and artificially increasing the contribution from the post-MS contribution up to a factor of 2.

#### 4.2.1. *AGB Stars*

The presence of bright AGB stars (up to $M_{bol} = -5.5$, i.e., a value $\sim 1.5$ mag brighter than what is observed in Galactic globular clusters) was first established by Freedman (1989) with deep $I_C$ photometry and then confirmed by IR observations of Freedman (1992), Davidge & Nieto (1992), and Elston & Da Silva (1992).

Due to its resemblance to the extended giant branch in the *C-M* diagrams of young globular clusters in the Magellanic clouds and in the M31 field (Rich & Mould 1991; Rich, Mould, & Graham 1993), this feature has been promptly raised as the most direct proof of a stellar population of intermediate age ($\sim 5$ Gyr) in M32.

Now, there is an obvious danger that must be more carefully taken into account, dealing with the proper handling of extreme crowding conditions when performing photometry of stars in external galaxies. We have reason to believe, for instance, that *all* the current luminosity functions for M31 and M32 suffer from a much higher degree of incompleteness than claimed by many authors and tend to display a brighter tail simply due to the extensive presence of unresolved blended stars. It is instructive in this regard to see the experiment of DePoy et al. (1993). For instance, a more conservative estimate of the crowding bias has convinced Rich et al. (1993) to decrease the luminosity of the brightest stars in M31 by $\sim 1$ mag down to values that nearly match the luminosity function in the Galactic bulge (Frogel & Whitford 1987).

Turning more specifically to Freedman's (1992) *K* photometry of M32, for example, and complementing Renzini's (1993) discussion relying on the fuel consumption theorem (Renzini & Buzzoni 1986), we have that, in the case of an old AGB lasting $15 \times 10^6$ yr, $\sim 3500$ stars should be expected in the observed field. Assuming Freedman's seeing FWHM as a spatial effective resolution element and using some elementary binomial statistics (disregarding for a moment all the non-AGB stars), one obtains that $\sim 84\%$ of the "resolution cells" are empty (in the sense that they contain no AGB stars), $\sim 14\%$ cells contain one star (and therefore 2850 AGB stars might be seen as individual objects once we go deep enough), $\sim 250$ detected objects are in fact a blend of two AGB stars (and appear therefore 0.75 mag brighter), and $\sim 50$ objects are blends of three or more stars (i.e., at least 1.2 mag brighter). This partition definitely gives a lower limit to the fraction of blended objects, as we are not considering the contribution of bright RGB stars (which are at least as numerous as the AGB members).

Now, as Freedman (1992) has revealed the 125 brightest objects in the field (and 50 of them are brighter than $M_{bol} \sim -4.0$), one expects that she is seeing almost purely unresolved clumps of one or more magnitudes fainter real AGB stars. Therefore, the luminosity of the giant tip might be drastically reduced, to be consistent with that of metal-rich Galactic globular clusters.

On the other hand, if we assume that Freedman is correctly sampling the M32 bright AGB population, then under those crowding conditions (i.e., by assuming that just less than one star is in fact a blended object) there would be space for a total of at most 140 AGB stars (15 of which are fainter than the magnitude limit), and we derive that the AGB phase lasts in total a factor (140/3500) less than assumed, that is, $\sim 600{,}000$ yrs. According to Renzini (1993), this is at least a factor of 2 less than what is currently predicted by models for 3–9 $M_\odot$ stars (e.g., Becker & Iben 1980) and almost one order of magnitude less than what is expected for a 5 Gyr stellar population with typically 1–1.5 $M_\odot$ stars evolving off the TO point (Gingold 1973; Iben & Renzini 1983).

#### 4.2.2. *TO Location*

The stellar TO group for M32 suggested by O'Connell (1980) on the basis of his fitting model turns to be about F6–9 V. However, no HB stars earlier than spectral type G5 III are included in his code, the only blue stars implicitly admitted being those included tout court in a "metal-poor" ([Fe/H] $\sim -1.5$) SED averaging the spectrum of the globular clusters M15 and M5. As stressed by O'Connell (1980), none of this metal-poor component was required by the optimum fit, and this led to such a bluer F8 V TO attributed to a 5 Gyr SSP with solar metallicity. Now, we know that, in addition to a main bulk of stars of about solar metallicity (Freedman 1989, 1992; Elston & Da Silva 1992), an old ($\sim 15$ Gyr) metal-poor component as low as [Fe/H] $= -2.2$ is present in the galaxy (Freedman 1989; Davidge & Jones 1992), so that this would require us to move the TO of the metal-rich stellar population to redder colors (i.e., to an older age).

#### 4.2.3. *Metallicity Calibration*

A metallicity calibration of M32 by means of high-resolution spectral features in the UV range about 3500 Å has been provided by Rose (1985c) and Boulade et al. (1988). The two main conclusions achieved in these works were that at 4000 Å a large amount, $\sim 70\%$, of the light in M32 was supplied by MS dwarf stars and that the luminosity-weighted mean metallicity is about solar (i.e., [Fe/H] $= -0.10 \pm 0.15$), derived from the UV features with no appreciable changes with respect to the determinations resting, for instance, on visual or IR wavelengths. The authors noted therefore that a composite stellar population with a noticeable spread in age but with fixed solar metallicity should be fully able to reproduce the spectral properties of M32.

We are inclined to believe that most of the arguments of Rose (1985c) and Boulade et al. (1988) come, in fact, from a subtly misleading interpretation of their observations and can be easily reversed. Concerning the claimed partition between dwarfs and giants in the UV light, these authors proceed similarly resting mainly on the study of the location of M32 in the plane of Sr II/Fe I or $\lambda 3550/\lambda 3544$ indices plotted versus H$\delta$/Fe I, comparing this location with the mean locus observed for giants and dwarfs (cf. Fig. 12 in Rose 1985c or Fig. 17 in Boulade et al. 1988). As discussed, the strategy leading to this combination of indices would maximize the dependence on the stellar gravity through the Sr II/Fe I and $\lambda 3550/\lambda 3544$ indices, while H$\delta$/Fe I would better trace the stellar temperature (preserving in any case a negligible dependence on [Fe/H]).

Clearly, on the basis of the Rose (1984) and Boulade et al. (1988) calibration, for M32 it is straightforward to derive that dwarfs about spectral type G5 (*i.e., the TO stars of the metal-rich stellar component*) are the main contributors to the integrated H$\delta$/Fe I index. The same also holds for most of the other

indices that better trace [Fe/H], for example, $p(3500)$ (cf. Fig. 11 in Boulade et al. 1988). It is no surprise therefore that those stars also lead to a constant solar value for the inferred metallicity. In other words, this stems from the fact that, quite perversely, in the UV range authors are testing the moderately cool component of the metal-rich stellar bulk of M32, and not its warmer (metal-poor) stars.

Rather than pointing to an important contribution from stars of intermediate age, we should instead conclude that the data of Rose (1985c) and Boulade et al. (1988) strongly support the presence of an old metal-rich stellar population and are not in conflict with the observed spread in metallicity. Incidentally, the claimed 70% contribution at 4000 Å from the MS stars can be consistently compared with a ~60% suggested by the 15 Gyr metal-rich SSPs in Paper I.

Accordingly, as remarked by Rose (1985c), the higher mean gravity displayed by stars contributing to the integrated Sr II/Fe I in M32 with respect to reference metal-rich globular clusters simply indicates a metallicity effect, as the G5 stars in the Sr II/Fe I "barycenter" of M32 are more metal rich than those of the reference globular clusters (see Fig. 5, by increasing [Fe/H] the mean gravity of the $B$ stellar contributors in an SSP slightly increases).

#### 4.1.4. *Radial Gradients*

In a recent spectroscopic study in search of radial gradients of some spectral features, Hardy et al. (1994) found for M32 a constant Hβ index of ~1.74 ± 0.05 Å with no significant gradients across the galaxy surface.

We discussed in § 2.2 the relevance of this feature as a powerful tracer of age in an SSP, and in Figure 13 we compare the observed value with the SSP models of Buzzoni et al. (1994). Also marked in the figure is the expected Hβ index for the old metal-poor component that is seen in the galaxy (its exact value would depend in part on the precise [Fe/H] and on the HB morphology). The result is that *disregarding any presence of metal-poor stars* there is no chance to fit the observations by any mix of metal-rich SSPs younger than 10 Gyr. Indeed, this is a safe lower limit since an even older population must be advocated to compensate for an otherwise stronger feature deriving from the fraction of stars at low metallicity.

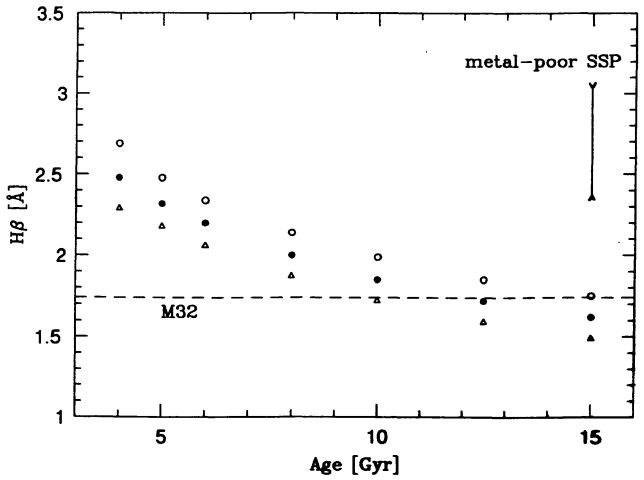


FIG. 13.—Expected trend in the Hβ index for metal-rich SSPs with increasing age. Open dots are for [Fe/H] = 0.25, solid dots are for [Fe/H] = 0.0, and open triangles are for [Fe/H] = +0.22. The integrated Hβ index for M32 is displayed by the dashed line, while the expected index for the old metal-poor component observed in the galaxy is marked by the vertical bar (according to different HB morphologies).

The fit of Hβ in M32 requires metal-rich SSPs no younger than 10 Gyr.

In addition, the lack of any significant Hβ radial gradient in the galaxy does not support any relevant gradient in the mean age of the stellar population, contrary to what has been concluded by Davidge & Nieto (1992) and Davidge & Jones (1992) on the basis of photometry in two fields (core and outer region) with extremely different crowding conditions.

We will return in § 7.1 to a possible model for M32 in terms of old SSPs with a spread in either metallicity or age.

### 4.3. *The Age-Metallicity Dilemma Revisited*

The evolutionary scenario emerging from the analysis of M32 seems to indicate that a bulk of old metal-rich stellar populations is required to adequately match the overall spectral properties of the galaxy.

Metal-poor stars are also a common ingredient of the stellar mix and are to be expected for giant ellipticals and the other ETGs. In the canonical framework of dynamical evolution they could be the earliest generations of stars formed, as long as gravitational collapse proceeded, anticipating the metal-enrichment process. It is reasonable to assume that the fraction of metal-poor stars over the whole stellar population in an ETG sharply correlates with the dynamical timescale, in the sense that the larger the free-fall time was, the more slowly the metal enhancement should have proceeded. Moreover, the so-called SN wind phase, causing an abrupt stripping of the residual gas, should have dramatically affected the chemical evolution in dwarf systems.

As a result, in a scenario basically dominated by coeval old stellar populations with a spread in metallicity, low-mass ellipticals should display a more important contribution from the metal-poor stellar component.

Direct evidence of the fact that a current age of 15 Gyr could be consistent with the observed photometric properties of the population of ETGs can be obtained by plotting the galaxy distribution in the $(B - V, V - K)$-plane. As we discussed in § 2.1, this combination of colors would maximize a selective response to age-metallicity effects, with [Fe/H] mainly running along the $V - K$ axis and age running along the $B - V$ axis. In Figure 14 we compare observations for a set of 94 ellipticals (52 galaxies with original $BVK$ photometry taken from Persson, Frogel, & Aaronson 1979, plus 42 galaxies with data for $B - V$ from Faber et al. 1989 and $V - K$ from Frogel et al. 1978). Reported in the figure is the theoretical sequence with increasing metallicity expected for 15 Gyr SSPs with Salpeter IMFs. The effect of decreasing age to 4 Gyr is shown for solar and supersolar metallicity.

One can see from the figure that the point distribution closely tracks the 15 Gyr model sequence with the exception of a few peculiar active or star-forming galaxies like NGC 4742, marked in the figure, that are better accounted for by a younger age. The barycenter of the whole sample of galaxies (see Table 5) indicates that [Fe/H] = +0.10 ± 0.35 (1 σ error bar from the $V - K$ dispersion), in fairly good agreement with the mean

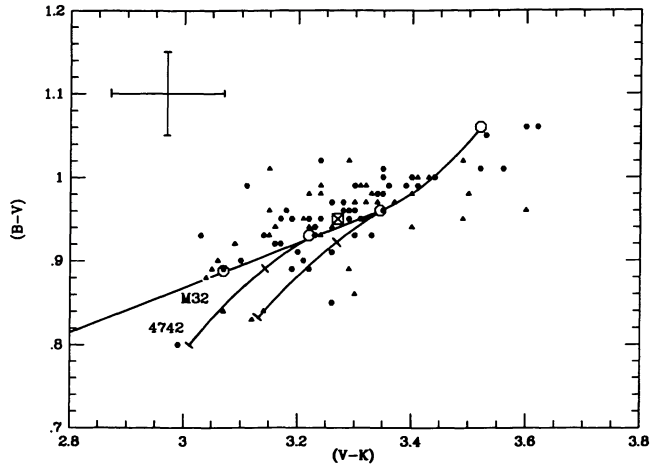


FIG. 14.—Color distribution of ETGs. Plotted is a sample of 52 galaxies with optical and IR photometry from Persson et al. (1979; *filled dots*) and 42 galaxies with $B - V$ from Faber et al. (1989) and $V - K$ from Frogel et al. (1978; *triangles*). The $B - V$ for M32 is from Sharov & Lyutyi (1983). Star-forming galaxy NGC 4742 is marked in the figure (see text for discussion). The barycenter of the whole population is displayed (*crossed square*), while in the top left is the typical error bar of observations.

The solid line is the sequence of 15 Gyr Salpeter SSPs with increasing metallicity. Open dots mark models with [Fe/H] = −0.25, 0, +0.22, and +0.87 in the sense of increasing $V - K$. Models at [Fe/H] = 0 and +0.22 are, respectively, the S and SS models referred to in the text and in Table 5. The effect of decreasing age to 10 and 4 Gyr is displayed for these two cases with tick marks along the two curves below the 15 Gyr sequence.

metallicity derived from the $Mg_2$ distribution (Buzzoni et al. 1992). In addition to the models of Paper I, a supplementary set has been included for [Fe/H] = +0.87 ($Z = 0.1$) based on the isochrones of Vandenberg & Laskarides (1987) and using the same prescriptions as in Paper I. The relevant parameters for these new models are summarized in Table 7.

As is well known, to a large extent the main contributors to the integrated $B - V$ of a galaxy are the MS stars, and especially those about the TO region. This is why $B - V$ is such a good age tracer, as we showed in § 2.1. On the other hand, it is clear from our previous discussion that any age-dating method relying solely on the (indirect) recognition of the TO temperature (as, e.g., optimized synthesis is) is prone to a subtle ambiguity, and in fact we have seen from the results in Table 5 how drastically different inferences can stem from a substantially coherent set of models.

For example, our 15 Gyr S and SS models of Figure 12 place the stellar TO in the spectral range G3–6 V. Accordingly, Pickles (1985) suggests for NGC 1404 a TO in the range G5–8 V but, however, derives an age of only 6.8 Gyr. Again, the age-metallicity dilemma crucially appears through a twofold bias.

A first source of ambiguity derives from the fact that Pickles's synthesis estimates only the temperature of the *warmest* stars about the TO, and not their absolute magnitude as well. So, a younger age is permitted if a higher metallicity is assumed. Second, in case we deal with a coeval stellar population displaying a spread in metallicity, the luminosity-weighted [Fe/H] to be attributed to such a TO group is *lower* than what is obtained by simply weighting in mass, as done by Pickles (remember that at a fixed age an SSP tends to become intrinsically bluer and brighter, i.e., with a lower $M/L$ ratio, with decreasing [Fe/H]). Therefore, despite any reasonable difference in the reference isochrones, we are of the opinion that most of the discrepancy in the age-dating procedure originally adopted by Pickles (1985) with respect to our results resides in such a systematic overestimate of the effective metallicity in ETGs. On the other hand, it is encouraging to note that a large revision occurred in Pickles's (1989) more recent work probing the ages of elliptical galaxies in distant clusters. In this case, resting on Vandenberg's isochrones, a lower effective metallicity is attributed to galaxies and an absolute age of 11–12 Gyr derives for galaxies at $z \sim 0.2$–0.3, fully reconciling the previous apparent discrepancy with the present results (see Buzzoni, Chincarini, & Molinari 1993).

### 4.4. *Age Dispersion*

An attempt to link our previous conclusions about the absolute age of ETGs with the currently accepted scenarios for gal-

TABLE 7

SUPER METAL-RICH SSPs

(Age = 15 Gyr; $Z = 0.1$; [Fe/H] = 0.87; $Y = 0.35$; R-HB)

| PARAMETER | MODEL 1 | 2 | 3 | 4 | NOTE |
|---|---|---|---|---|---|
| $s$ | 2.35 | 2.35 | 1.35 | 3.35 | |
| $\eta$ | 0.30 | 0.50 | 0.30 | 0.30 | |
| $M_{TO}$ | 0.92 | 0.92 | 0.92 | 0.92 | 1 |
| $M_{rt}$ | 0.75 | 0.57 | 0.75 | 0.75 | 1 |
| $M_{pn}$ | 0.51 | 0.47 | 0.51 | 0.51 | 1 |
| $B_{11}$ | 2.03 | 2.22 | 2.22 | 1.67 | 2 |
| Bol | 0.00 | 0.09 | −1.03 | 1.35 | 3 |
| Bol − $V$ | −1.12 | −1.01 | −1.11 | −1.21 | |
| $U - V$ | 1.93 | 1.92 | 1.91 | 1.97 | |
| $B - V$ | 1.06 | 1.05 | 1.05 | 1.08 | |
| $V - R$ | 0.96 | 0.94 | 0.96 | 0.99 | |
| $V - I$ | 1.72 | 1.68 | 1.71 | 1.79 | |
| $V - J$ | 2.47 | 2.38 | 2.45 | 2.57 | |
| $V - K$ | 3.52 | 3.38 | 3.49 | 3.65 | |
| $Mg_2$ | 0.36 | 0.35 | 0.35 | 0.38 | 4 |
| Hβ | 1.29 | 1.30 | 1.32 | 1.23 | 4 |
| Fe52 | 4.52 | 4.53 | 4.51 | 4.49 | 4 |
| Fe53 | 4.16 | 4.17 | 4.15 | 4.13 | 4 |
| CO | 0.21 | 0.19 | 0.23 | 0.16 | |
| $H_2O$ | 0.20 | 0.17 | 0.20 | 0.25 | |
| %MS | 0.302 | 0.330 | 0.237 | 0.427 | 5 |
| %SGB | 0.082 | 0.090 | 0.089 | 0.068 | 5 |
| %RGB | 0.335 | 0.366 | 0.367 | 0.274 | 5 |
| %HB | 0.126 | 0.147 | 0.138 | 0.103 | 5 |
| %AGB | 0.149 | 0.059 | 0.163 | 0.122 | 5 |
| %PAGB | 0.005 | 0.009 | 0.006 | 0.004 | 5 |
| $M/L_{bol}$ | 4.90 | 5.30 | 1.90 | 17.00 | 6 |
| $M/L_b$ | 19.15 | 18.55 | 7.29 | 73.53 | 6 |
| $M/L_v$ | 12.89 | 12.60 | 4.95 | 48.58 | 6 |
| $M/L_k$ | 1.90 | 2.11 | 0.75 | 6.35 | 6 |

NOTES.—(1) $M_{TO}$, $M_{rt}$, and $M_{pn}$ = masses in solar units of stars at the TO point, RGB tip, and onset of post-AGB phases, respectively. (2) $B_{11}$ = specific evolutionary flux in units of $10^{-11}$ $L_\odot^{-1}$ $yr^{-1}$. (3) Bol = bolometric magnitude of the SSP normalized to model No. 1. (4) $Mg_2$, Fe52, Fe53, and Hβ according to Buzzoni et al. 1992, 1993. (5) Relative contributions of the evolutionary phases to bolometric light. (6) $M/L$ in solar units. Only the *bright* mass is accounted for in the ratio.

axy formation would strongly prefer those mechanisms leading to a quick dissipative collapse of the primeval gas cloud. This would naturally account for old coeval galaxies, especially when considering the shorter dynamical free-fall time in the high-density regions in the universe, like the cores of clusters ($t_{ff} \propto 1/\sqrt{\rho}$). To some extent, we can understand the well-established evidence that ETGs seem to obey such a segregation effect (Dressler 1980), and up to $\frac{3}{4}$ of cluster galaxies are thus found to be E+S0 (Oemler 1974).

However, though the fraction of ETGs fades to 20% or less when considering the low-density field (Sandage & Tammann 1981), it remains to be clarified whether galactic genesis in the field has been the same as in the clusters or whether we have to expect the more likely case that the different environments play a role (cf. Whitmore 1990 for a recent discussion).

The two basic differences between field and cluster environments are that (1) the low-density regime in the field leads us to expect a larger spread in the timescales for a dissipative collapse converting gas into stars and (2) the dynamical interactions among galaxies are eased in low-density environments (e.g., in loose or even compact groups), allowing a more effective transfer of momentum and inducing therefore a more profound change in the structure and morphology of interacting members (Toomre 1977).

In the most basic terms, the question of ETG formation leads us to conceive two possible ways, hard to say whether antagonistic or complementary. On one hand, we might envisage a dissipative collapse eventually ending up with firing stars in the galaxy. On the other hand, an ETG might stem from dissipationless interactions among (disk) galaxies, feeding stars and eventually ending up with a merging. Cluster environments might be more favorable to the former case, while field conditions might be more suitable for the latter case (but this would call for a primary role of the compact groups). However, it has been proved (Stiavelli, Londrillo, & Messina 1991; Governato, Reduzzi, & Rampazzo 1993) that on the basis of a study of the galactic morphological features alone one cannot univocally discriminate between the different mechanisms of formation.

*N*-body simulations have shown that the evolutionary timescale over which a bulge galaxy can form via merging in a compact group spans a large range, going from a lower limit given by the crossing time of the group (White 1979; Barnes 1988) up to a large fraction of the Hubble time, if a suitable partition of the total energy between momentum and internal energy is provided (Governato et al. 1991).

Possible support for a differentiate genesis of cluster and field ETGs comes from the work of De Carvalho & Djorgovski (1989), who find a statistically significant difference between the two populations of galaxies, with field ellipticals displaying a larger spread in any of the distinctive dynamical and photometric parameters.

This problem has been addressed by Bower, Lucey, & Ellis (1992a, b) through a wide set of observations for a sample of ETGs in the two local clusters of galaxies in Virgo and Coma. Complementary work in this regard has been also carried out by Recillas-Cruz et al. (1990, 1991) providing accurate IR magnitudes and colors.

A comparison of these data with our models is displayed in Figures 15 and 16. *UVK* observations for a total of 48 galaxies

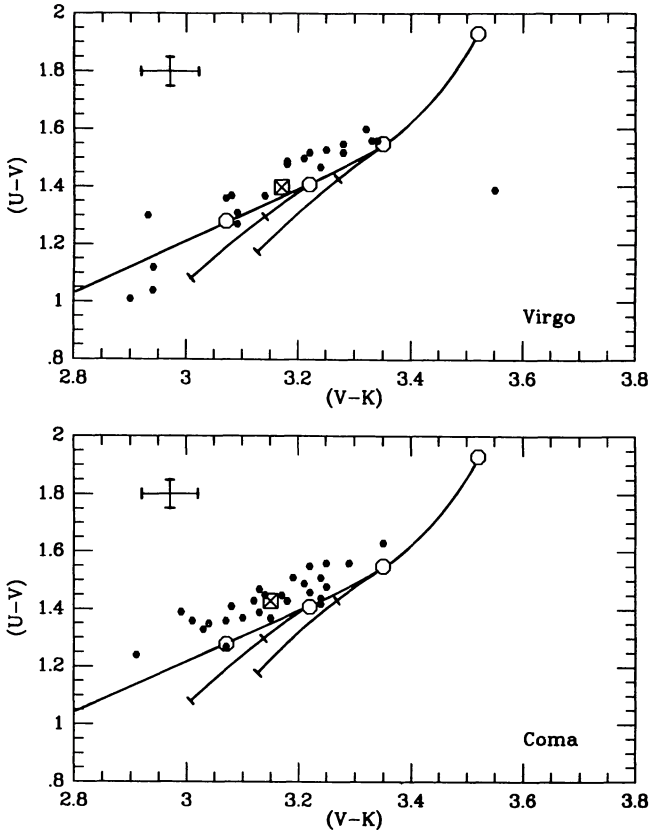


FIG. 15.—Same as in Fig. 13, but for *UVK* photometry of 21 ETGs in Virgo and 27 in Coma taken from Bower et al. (1992a).

(21 in Virgo and 27 in Coma) are available from Bower et al. (1992a), while 57 galaxies (28 in Virgo and 29 in Coma) have *K* photometry from Recillas-Cruz et al. (1990, 1991) and $B - V$ color from Davies et al. (1987). Just a glance at both figures makes evident the fact that ETGs in clusters seem to represent a quite homogenous population. Again, 15 Gyr models are fully able to match the data, and the little intrinsic scatter of the observations, especially in the *UV* photometry of Figure 15, strongly points to little spread in age, with galaxies being old coeval objects.

When comparing the *UVK*-selected sample of Bower et al. with the *BVK*-selected one of Recillas-Cruz et al., there is evidently a little systematic difference in the $V - K$ distribution, with the former having a bluer $V - K$ barycenter, especially for the Virgo sample. This difference is almost entirely due to aperture effects in the photometry (Bower et al. used a larger aperture), as the mean $V - K$ for the 13 galaxies in common to both samples results in $0.18 \pm 0.09$ mag bluer in Bower et al.

One more remark stemming from the figure is that there is a tendency of galaxies to lie above the theoretical sequence, especially in the Bower et al. sample. We believe that most of this shift should be accounted for by the uncertainty in the absolute zero point of the photometry. It is remarkable to note, however, that the effect is in the sense of disfavoring dwarf-dominated ($s \geq 2.35$) SSPs, an issue that we will discuss more extensively in the next section.

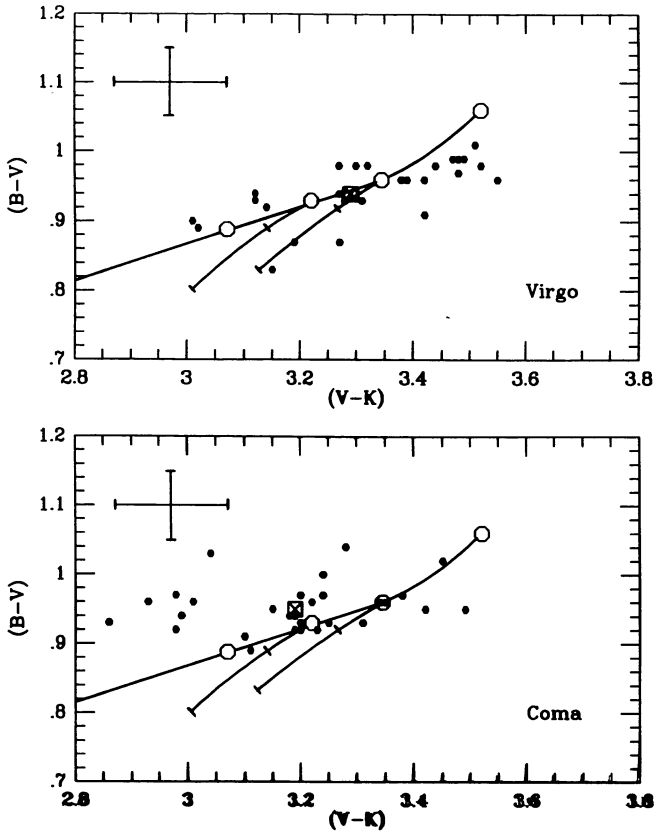


FIG. 16.—Same as in Fig. 13, but for *BVK* photometry of 28 ETGs in Virgo and 29 in Coma. $V-K$ is from Recillas-Cruz et al. (1990, 1991) and $B-V$ from Davies et al. (1987).

An effective test to investigate the age distribution among ETGs in clusters and in the field has been suggested by Bower et al. (1992b). In essence, it relies on the observed relationship between broadband colors or spectral indices and velocity dispersion ($\sigma_V$). This would thus allow us to account empirically for and remove any dependence of the index on metallicity, singling out only its dependence on age. The physical rationale in this case is that $\sigma_V$ is related to the mass of a galaxy and consequently to its metallicity through the following chain: higher $\sigma_V \rightarrow$ higher total mass $\rightarrow$ higher gravitational potential $\rightarrow$ higher efficiency in the metal enrichment via SN events $\rightarrow$ higher metallicity.

Therefore, one could assume that statistically any difference in color between galaxies with the same $\sigma_V$ should to be regarded as a difference in the absolute age of their stellar populations. On the basis of the small spread in the observed ($U-V$) versus $\sigma_V$ relationship, Bower et al. (1992b) concluded that a high degree of uniformity in star formation history should be envisaged for ETGs in Virgo and Coma. The authors therefore place the epoch of galaxy formation beyond $z_f \geq 2$, while later additions from more recent star formation should provide no more than 10% of the present luminosity of the galaxies.

A more refined extension of the Bower et al. (1992b) test to the field galaxies in the Davies et al. (1987) sample can be attempted by using the $Mg_2$ calibration of Buzzoni et al. (1992) instead of UV broadband colors. For the total sample of 455 ellipticals, Burstein et al. (1988b) derived the dependence of the index on $\sigma_V$ as

$$Mg_2 = 0.175 \log \sigma_V - 0.11 . \quad (4)$$

The residual distribution about the relations is displayed in Figure 17*c*. Its 1 $\sigma$ spread is 0.024 mag, and it is quite evidently skewed a little toward negative residuals. Burstein et al. (1988b) correctly pointed out that this would indicate the presence of a significant spread in age among galaxies, as the standard deviation exceeded the observational 1 $\sigma$ error bar, estimated in $\pm 0.016$ mag.

We tried a simple experiment by degrading an exponential residual distribution like that in Figure 17*a* with the quoted Gaussian error distribution. The result of the convolution is shown in Figure 17*b*. It is fair to note that the residual distribution obtained closely reproduces the observed one (both having $\sigma = 0.024$ mag and the same degree of skewness). Calibrating the scale of the $Mg_2$ residuals in terms of age difference via equation (8) in Buzzoni et al. (1992), we find that a rate of galaxy formation can be inferred for ETGs in the field such that the number $\phi_t$ of ETGs with current age $t_{gal}$ is

$$\phi_t \propto t_{gal}^{2.5} . \quad (5)$$

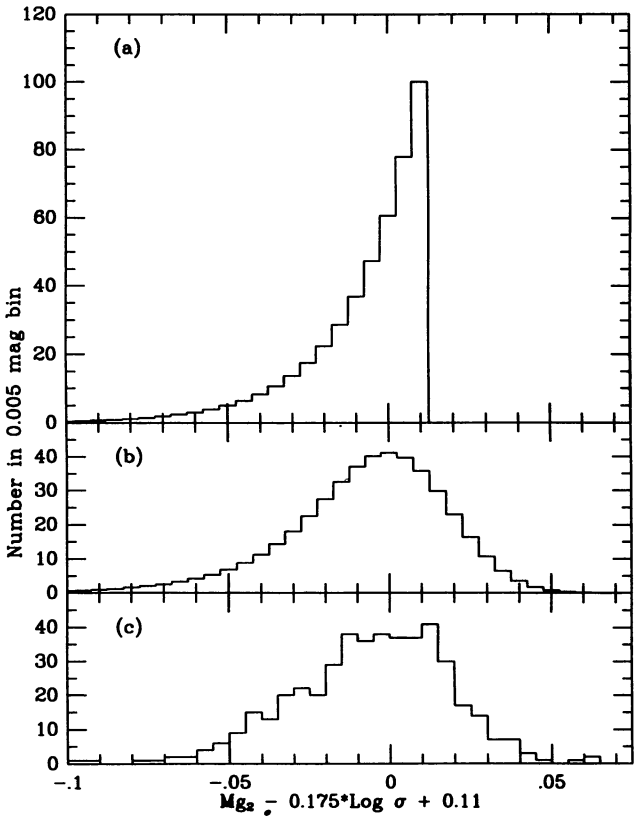


FIG. 17.—(*a*) Assumed real distribution of the residuals following an exponential law. This theoretical distribution is convolved with the Gaussian error in Burstein's et al. (1988b) observations ($\sigma(Mg_2) = 0.016$ mag) obtaining the histogram in (*b*). It is remarkable to note a distribution substantially similar to the observed one. See text for discussion. (*c*) Histogram of $Mg_2$ residuals for the Burstein et al. (1988b) sample of 455 ETGs.

Assuming 15 Gyr for the current age of the *oldest* ellipticals, this means that the *mean* age of the ETGs in the field is 11.5 Gyr. Three galaxies out of four are expected to be older than 10 Gyr, while only 2% should be younger than 5 Gyr. In terms of redshift of formation, we find that just one elliptical galaxy out of 50 is expected to form at $z_f \leq 0.4$ in an $H_0 = 50$ km $s^{-1}$ $Mpc^{-1}$ universe. Clearly, this point does not support any relevant contribution of star-forming ellipticals to the Butcher-Oemler effect (Butcher & Oemler 1978) in the clusters at intermediate distance.

A similar approach can be applied to a sample of 26 ETGs in the Virgo Cluster with available $Mg_2$ index and $\sigma_V$ from Faber et al. (1989). The residual distribution is displayed in Figure 18. The mean residual is $+0.003 \pm 0.022$ mag (1 $\sigma$ standard deviation), while the original data have $\langle Mg_2 \rangle = 0.277 \pm 0.047$, in good agreement with the mean value found in Buzzoni et al. (1992), showing no significant difference in metallicity between field and cluster galaxies.

The intrinsic spread in the $Mg_2$ residual distribution, once we take into account the observational error bar, is only 0.015 mag, which with our adopted age calibration translates into a $\pm 20\%$ spread in the current age. If we assume ETGs to be 15 Gyr old, this means that we derive only a $\pm 3$ Gyr dispersion for ETGs in Virgo.

In conclusion, a difference in formation histories could be invoked for ETGs in the field and in clusters. Although we can single out a bulk older than 10 Gyr for field ellipticals, they display a spread in age larger with respect to cluster members, the latter being essentially coeval objects formed earlier than $z_f > 3$. Our results fully support Yoshii & Takahara's (1988) work that suggests $z_f > 5$ for elliptical galaxies, while it would hardly match Wyse's (1985) claim of a much more recent redshift of formation ($z_f < 3$). Moreover, our results further strengthen the use of ETGs in distant clusters as reliable standard candles for cosmological tests (Buzzoni et al. 1993).

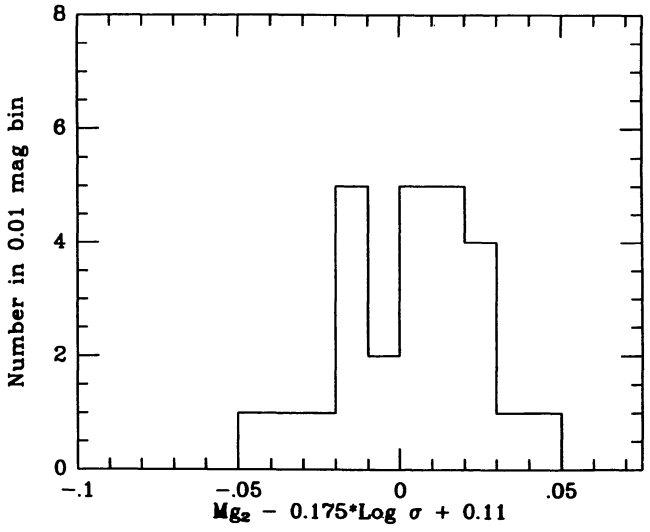


FIG. 18.—Distribution of $Mg_2$ residuals for a sample of 26 ETGs from Faber et al. (1989) belonging to the Virgo cluster. Galaxies seem coeval, with only a 20% spread in age. See text for discussion.

## 5. THE IMF

A second important point concerning ETGs that deserves to be investigated deals with the determination of the IMF of their stellar populations. In other words, it could be relevant to establish whether star formation in elliptical galaxies proceeded by more likely producing giant stars (i.e., flat IMF) or low-mass dwarfs (steep IMF).

It is a well-recognized feature that a power law with fixed exponent, such as $\phi(M) \propto M^{-s}$, is a useful although probably oversimplified assumption for describing the IMF. More accurate determinations of the IMF in the solar neighborhood indicate that more complex behavior might be expected, requiring the power-law index to be a function of the different mass ranges of stars (Scalo 1986; Rana 1987; Ferrini 1991). Moreover, there might be observational signs (Rana 1987), also supported by the theory (Ferrini, Palla, & Penco 1990), for bi- or multimodality of the IMF in the Galaxy.

Nevertheless, it is clear that what really plays a role in inducing the photometric features of ETGs is only the fraction of bright stars, that is, the low-mass stellar component with $M \leq 1\ M_\odot$; an extension of the IMF that includes massive (yet dead) stars enters rather into the computation of the $M/L$ ratio of a galaxy.

What we might hope to constrain from observations is, therefore, the slope of the IMF in the narrow range of mass between $0.1 \leq M \leq 1.0$. From the observational point of view, an optimized approach to the problem would likely involve selected spectral indices, possibly maximizing the sensitivity to stellar gravity. In addition, we would prefer infrared indices that better respond to the cooler component in a stellar population, that is, to bright AGB stars and faint low-MS dwarfs. This would maximize the range in stellar mass within the population. One more advantage in using narrowband indices is that they are reddening free, thus relaxing any critical correction of the observations in this sense.

As we discussed in § 2.2, the two CO and $H_2O$ indices are, in principle, ideal tools to investigate the IMF in ETGs (Tinsley & Gunn 1976), as they work so selectively on dwarf and giant stars. In Figure 19 we compare the database of 50 elliptical galaxies with measured CO from Frogel et al. (1978) and/or $H_2O$ from Aaronson et al. (1978) with theoretical sequences of models for 15 Gyr SSPs with IMF power-law index in the range $1.35 \leq s \leq 3.35$ (recall that the Salpeter value is here $s = 2.35$). It is fair to note that a Salpeter IMF is fully able to match the data, and in particular a steeper index (i.e., a dwarf-dominated SSP) is strongly disfavored.

In order to test how confidently we can support our conclusions, we show in Figure 20 an explanatory plot giving, in addition to the direct dependence of the indices on the IMF, also their expected variations versus selective changes in age, metallicity, and stellar mass loss. One can see that while mass loss has no effect in constraining the IMF from the models, it is confirmed that a younger age would strongly worsen the match to the data, requiring a much steeper IMF (and then inducing an unrecoverable discrepancy in other parameters, such as the $Mg_2$ index or $V - K$).

A comparison of the data versus the $Mg_2$ index is provided in the two panels of Figure 21, showing that CO is a better

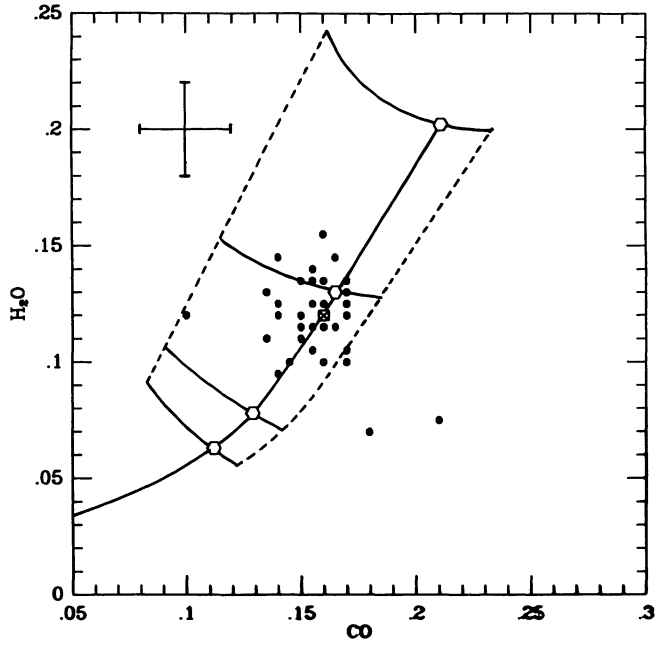


FIG. 19.—Galaxy distribution in the CO vs. $H_2O$ plane. Data are for 50 ETGs from Frogel et al. (1978) and Aaronson et al. (1978). The crossed square marks the barycenter of the population, while typical error bars in the observations are reported at top left.

Open dots are the sequence of 15 Gyr Salpeter SSPs with increasing metallicity ([Fe/H] = −0.25, 0, +0.22, and +0.87 in the sense of increasing indices). Also displayed is the change expected a change in the IMF. Upper and lower dashed lines are the envelope for $s$ = 3.35 and 1.35, respectively.

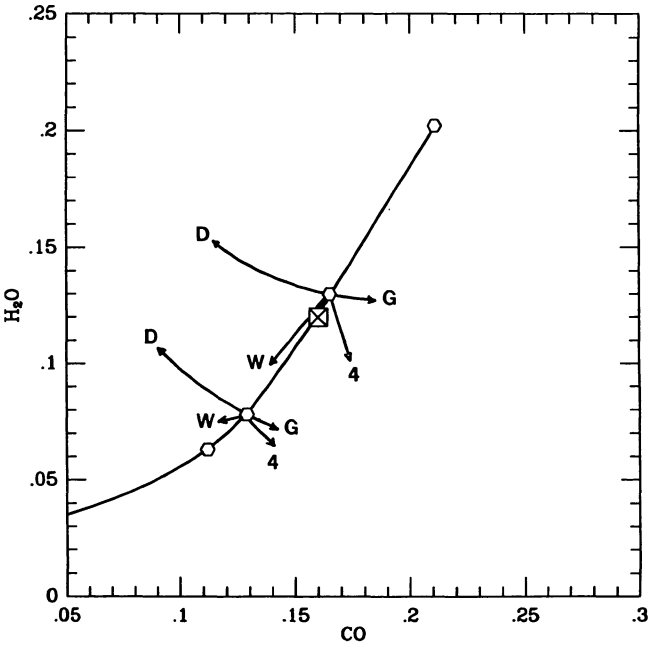


FIG. 20.—Same as in Fig. 18, but exploring the index dependence on the IMF (label "D" is for dwarf-dominated models with $s$ = 3.35, while label "G" is for giant-dominated SSPs with $s$ = 1.35), age (label "4" is the change from 15 Gyr to 4 Gyr), and mass loss (label "W" indicates the change from increasing the mass-loss parameter $\eta$ from 0.3 to 0.5). The crossed square marks the mean value observed for ETGs.

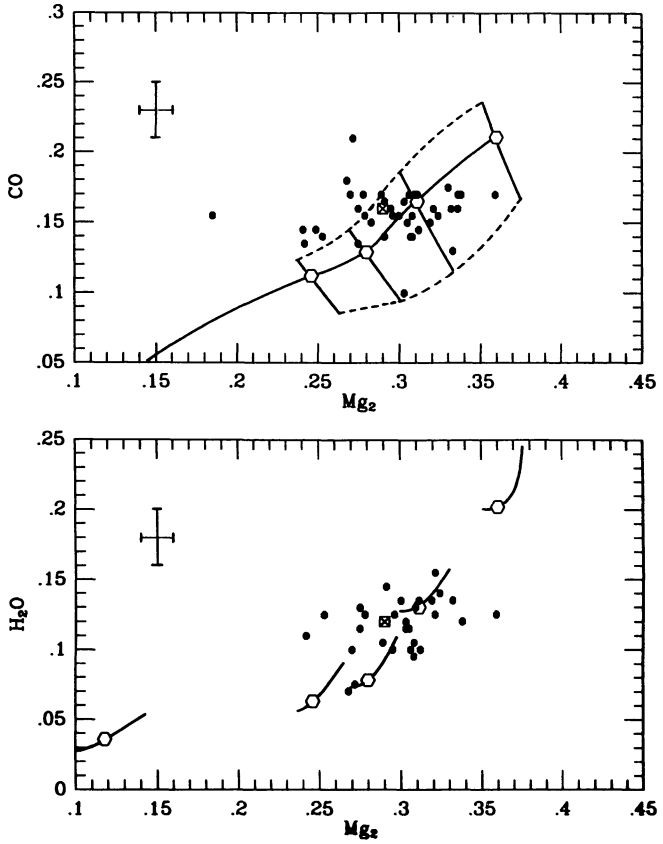


FIG. 21.—Galaxy distribution in the CO and $H_2O$ vs. $Mg_2$ planes. Data are for 38 ETGs with CO from Frogel et al. (1978) and 29 galaxies with $H_2O$ from Aaronson et al. (1978). In both panels $Mg_2$ is from Faber et al. (1989). The crossed square marks the barycenter of the population, while typical error bars in the observations are reported at top left.

Open dots and lines have the same meaning as in Fig. 19 (but the $s$ = 3.35 and 1.35 envelopes are, respectively, the lower and upper dashed lines). Due to the rather complex dependence of $H_2O$ on the distinctive parameters of the models in the lower panel, we avoid tracing any line envelope, only reporting for each metallicity the sequence resulting from changing the IMF index (in the sense of increasing $Mg_2$ with increasing $s$).

tracer of the IMF, while $H_2O$ displays a less univocal trend due to its composite dependence on both giant and dwarf stars (cf. Fig. 9).

We believe that the emerging consistency of our results with a power-law IMF à la Salpeter or with a slightly flatter power index is an important point in spite of whether the Salpeter law might yet be regarded as an unfashionable representation of the real data. On the other hand, more recent studies such as that of Rana (1987) also indicate a local power index in the range $1.5 \leq s \leq 2.2$ for stars of $\sim$0.5–1 $M_\odot$, while in the same range of mass Ferrini (1991) and Scalo (1986) find $s \sim 1.3$.

### 5.1. *The M/L Ratio*

The slope of the IMF has a direct impact on the $M/L$ ratio of a galaxy, as it defines a sort of efficiency in the way the overall integrated luminosity is contributed by stars of different mass. As is well known, more light can be derived per gram of matter

in massive stars ($M_*/L_* \sim M_*^{-2.5}$ in bolometric for stars in the MS), so that a stellar population with a flatter IMF has higher intrinsic luminosity per unit total mass, that is, a lower $M/L$ ratio.

The total luminosity of coeval SSPs with fixed IMF is expected to change with [Fe/H], depending on the wavelength of observation. As metal-poor isochrones have a brighter and bluer TO, when considering, for example, $M/L_B$ we find that it decreases with decreasing metallicity. The effect is quantified in Figure 22 for 15 Gyr SSPs with Salpeter IMF. One can see that stellar populations like those in the globular clusters (say at [Fe/H] $\sim -1.5$) are $\sim 1$ mag brighter per unit total mass than those more metal rich in ETGs. Of course, this difference is much reduced in the IR (we find $\sim 0.2$ mag in $K$ band from the models of Paper I), as metal-rich SSPs become brighter, and $M/L_K$ is nearly constant with changing [Fe/H].

The dependence of the luminosity of an SSP on the slope of the IMF is explored in Figure 23 for a 15 Gyr SSP with solar metallicity. We have a bimodal trend due to a complementary action of high- and low-mass stars. For low values of $s$, that is, for a flatter IMF, we find that a lot of mass is locked into dead stars of mass higher than the TO mass. For opposite reasons, a steeper IMF ($s \geq 2.35$) produces a huge number of unevolved dwarf stars. In both these extreme cases, most of the total mass of the population is locked into faint/dark stars that negligibly contribute to the total luminosity. This leads to a similar result with lower luminosity per unit total mass, that is, a higher $M/L$ ratio.

It is curious to see from Figure 23 that an SSP reaches maximum luminosity (the minimum $M/L$ ratio) at fixed total mass for an IMF about the Salpeter slope. This can be easily understood by the following plain analytical argument, which recalls the one originally stated by Tinsley (1973). Considering an IMF in the canonical form

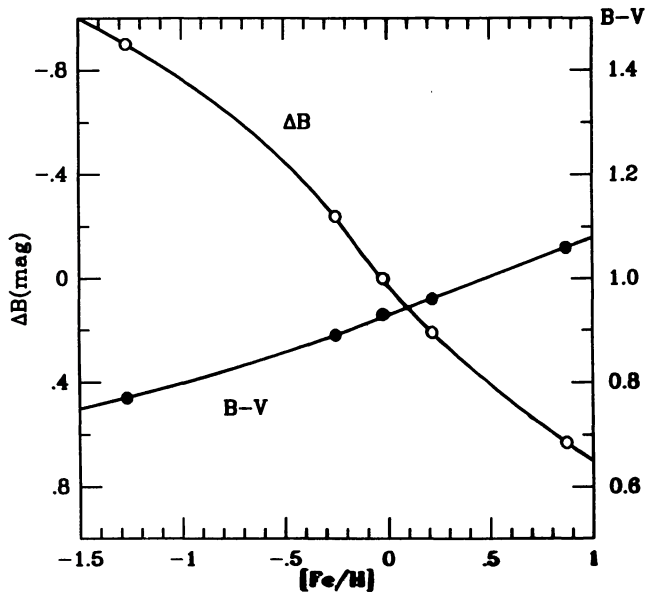


FIG. 22.—$B$-luminosity of a 15 Gyr Salpeter SSP for fixed total mass and changing metallicity. Magnitude differences $\Delta B$ (*left-hand scale*) are with respect to the reference model at [Fe/H] = 0. Also the color $B - V$ of the population is reported (*right-hand scale*).

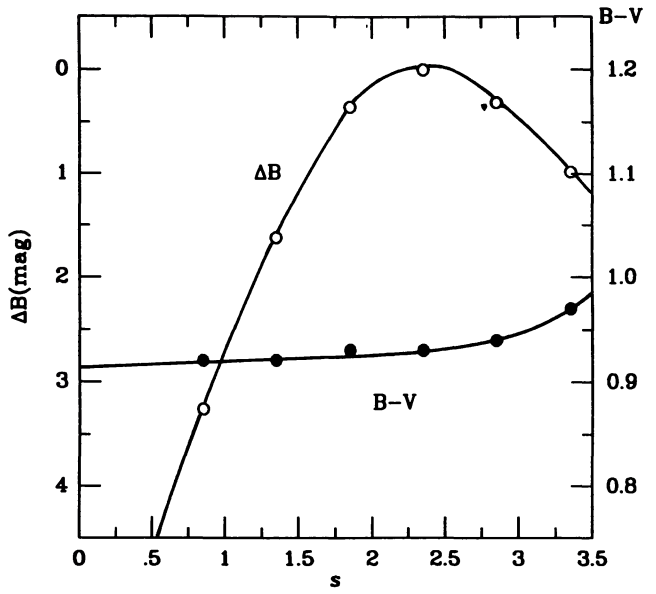


FIG. 23.—$B$-luminosity of a 15 Gyr SSPs ([Fe/H] = 0) for fixed total mass and changing IMF parameter $s$ (*left-hand scale*). The maximum luminosity (i.e., the minimum $M/L$ ratio) is for $s$ about the Salpeter value $s = 2.35$. Also reported is the $B - V$ of the population (*right-hand scale*).

$$\phi(M) = AM^{-s}, \tag{6}$$

$A$ being a normalization constant, the total mass of an SSP (for $s \neq 2$) is

$$M_{\rm TOT} = \frac{A}{2-s}[M^{2-s}]_{M_l}^{M_u}. \tag{7}$$

Assuming for the sake of simplicity a common power-law dependence of the stellar mass and luminosity, such as $L_* = M_*^{3.5}$, one has that the total luminosity of an SSP (for $s \neq 4.5$) is

$$L_{\rm TOT} = \frac{A}{4.5-s}[M^{4.5-s}]_{M_l}^{M_{\rm TO}}. \tag{8}$$

Restricting to the relevant range $2 < s < 4$ for the IMF, we have that $M_{\rm TOT}$ is mainly modulated by the lower limit of integration $M_l$, while $L_{\rm TOT}$ mainly depends on the TO mass ($M_{\rm TO}$). Therefore, to a first approximation, the $M/L$ ratio in solar units can be written in as

$$M/L \simeq \frac{4.5-s}{s-2}\left(\frac{M_l}{M_{\rm TO}}\right)^{2-s}\frac{1}{(M_{\rm TO})^{2.5}} \simeq \frac{4.5-s}{s-2}10^{s-2}, \tag{9}$$

where the last right-hand term assumes $M_{\rm TO} \sim 10\,M_l \sim 1\,M_\odot$. By deriving equation (9) with respect to $s$, it is immediate to obtain that the minimum of the function is for $s \sim 2.5$, the exact value weakly depending on the mass-luminosity relation assumed for stars and on the lower mass $M_l$.

A comparison of the theoretical expectations with the current estimates of $M/L$ for ETGs can be made by means of the three panels of Figure 24. Here we report a compilation for a

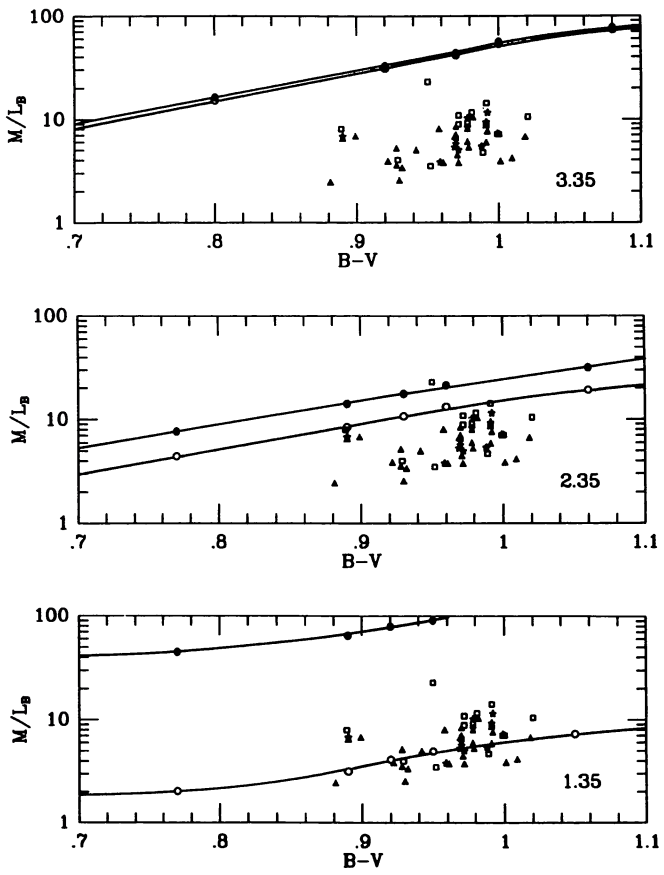


FIG. 24.—Mass-to-light distribution of ETGs vs. $B - V$. Data are for a total of 63 galaxies from Faber & Jackson (1976; *stars*), Schechter (1980; *squares*), and Michard (1980; *triangles*) and assume that $H_0 = 50$ km s$^{-1}$ Mpc$^{-1}$.

A comparison with models by changing the IMF index $s$ from 3.35 to 1.35 is performed in the three panels. Open dots in each panel are the sequence of $M/L$ ratios with increasing metallicity by accounting *only for the luminous mass* (i.e., summing up only the stars from MS to AGB), while filled dots are for the total mass integrating the IMF up to 100 $M_\odot$. The former estimate is a conservative lower limit for $M/L$, while the latter is an upper limit. Data seem to better fit a flat IMF.

total of 63 ellipticals, taken from the work of Faber & Jackson (1976), and from Schechter (1980) and Michard (1980). All the data in the figure are given for a Hubble constant $H_0 = 50$ km s$^{-1}$ Mpc$^{-1}$, while the source for $B - V$ is Faber et al. (1989).

A strip is defined by model sequences in each panel with increasing metallicity (i.e., increasing $B - V$), with a lower envelope given by the $M_{\rm lum}/L$ ratio of the luminous matter alone, and an upper envelope that accounts for the IMF integrated over the whole range in mass up to 100 $M_\odot$. While $M_{\rm lum}/L$ is a safe lower limit for the true ratio (apart from the uncertainty related to the assumed lower cutoff in the stellar mass of the IMF), the upper envelope of the strip might largely overestimate the real value, given the empirical IMF in the solar neighborhood which seems to indicate a very prominent relative "deficiency" of massive stars ($M \geq 2\ M_\odot$) with a steeper slope ($s \geq 3$) in this range (van Buren 1983; Scalo 1986). Two main points from Figure 24 are worthy of attention.

1. Even accounting for the uncertainty affecting the exact knowledge of the low-mass cutoff of the IMF (which we have assumed to be 0.1 $M_\odot$), observations definitely rule out a steep IMF with a large contribution in mass from dwarf stars (the logarithmic mean for the whole set of galaxies is $M/L_B = 6.3^{+3.5}_{-2.2}$). This is not a new issue but confirms on more solid quantitative bases a hint originally figured out by, among others, Tinsley (1978).

2. According to Michard (1980), a trend with color can be derived for observations of the different sources, with a slope of $M/L_B$ versus $B - V$ that is in agreement with the model expectations considering a pure dependence of $M/L$ on metallicity. A fit to the data gives

$$\log (M/L_B) = 1.4 \pm 0.3(B - V) - 0.49 \pm 0.01 + \log (H_0/50) \quad (10)$$

(error bar at 1 $\sigma$ level) for the Faber & Jackson (1976) sample,

$$\log (M/L_B) = 1.1 \pm 0.2(B - V) - 0.18 \pm 0.01 + \log (H_0/50) \quad (11)$$

for Schechter (1980), and

$$\log (M/L_B) = 1.9 \pm 0.2(B - V) - 1.11 \pm 0.01 + \log (H_0/50) \quad (12)$$

for Michard (1980). A fit to the whole sample (53 galaxies with available color) gives

$$\log (M/L_B) = 2.0 \pm 0.1(B - V) - 1.108 \pm 0.005 + \log (H_0/50), \quad (13)$$

while models predict for $\partial \log (M/L_B)/\partial(B - V)$ a value of $1.81 \pm 0.05$ for $s = 1.35$, $2.15 \pm 0.05$ for $s = 2.35$, and $2.47 \pm 0.06$ for $s = 3.35$ (error bars at 2 $\sigma$ levels).

A dependence on color would translate into a dependence on the absolute luminosity of a galaxy if a color-magnitude relation, mainly driven by metallicity effects, is accounted for, as found, for example, by Visvanathan & Sandage (1978) for ETGs in clusters.

The empirical dependency of $M/L$ on $L$ is still a highly controversial question. The relationship originally suggested by Faber & Jackson (1976) in the form $M/L_B \propto L_B^{1/2}$ has not found general support, in the sense that different authors found a consistency of the power index with zero (Schechter & Gunn 1979; Leach 1979; Schechter 1980), while others maintain larger values, but less than the 0.5 of Faber & Jackson, ~0.3 (Michard 1980; Recillas-Cruz et al. 1991). We note that a higher value for the power index in the $(M/L)$-$L$ relation would imply a steeper slope in the color-magnitude relationship. As Visvanathan & Sandage (1978) find $B - V \propto 0.037 \log L_B$, this would hardly reconcile with a power index for the $(M/L_B)$-$L_B$ relation larger than 0.1.

### 5.2. *Spread in the IMF*

A relatively flat IMF for the stellar populations in ETGs could have important consequences for different problems

dealing, for instance, with the dynamical evolution of galaxies. For example, from a certain point of view, the lack of a dominant fraction of dwarf stars in the luminous body of a galaxy would also tend to decrease the role of low-mass stars as potentially relevant contributors to the dark halos detected in elliptical galaxies (Schweizer 1987 derives $M/L_B \sim 50 \pm 12[H_0/50]$ over scale lengths of 100 kpc for elliptical galaxies in binary systems). On the other hand, if evolution on conveniently short timescales can be envisaged, leading to a mass segregation for stars, then the relative lack of dwarfs in the core would, on the contrary, call for their massive presence in the outermost regions of galaxies.

In this regard, it is important to check whether the IMF seen at the present time is constant or rather displays any sign of evolution among ETGs depending on the overall dynamical parameters of the systems. A possible answer could reside in the well-recognized $L$-$\sigma$ relationship of Faber & Jackson (1976). Coeval galaxies with the same velocity dispersion should also have the same total mass, and for the reasons previously stated, it is reasonable to assume they also have the same metallicity. Therefore, one effective possibility to explain any difference in their absolute magnitudes exceeding the observational uncertainties might rest on a difference in their IMFs.

We performed a test on the Virgo and Coma galaxy sample of Bower et al. (1992b). The authors were able to verify Faber & Jackson's relation for the ETG population in both clusters, finding

$$V_T = -7.53 \log \sigma + 27.33 \quad (14)$$

for Virgo E+S0 galaxies, and

$$V_T = -8.35 \log \sigma + 32.83 \quad (15)$$

for Coma.

We computed the residual magnitude scatter about these relations by using the published photometry of Bower et al. (1992a). The results, restricting to the sample of galaxies with $\log \sigma \geq 2.0$ to avoid peculiar low surface brightness objects, are displayed in Figure 25. It is remarkable to see that in the relevant range no systematic drift is present for either the Virgo or Coma samples, and virtually all the points are contained in a strip of width $\Delta V \sim 2$ mag. With the help of Figure 23 (the expected trend in $V$ is very similar to that in $B$, as $B - V$ of the SSPs does not change sensibly with $s$) one can easily derive that the whole sample of galaxies displays a rather tuned IMF, with a spread in the power index that should be less than $\Delta s \leq 1$.

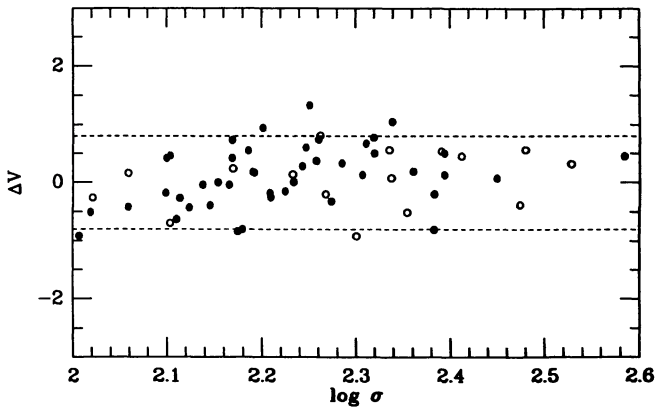


FIG. 25.—Magnitude residuals vs. velocity dispersion for 59 ETGs in Virgo (*open dots*) and Coma (*filled dots*). Data are from Bower et al. (1992a). The spread of the residuals is consistent with a spread of only ±1 in the IMF index $s$.

Of course, this cannot be regarded as conclusive evidence against the possibility that a mass segregation has occurred in the galaxies by stripping dwarf stars from the core or that a strong change in the IMF has to be expected in the very outer regions of a galaxy. Moreover, a population of dwarf stars has sometimes been suggested as a possible result of galaxy cooling flows (Cowie & Binney 1977). Quite amazingly, however, in the former case a mechanism would be invoked that to a large extent would not depend on the total mass of a galaxy (and therefore on its gravitational potential). In the latter case, it is hard to realize how a relevant component of dwarf stars (of mass comparable to the rest of the galaxy) could escape any detection, given its repercussion on the galactic colors.

## 6. STELLAR MASS LOSS AND INTERNAL REDDENING

It is a common feature that ETGs are gas-deficient systems. The main observational probe in this sense is a lack of strong emission lines in the spectra as well as no explicit evidence for H II regions or other extended gas structures in the bodies of the galaxies. On the other hand, there are yet increasing reasons to believe that this might be a somewhat simplified picture.

X-ray–emitting hot gas ($T \sim 10^7$ K) is certainly present, extending in dark halos around ellipticals (Forman et al. 1979; Trinchieri, Fabbiano, & Canizares 1986; Canizares, Fabbiano, & Trinchieri 1987). It is possible that the dark matter locked into this form is some 10%–100% of the luminous mass, extending much beyond the visible size of the galaxy. In addition, ETGs sometimes also show signs of the presence of a cold gas component, detectable with H I radio observations, with a typical size of $10^6$–$10^7$ $M_\odot$ or less (Sanders 1980).

To a large extent, both these components often seem dynamically decoupled from the luminous matter, participating in a different dynamical environment. This leads us to attribute their origin to external interactions, especially for cluster galaxies like the cDs, even if it might be reasonable that chemical enrichment in this matter occurred via a substantial contribution from galactic winds feeding mass from stars both via SN events and via quiescent stellar wind (Ciotti et al. 1991).

A full discussion of the mechanisms modulating the interaction between ETGs and the external environment is beyond the scope of this work (see, e.g., Volkov 1990 for a comprehensive review in this sense), and the impact on the photometric properties of ETGs is expected to be negligible. Rather, we are more interested here in considering quiescent stellar mass loss as providing an important (and possibly unique) source of the ISM in ETGs along the entire life of a galaxy. Moreover, chemically enriched matter is the basic ingredient of dust, and we know that dust is the basic ingredient of the ISM, causing reddening and able in principle to affect the SED of a galaxy.

A full treatment of the problem of the rate of mass return from stars to the ISM in ETGs has been given in Renzini & Buzzoni (1986), and it is worth recalling here only the relevant relation:

$$\dot{M}/L_{\rm TOT} = B\Delta M_* \sim 2\times 10^{-11}\Delta M_* \,(M_\odot\,{\rm yr}^{-1}\,{\rm L}_\odot^{-1})\,, \quad (16)$$

where $B$ is the specific evolutionary flux and $\Delta M_*$ is the mass lost by a star with $M = M_{\rm TO}$ along the post-MS phases. The equation states, for example, that for a $10^{11}\ L_\odot$ system we expect no more than 2 $M_\odot\ {\rm yr}^{-1}$ supplied to the ISM by stellar mass loss (as, obviously, $\Delta M_* \le M_{\rm TO} \sim 1\ M_\odot$).

With little arithmetic, from equation (16) it is immediate to derive the time dependence of the $M/L$ ratio of the ejecta in an SSP. Assuming for the total luminosity a power-law evolution, such as $L_{\rm TOT} \propto t^{-\alpha}$ (see next section), and considering to a first approximation that the right-hand term of equation (16) is roughly constant (because $B$ is a function weakly dependent on time and $\Delta M_*$ does not change by more than 50% in a wide range of stellar masses), we have that

$$M_{\rm ej}/L \propto t\,. \quad (17)$$

The most immediate consequence in this regard is that, if dust is related to the amount $M_{\rm ej}$ of chemically enriched matter in a galaxy, then we have to expect that *internal reddening in ETGs (as well as in most disk galaxies) should increase with time.* It is worth noting that this is opposite to what was suggested by Wang (1991a, b), with the obvious repercussions on the expected spectral properties of the primeval galaxies.

Stellar mass-loss efficiency plays a dual role when considering the photometric properties of galaxies. On one hand, it strongly constrains the IR emission of a stellar population by acting on the development of the RGB and AGB. On the other hand, it regulates the mass return to the ISM (and therefore, in principle, also the rate of production of dust) via $\Delta M_*$ in equation (16).

In the models of Paper I, mass loss has been accounted for via the tuning factor $\eta$ in the Reimers (1975) notation, where $\dot{M} \propto \eta LR/M$ (see Paper I for details). Owing to the fact that in Galactic globular clusters the AGB tip never seems to exceed in luminosity the RGB tip, Fusi Pecci & Renzini (1976) calibrated the Reimers formula by adopting $\eta = 0.4$ for low-metallicity stellar systems. A little revision is now necessary in this context, as Fusi Pecci & Renzini's calibration originally relied on the old Yale isochrones (Ciardullo & Demarque 1977), predicting too cool a temperature (i.e., too low a surface gravity) for the RGB + AGB and leading therefore to a higher mass-loss rate. In Figure 26 we present the new calibration of stellar mass loss for 15 Gyr SSPs resting on Vandenberg's isochrones and assuming an AGB tip equal to 0.5 and 1.0 bolometric magnitudes brighter than the RGB tip. One can see that, while $\eta \sim 0.3$–$0.4$ is still suitable for metal-rich SSPs, a larger value $\sim$0.5–0.7 is needed to match the observed mass-loss rate for globular clusters.

We know that, when increasing metallicity in the models, redder stellar populations are obtained. Figure 27 demonstrate how strictly this result mimics the effect of intervening (internal and/or external) reddening on the SED of a galaxy. In the figure we compared the color excess induced by reddening with the change in color induced in the models by a change in metallicity. Of course, the change in color with changing [Fe/H] cannot be regarded properly as a "color excess," but rather as the ratio

$$\frac{\Delta{\rm Color}}{\Delta(B-V)} = \frac{\partial{\rm Color}}{\partial[{\rm Fe/H}]}\,\frac{\partial[{\rm Fe/H}]}{\partial(B-V)}\,, \quad (18)$$

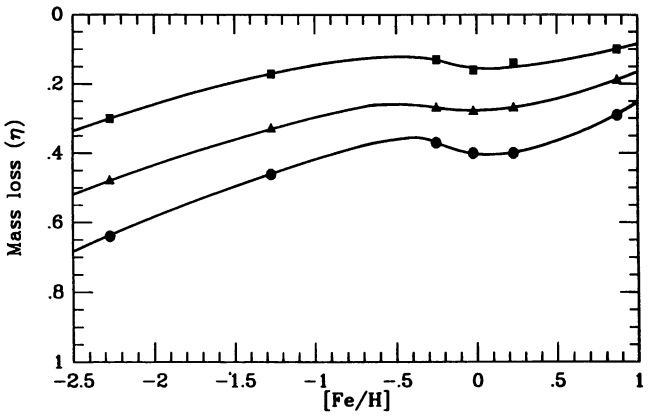


FIG. 26.—Calibration of the Reimers (1975) mass-loss parameter $\eta$ vs. metallicity. Displayed are the values required to locate the luminosity of the AGB tip at the same level as the RGB (*filled dots*), 0.5 mag brighter (*triangles*), or 1.0 mag brighter (*squares*).

where the partial derivatives can be taken, for example, from Table 1.

It is relevant to remark from the figure, however, that the [Fe/H]-induced color change in an SSP is almost equivalent to a reddening-induced color excess, such as

$$E(B-V) \sim 0.14\Delta[{\rm Fe/H}]\,, \quad (19)$$

the only relevant differences residing in the trend at the extreme wavelengths in the IR or in the UV. This means that, if reddening is not properly accounted for in correcting broadband photometry, we expect a consequent uncertainty in the metallicity calibration (Zinn 1980) which we estimate at $\sim$1 dex in $\sigma$[Fe/H] per 0.1 mag in $\sigma E(B-V)$. Fortunately, narrowband spectral indices are free from the effect, but nevertheless this is an instructive example of the way such uncertainties ramify, affecting the correct interpretation of the observations.

In Buzzoni et al. (1992) we were able to set an upper limit to the internal reddening in ETGs of $\sim E(B-V) \le 0.04$, which agrees with the observational evidence of a small amount ($10^3$–$10^6\ M_\odot$) of residual gas found in ETGs (Caldwell 1984; O'Connell 1976). From equation (19) this implies an uncertainty of $\le \pm 0.3$ dex in the inferred [Fe/H] from broadband photometry.

### 6.1. *Mass Loss and UV Excess in ETGs*

Another problem that might be strictly related to the treatment of the quiescent stellar mass loss is the UV excess detected shortward of 2500 Å in the spectra of some ETGs (Bertola, Capaccioli, & Oke 1982; Burstein et al. 1988a). A general effort has been made in recent years to consistently account for this effect in the theoretical framework of stellar evolution (Nørgaard-Nielsen & Kjægaard 1981; Renzini & Buzzoni 1986; Burstein et al. 1988a; Bertelli, Chiosi, & Bertola 1989; Brocato et al. 1990; Greggio & Renzini 1990). Among the different evolutionary scenarios envisaged to explain the UV emission, it has immediately become clear that a major role should be played by stars in the very late evolutionary stages dealing with the double-shell burning phase that sets in after the HB.

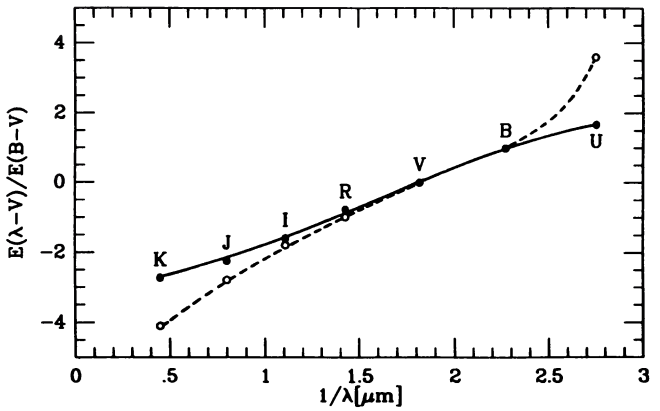


FIG. 27.—Solid line shows the color excess induced by reddening; dashed line is the color excess in terms of $\Delta\text{Color}/\Delta(B-V)$ for 15 Gyr SSPs with different metallicity with respect to a reference model at [Fe/H] = 0. One can see that the modulation in the SED of an SSP with increasing metallicity is nearly identical to the effect of increasing reddening. An equivalence such as $\Delta(B-V) = 0.14\Delta[\text{Fe/H}]$ can be derived. Except, in the extreme-UV or IR, the trends are different.

A more systematic exploration in the phase space of the models allowed us to refine the analysis in this sense, paying special attention to the problem of the energetics required for an SSP to supply the right amount of UV emission. In this framework, the original picture relying on the UV contribution from hot post-AGB stars (i.e., the nuclei of planetary nebulae) has been progressively replaced by the possibility, indicated by the new generation of stellar tracks, that under specific physical conditions the double-shell evolution might occur at high temperatures, totally or partially escaping the AGB phase (the so-called AGB-manqué stars of Greggio & Renzini 1990). Such a feature was first recognized in the models of Gingold (1976) but was then extensively explored by the Frascati group (Brocato et al. 1990; Castellani & Tornambè 1991; Castellani, Limongi, & Tornambè 1992) who demonstrated the full ability of these stars to reproduce the observed behavior of ellipticals in the UV range.

In short, the crucial condition required by models to allow stars to spend their double-shell burning phase at high temperatures is that they terminate the HB phase with $M \leq 0.54\ M_{\odot}$. Indeed, this condition can be marginally accounted for within the normal range of the relevant parameters by assuming a very efficient mass loss ($\eta \sim 1$ in our notation) and/or a supersolar metallicity ($Z \geq 2\ Z_{\odot}$) possibly coupled with an enhanced helium content (cf. Renzini 1993 for an enlighting discussion in this regard).

In order to preserve physical self-consistency however, the fuel consumption theorem requires that the fuel spent by an SSP to produce UV light via AGB-manqué stars must of course be diverted from the IR. Thus a positive correlation should be expected in this sense, and UV-bright ellipticals should at the same time be IR-deficient.

In Figure 28 we attempt a test in this by locating in the ($B-V$, $V-K$)-plane galaxies with the largest UV excess (1550 − $V$ color less than 3.0, from Burstein et al. 1988a). For comparison, model sequences with increasing mass loss are also reported, together with the extreme case of abruptly removing the whole post-HB evolution. Although UV-bright ellipticals are consistent with super–metal-rich stellar populations as correctly predicted by Castellani & Tornambè's (1991) models, one can see that a problem seems to arise with the AGB-manqué solution as UV galaxies still show too large an IR emission (i.e., too red a $V-K$) consistent with $0.3 < \eta < 0.5$. This is a sign supporting the possibility that stellar populations in ETGs still fully develop the early-AGB phase (cf. Iben & Renzini 1983 and Castellani et al. 1992 for its definition) climbing to a luminosity $\log (L/L_{\odot}) \sim 3.0$ decidedly higher than that postulated by Castellani & Tornambè's (1991) models. Incidentally, things get even worse if we consider a composite stellar population including a fraction of metal-poor stars.

The only way to reconcile the UV excess and the IR emission from AGB-manqué stars seems to require somehow ad hoc conditions with a full exploitation of the early-AGB phase and with the stellar envelope stripped by the superwind phase just before the onset of the thermal pulses (Iben & Renzini 1983). Although observational evidence supports a possible primary role of metallicity in triggering the UV-excess effect (colors of the UV-bright galaxies in Fig. 28 are consistent with $Z \sim 2\ Z_{\odot}$), it is clear that such critical constraints about mass loss do not strengthen the envisaged evolutionary scenario, and in our opinion the question remains to be more carefully examined.

## 7. COMPOSITE STELLAR POPULATIONS

Our standard picture adopted in the previous sections to describe the present-day evolutionary status of ETGs tacitly admits that SSPs are convenient approximations of the real stellar populations in the galaxies. Now, the validity of this assumption needs to be verified, as it is certain that a link does exist between early dynamical evolution and early chemical evolution in ETGs, leading to different evolutionary paths de-

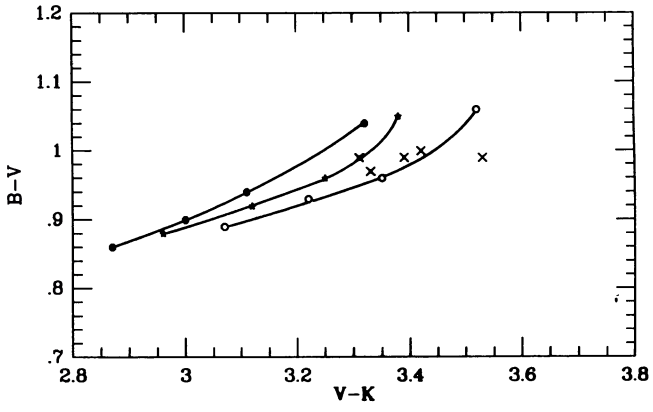


FIG. 28.—Location in the $B-V$ vs. $V-K$ diagram of ETGs with UV excess (*crosses*). The galaxies are all those classified as "quiescent" systems with the 1550 − V color less than 3.0 in the Burstein et al. (1988a) sample and with available $B-V$ photometry from Faber et al. (1989) and $V-K$ from Frogel et al. (1978), Persson et al. (1979), or Bower et al. (1992a). They are NGC 4889, NGC 4552, NGC 4649, NGC 1399, and NGC 1407 in the sense of increasing $V-K$.

For comparison the model sequences for 15 Gyr Salpeter SSPs are also displayed with mass-loss parameter $\eta = 0.3$ (*open dots*) and 0.5 (*stars*), and abruptly removing from the models the post-HB evolution (*filled dots*). Observations seem to indicate that a full development of the AGB in the galaxies is necessary to fit the IR colors. See text for discussion.

pending on the total mass involved in the primeval collapse (Arimoto 1988). In particular, chemical enrichment proceeded over short but finite timescales, inducing a spread in metallicity among quasi-coeval generations of stars.

As a result, in ETGs we should deal at present with a major bulk of metal-rich stars, but a metal-poor component *must* exist (the case of M32 is enlightening in this regard), its real weight depending on the primeval evolutionary features. There are signs that such a metal-poor component is a common ingredient in ETGs (Buzzoni 1993), and it is important therefore to study this question and quantify this component's contribution to the integrated SED.

The case of a composite stellar population (CSP) for ETGs has been approached by assuming three basic reference models with the same age (15 Gyr) and extreme values of metallicity. In the following we will refer therefore to a *P* model given by a metal-poor SSP with [Fe/H] = −2.27, an S model with solar metallicity, and an R model given by a super–metal-rich SSP with [Fe/H] = +0.87. All of the three reference templates have a Salpeter IMF ($s$ = 2.35), while mass loss has been tuned in order to preserve equality in the luminosity at the tips of the AGB and the RGB. This required $\eta$ = 0.3 for models S and R and $\eta$ = 0.7 for model P. The latter also assumes an HB of intermediate morphology (I-HB in the notation of Paper I) while a red clump (R-HB) has been assumed for models S and R. More details on the photometric properties of the S and R models can be found in Tables 5 and 7 (the R model is No. 1 in Table 7), respectively. The P model is summarized in Table 8.

Among the different CSPs that can be obtained by mixing the three templates, we searched for those combinations that matched the properties (UV, visual, and IR broadband colors, as well as spectral indices) of real ETGs according to the mean observed values reported in Table 5. In Figure 29 we show the family of solutions obtained for the photometric features. Plotted in the figure are the allowed combinations, in terms of percentage contribution to the total bolometric light of the CSP, of the P and S models able to reproduce a given color of spectral index (the R contribution is immediately derived as %P + %S + %R = 100%).

Indeed, one can see that the combined action of the CO and $H_2O$ indices with the rest of the colors can very effectively constrain the stellar mix and, in particular, the metal-poor stellar component. In fact, a general trend in the fitting curves shows that any increase in the P contribution would also require a parallel increase in the R model to be compensated (this, of course, to the detriment of the solar SSP). An optimum mix can be achieved by assuming a CSP with 5% bolometric contribution from the P model, while the remaining light is divided into $\sim\frac{2}{3}$ contributed by the S bulk (57% of the total) and $\frac{1}{3}$ by the R model (38% of the total). In this case, the luminosity-weighted mean metallicity of the mix would be $[Fe/H]_{bol} = +0.21$.

The resulting SED from such a mix is compared in Figure 30 with that of an SSP with [Fe/H] = +0.22 (it is model SS in Table 5; cf. also Paper I). The agreement is nearly perfect, and the models could hardly be distinguished except for their different behavior in the extreme-UV shortward of 2500 Å. A comparison with the observed mean colors and spectral indices for ETGs is done in Table 9A.

TABLE 8

METAL-POOR MODEL (P Model)

($Z$ = 0.0001; [Fe/H] = −2.27; $Y$ = 0.23; $s$ = 2.35; $\eta$ = 0.7; I-HB)

| Parameter | Value |
|---|---|
| Age (Gyr) | 15.0 |
| $M_{TO}$ | 0.79 |
| $M_{rt}$ | 0.59 |
| $M_{pn}$ | 0.48 |
| $B_{11}$ | 1.83 |
| Bol − $V$ | −0.34 |
| $U-V$ | 0.63 |
| $B-V$ | 0.60 |
| $V-R$ | 0.61 |
| $V-I$ | 1.07 |
| $V-J$ | 1.52 |
| $V-K$ | 2.13 |
| $Mg_2$ | 0.04 |
| Hβ | 3.04 |
| Fe52 | 0.35 |
| Fe53 | 0.20 |
| CO | 0.00 |
| $H_2O$ | 0.03 |
| %MS | 0.378 |
| %SGB | 0.089 |
| %RGB | 0.367 |
| %HB | 0.086 |
| %AGB | 0.074 |
| %PAGB | 0.007 |
| $M/L_{bol}$ | 2.40 |
| $M/L_b$ | 3.00 |
| $M/L_v$ | 3.08 |
| $M/L_k$ | 1.63 |

NOTE.—See notes to Table 7.

### 7.1. *A CSP for M32*

As anticipated in § 4, a discussion in terms of old CSPs with a large spread in metallicity might help in accounting for the nature of the observed spread in the stellar population of M32. It could be useful, therefore, to search for an optimized mix in terms of the P, S, and R reference models fitting the observed colors summarized in Table 9B. The results show that a bolometric fraction of metal-poor stars of ∼15% is allowed for M32, while the remaining fraction of light is roughly shared between the solar and supersolar stellar components. Assuming a mix such as (P, S, R) = (15%, 45%, 40%) (mean luminosity-weighted [Fe/H] = 0.0) we are fully able to reproduce the observations with the exception of only the $Mg_2$ index, which appears 0.04 ± 0.01 mag more enhanced in the synthetic model (Table 9B).

Note, on the other hand, from Table 9B that any tried mix including 4 Gyr metal-rich SSP (referred to as models S4 and R4 in the table, with [Fe/H] = 0.0 and +0.22, respectively) in addition to the P model would dramatically fail in reproducing both the Hβ index and the integrated $B-V$ (cf. Fig. 13 and Table 5 in Buzzoni 1989), and in addition would not allow any presence of metal-poor stars due to exceedingly blue colors of the young metal-rich SSPs.

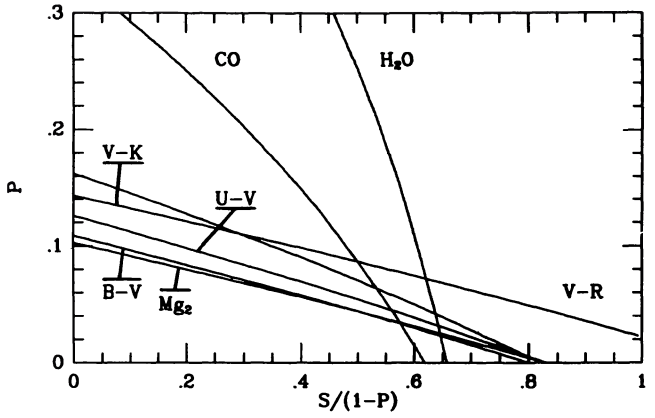


FIG. 29.—Allowed combinations of composite stellar populations reproducing mean observed colors and spectral indices for ETGs. A mix of three 15 Gyr Salpeter SSPs (P, S, and R models in the text) is considered, with [Fe/H] = −2.27, 0, and +0.87, respectively. Each curve in the plot is the locus of the allowed combination reproducing a given feature in terms of percent to bolometric light from the P and S models. Contribution from the R model derives from the condition %P + %S + %R = 100% in bolometric. The crossing between the curves for the IR indices and those for other broadband colors indicates that a mix such as (%P, %S, %R) = (5%, 57%, 38%) could be a good combination fitting the ETG stellar populations.

## 8. BACK-IN-TIME EVOLUTION

At the end of our analysis on the present evolutionary status of ETGs it becomes relevant to also track galaxy evolution back in time. Its relevance for cosmological tests is obvious. Indeed, by using distant galaxies as standard candles we cannot escape the problem of a reliable reconstruction of their intrinsic photometric properties at high redshift, that is, at earlier epochs.

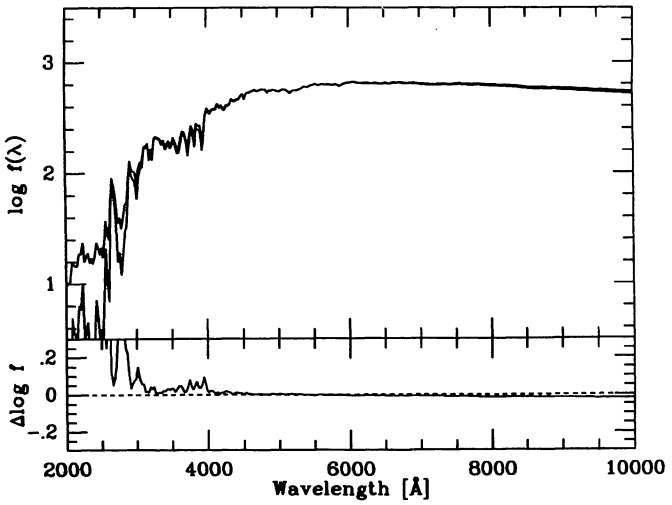


FIG. 30.—Comparison between SED of the SS model for SSP (cf. text and Table 5) and the fiducial composite stellar population for ETGs of Fig. 28. Plotted in the lower panel are the residuals vs. wavelength in the sense (CSP-SSP) normalized at $V$. It is evident that only shortward of 2500 Å there is an appreciable difference between the two models.

TABLE 9A

COMPOSITE STELLAR POPULATION OF ETGs

| (P, S, R) = (0.05, 0.57, 0.38) | | | |
|---|---|---|---|
| Parameter | Synthetic | Observed | Reference |
| [Fe/H][a] ..... | 0.22 | ... | |
| $U-V$ ..... | 1.45 | 1.47 ± 0.16 | 1 |
| $B-V$ ..... | 0.93 | 0.95 ± 0.06 | 1 |
| $V-R$ ..... | 0.89 | 0.88 ± 0.05 | 1 |
| $V-K$ ..... | 3.27 | 3.27 ± 0.16 | 1 |
| Hβ ..... | 1.69 | 1.60 ± 0.30 | 2 |
| $Mg_2$ ..... | 0.28 | 0.29 ± 0.04 | 3 |
| CO ..... | 0.16 | 0.16 ± 0.02 | 4 |
| $H_2O$ ..... | 0.12 | 0.11 ± 0.02 | 5 |

[a] Mean luminosity-weighted [Fe/H] from the bolometric partition.

REFERENCES.—(1) Persson et al. 1979; (2) Salsa 1993; (3) Davies et al. 1987; (4) Frogel et al. 1978; (5) Aaronson et al. 1978.

In view of the importance of ETGs in observational cosmology (Sandage & Hardy 1973; Lebofsky 1981; Lilly & Longair 1984; Yoshii & Takahara 1988), here we will just summarize some basic concepts, deferring to a future paper of this series a more systematic study of the spectral properties of the primeval galaxies.

### 8.1. *Luminosity Evolution*

Since an elliptical galaxy can be conveniently represented by an SSP of "effective" metallicity slightly higher than solar (hereafter we will adopt [Fe/H] = +0.22 as a reference value), it is immediate to reconstruct its luminosity evolution on the basis of the models of Paper I. Figure 31 shows that a fairly linear law exists in the ($\log l$, $\log t$)-plane. The general trend of the models is in the sense of increasing luminosity in the past. This is easily understood remembering that in a burst stellar population the number of luminous stars decreases with time (as bright massive stars die and are no longer replaced). The

TABLE 9B

CASE OF M32

| | Spread in | | |
|---|---|---|---|
| Parameter | Age[a] | Metallicity[b] | Observed |
| [Fe/H][c] ..... | +0.2 | 0.0 | |
| $A(B)$ ..... | | | 0.30[d] |
| $B-V$ ..... | 0.82 | 0.88 | 0.88 ± 0.03[e] |
| $V-K$ ..... | 3.11 | 3.16 | 3.14 ± 0.10[f] |
| Hβ ..... | 2.38 | 1.65–1.92[g] | 1.74 ± 0.05[h] |
| $Mg_2$ ..... | 0.21 | 0.24 | 0.20 ± 0.01[h] |
| CO ..... | 0.17 | 0.15 | 0.15 ± 0.02[f] |

[a] Bolometric partition (P, S, R) = 0.15, 0.45, 0.40).
[b] Bolometric partition (P, S4, R4) = (0.00, 0.20, 0.80).
[c] Mean luminosity-weighted [Fe/H] from the bolometric partition.
[d] Faber et al. 1989.
[e] Sharov & Lyutyi 1983.
[f] Frogel et al. 1978.
[g] Depending on HB morphology assumed for the P model.
[h] Hardy et al. 1994.

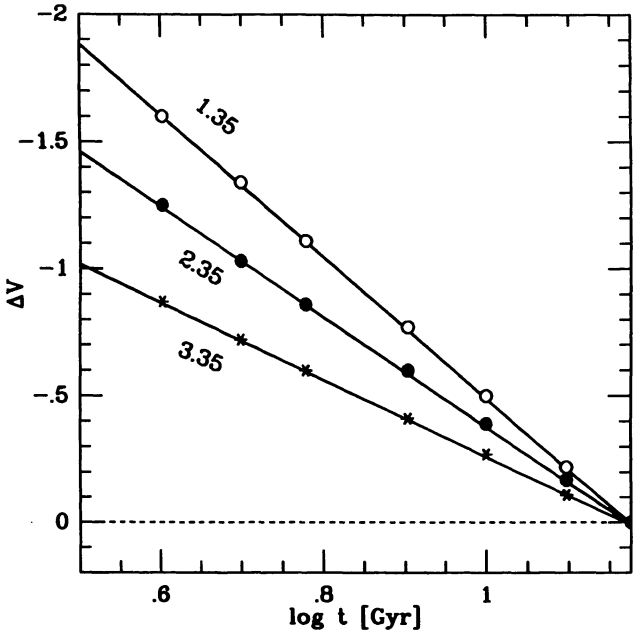


FIG. 31.—$V$-luminosity evolution for SSPs with different IMFs (each curve is labeled with the IMF index $s$). Model magnitudes are normalized at an age of 15 Gyr. A giant-dominated SSP with a flatter IMF displays stronger evolution. Magnitudes are intended in the galaxy rest frame.

twofold effect is therefore to reduce the luminous contributors and move the barycenter of the population to fainter magnitudes and redder colors (see Buzzoni 1993 for a quantitative evaluation in this sense).

The way luminosity changes with time strongly depends on the IMF. As a general trend we should expect that evolution is milder in dwarf-dominated SSPs. In fact, in steeper IMFs a higher fraction of the total light is supplied by unevolved dwarf stars in the lower MS, and it scarcely depends on the age of the SSP. The opposite holds of course for a giant-dominated population, as shown in Figure 31.

The rate of change in luminosity derived from the figure suggests that $M_V \propto -\alpha \ln t$, with $\alpha$ almost totally depending on the IMF slope (while it is very insensitive to metallicity). A fit to the models gives

$$\partial M_V / \partial \ln t = 1.30 - 0.27(s - 1), \tag{20}$$

which matches exactly Tinsley's former relation (Tinsley & Gunn 1976; Tinsley 1978).

The $L$-$t$ dependence can be explained by stellar population theory on the basis of these simple arguments. Let us suppose a mass-luminosity relation such as $L_* \propto M_*^{3.5}$ holds for MS stars ($L$ is intended in bolometric). Hence, a stellar lifetime $t_* \propto M_*/L_*$ implies $t_* \propto M_*^{-2.5}$.

The MS bolometric contribution can be written as

$$L_{\rm MS} \propto \int L_* M_*^{-s} dM_*, \tag{21}$$

where the integral is performed up to the TO stellar mass. For an age $t$ pertinent to $M_{\rm TO}$ we finally have

$$L_{\rm MS} \propto M_{\rm TO}^{4.5-s} \propto t^{0.4s-1.8}. \tag{22}$$

For a Salpeter IMF this leads to $L_{\rm MS} \propto t^{-0.86}$, in agreement with the power index of the more detailed models. A different treatment should be used for the post-MS contribution. In this case, from the fuel consumption theorem, and using the notation of Paper I, we have that

$$L_{\rm PMS} \propto \dot{M}_{\rm TO} M_{\rm TO}^{-s} \times \text{Fuel}. \tag{23}$$

The fuel spent by stars in post-MS phases does not strongly depend on mass (see Fig. 3 in Renzini & Buzzoni 1986), and to first degree we can regard it as a constant. We obtain therefore that the time dependence of the post-MS luminosity of an SSP is

$$L_{\rm PMS} \propto t^{0.4s-1.4}. \tag{23}$$

For a Salpeter IMF this gives $L_{\rm PMS} \propto t^{-0.46}$. We can therefore imagine the time evolution of the whole SSP following a power law as well, with an intermediate index depending on the relative weight of the post-MS/MS contributions.

It is interesting to note that this ratio becomes

$$\frac{L_{\rm PMS}}{L_{\rm MS}} \propto t^{0.4}, \tag{24}$$

meaning that the photometric relevance of the post-MS phases slowly increases with increasing time at a rate not directly depending on the IMF.

### 8.2. *k-Corrections and Color Evolution*

More useful for a direct match with observations of galaxies at cosmological distances is to compute the expected $k$-correc-

TABLE 10A

$(e + k)$-CORRECTIONS FOR $(H_0, q_0, z_f) = (50, 0, \infty)$

| $z$ | Age (Gyr) | $K(B)$ | $k(V)$ | $k(K)$ | $k(g)$ | $k(r)$ | $k(i)$ |
|---|---|---|---|---|---|---|---|
| 0.00 ..... | 19.54 | 0.00 | 0.00 | 0.00 | 0.00 | 0.00 | 0.00 |
| 0.05 ..... | 18.61 | 0.16 | 0.03 | −0.12 | 0.04 | −0.01 | −0.02 |
| 0.10 ..... | 17.76 | 0.34 | 0.06 | −0.21 | 0.10 | −0.01 | −0.03 |
| 0.15 ..... | 16.99 | 0.51 | 0.11 | −0.30 | 0.19 | 0.01 | −0.04 |
| 0.20 ..... | 16.28 | 0.66 | 0.19 | −0.39 | 0.31 | 0.04 | −0.05 |
| 0.25 ..... | 15.62 | 0.78 | 0.29 | −0.46 | 0.47 | 0.08 | −0.04 |
| 0.30 ..... | 15.02 | 0.91 | 0.44 | −0.52 | 0.65 | 0.10 | −0.03 |
| 0.35 ..... | 14.47 | 1.05 | 0.61 | −0.58 | 0.83 | 0.13 | −0.01 |
| 0.40 ..... | 13.95 | 1.23 | 0.79 | −0.63 | 0.98 | 0.17 | 0.02 |
| 0.45 ..... | 13.47 | 1.41 | 0.94 | −0.67 | 1.09 | 0.23 | 0.06 |
| 0.50 ..... | 13.02 | 1.62 | 1.05 | −0.70 | 1.16 | 0.30 | 0.09 |
| 0.55 ..... | 12.59 | 1.88 | 1.13 | −0.73 | 1.25 | 0.39 | 0.11 |
| 0.60 ..... | 12.20 | 2.17 | 1.19 | −0.75 | 1.35 | 0.52 | 0.14 |
| 0.65 ..... | 11.83 | 2.49 | 1.27 | −0.77 | 1.49 | 0.65 | 0.19 |
| 0.70 ..... | 11.48 | 2.83 | 1.38 | −0.80 | 1.68 | 0.79 | 0.24 |
| 0.75 ..... | 11.15 | 3.15 | 1.52 | −0.81 | 1.89 | 0.93 | 0.30 |
| 0.80 ..... | 10.84 | 3.46 | 1.71 | −0.83 | 2.14 | 1.05 | 0.38 |
| 0.85 ..... | 10.55 | 3.75 | 1.92 | −0.85 | 2.39 | 1.14 | 0.48 |
| 0.90 ..... | 10.27 | 4.03 | 2.13 | −0.87 | 2.64 | 1.19 | 0.60 |
| 0.95 ..... | 10.01 | 4.30 | 2.35 | −0.89 | 2.92 | 1.24 | 0.72 |
| 1.00 ..... | 9.75 | 4.56 | 2.58 | −0.91 | 3.19 | 1.28 | 0.83 |

TABLE 10B

$(e + k)$-CORRECTIONS FOR $(H_0, q_0, z_f) = (50, 0, 3)$

| $z$ | Age (Gyr) | $K(B)$ | $k(V)$ | $k(K)$ | $k(g)$ | $k(r)$ | $k(i)$ |
|---|---|---|---|---|---|---|---|
| 0.00 ..... | 14.68 | 0.00 | 0.00 | 0.00 | 0.00 | 0.00 | 0.00 |
| 0.05 ..... | 13.74 | 0.15 | 0.02 | −0.12 | 0.03 | −0.01 | −0.02 |
| 0.10 ..... | 12.90 | 0.32 | 0.04 | −0.21 | 0.08 | −0.02 | −0.04 |
| 0.15 ..... | 12.12 | 0.48 | 0.08 | −0.31 | 0.16 | −0.01 | −0.06 |
| 0.20 ..... | 11.41 | 0.60 | 0.15 | −0.40 | 0.27 | 0.01 | −0.07 |
| 0.25 ..... | 10.76 | 0.70 | 0.24 | −0.48 | 0.41 | 0.04 | −0.08 |
| 0.30 ..... | 10.16 | 0.82 | 0.37 | −0.55 | 0.57 | 0.05 | −0.07 |
| 0.35 ..... | 9.60 | 0.92 | 0.51 | −0.62 | 0.72 | 0.06 | −0.07 |
| 0.40 ..... | 9.08 | 1.06 | 0.65 | −0.69 | 0.83 | 0.07 | −0.06 |
| 0.45 ..... | 8.60 | 1.21 | 0.76 | −0.74 | 0.90 | 0.10 | −0.05 |
| 0.50 ..... | 8.15 | 1.38 | 0.84 | −0.79 | 0.95 | 0.15 | −0.05 |
| 0.55 ..... | 7.73 | 1.59 | 0.88 | −0.83 | 1.00 | 0.20 | −0.05 |
| 0.60 ..... | 7.34 | 1.83 | 0.91 | −0.88 | 1.07 | 0.29 | −0.05 |
| 0.65 ..... | 6.97 | 2.09 | 0.96 | −0.92 | 1.17 | 0.39 | −0.04 |
| 0.70 ..... | 6.62 | 2.37 | 1.03 | −0.96 | 1.31 | 0.49 | −0.01 |
| 0.75 ..... | 6.29 | 2.62 | 1.13 | −0.99 | 1.48 | 0.59 | 0.02 |
| 0.80 ..... | 5.98 | 2.84 | 1.28 | −1.03 | 1.68 | 0.68 | 0.07 |
| 0.85 ..... | 5.68 | 3.00 | 1.43 | −1.08 | 1.86 | 0.72 | 0.13 |
| 0.90 ..... | 5.41 | 3.16 | 1.58 | −1.12 | 2.06 | 0.74 | 0.20 |
| 0.95 ..... | 5.14 | 3.31 | 1.75 | −1.16 | 2.28 | 0.76 | 0.27 |
| 1.00 ..... | 4.89 | 3.46 | 1.94 | −1.21 | 2.50 | 0.77 | 0.34 |

TABLE 10D

$(e + k)$-CORRECTIONS FOR $(H_0, q_0, z_f) = (50, 0.5, 3)$

| $z$ | Age (Gyr) | $K(B)$ | $k(V)$ | $k(K)$ | $k(g)$ | $k(r)$ | $k(i)$ |
|---|---|---|---|---|---|---|---|
| 0.00 ..... | 11.42 | 0.00 | 0.00 | 0.00 | 0.00 | 0.00 | 0.00 |
| 0.05 ..... | 10.49 | 0.13 | 0.01 | −0.12 | 0.02 | −0.02 | −0.03 |
| 0.10 ..... | 9.68 | 0.28 | 0.01 | −0.23 | 0.05 | −0.04 | −0.07 |
| 0.15 ..... | 8.95 | 0.40 | 0.03 | −0.35 | 0.10 | −0.06 | −0.10 |
| 0.20 ..... | 8.29 | 0.49 | 0.07 | −0.45 | 0.18 | −0.05 | −0.13 |
| 0.25 ..... | 7.70 | 0.57 | 0.13 | −0.54 | 0.29 | −0.05 | −0.16 |
| 0.30 ..... | 7.17 | 0.64 | 0.22 | −0.64 | 0.41 | −0.06 | −0.18 |
| 0.35 ..... | 6.69 | 0.72 | 0.34 | −0.72 | 0.53 | −0.08 | −0.20 |
| 0.40 ..... | 6.25 | 0.85 | 0.46 | −0.79 | 0.63 | −0.07 | −0.20 |
| 0.45 ..... | 5.84 | 0.99 | 0.56 | −0.85 | 0.69 | −0.06 | −0.20 |
| 0.50 ..... | 5.47 | 1.12 | 0.61 | −0.92 | 0.72 | −0.04 | −0.22 |
| 0.55 ..... | 5.13 | 1.31 | 0.64 | −0.98 | 0.76 | 0.00 | −0.23 |
| 0.60 ..... | 4.82 | 1.54 | 0.67 | −1.03 | 0.81 | 0.08 | −0.24 |
| 0.65 ..... | 4.52 | 1.78 | 0.71 | −1.08 | 0.91 | 0.15 | −0.24 |
| 0.70 ..... | 4.26 | 2.04 | 0.77 | −1.12 | 1.03 | 0.24 | −0.23 |
| 0.75 ..... | 4.00 | 2.26 | 0.86 | −1.16 | 1.19 | 0.33 | −0.20 |
| 0.80 ..... | 3.77 | 2.45 | 1.00 | −1.21 | 1.38 | 0.41 | −0.17 |
| 0.85 ..... | 3.55 | 2.61 | 1.16 | −1.24 | 1.57 | 0.47 | −0.10 |
| 0.90 ..... | 3.35 | 2.76 | 1.32 | −1.28 | 1.78 | 0.51 | −0.03 |
| 0.95 ..... | 3.16 | 2.91 | 1.50 | −1.32 | 2.00 | 0.54 | 0.05 |
| 1.00 ..... | 2.98 | 3.06 | 1.70 | −1.35 | 2.23 | 0.57 | 0.13 |

tion and color evolution as a function of redshift. In its classical form (Whitford 1975), $k$-correction is defined as the offset to apply to the observed magnitude of a galaxy at redshift $z$ to reproduce its magnitude at the same distance but in the rest frame. We have therefore $m(z) - m(0) = k(z)$, where

$$k(z) = 2.5 \log (1 + z) - 2.5 \log \frac{\int \mathrm{SED}(\lambda, z) S(\lambda) d\lambda}{\int \mathrm{SED}(\lambda, 0) S(\lambda) d\lambda} \quad (25)$$

and $S(\lambda)$ is the bandpass profile for a given magnitude system.

However, the relevant rate of change in luminosity makes the ancestors of present-day ellipticals much more luminous, and this requires, in addition to the geometrical $k$-correction, an increasingly large evolutionary correction to galaxy magnitudes with increasing redshift. Following, for example, the definition of Bruzual (1983), the evolutionary $e$-correction gives the magnitude difference between a source at redshift $z$, with a SED corresponding to age $t(z)$, and a similar source

TABLE 10C

$(e + k)$-CORRECTIONS FOR $(H_0, q_0, z_f) = (50, 0.5, \infty)$

| $z$ | Age (Gyr) | $K(B)$ | $k(V)$ | $k(K)$ | $k(g)$ | $k(r)$ | $k(i)$ |
|---|---|---|---|---|---|---|---|
| 0.00 ..... | 13.05 | 0.00 | 0.00 | 0.00 | 0.00 | 0.00 | 0.00 |
| 0.05 ..... | 12.13 | 0.14 | 0.02 | −0.12 | 0.03 | −0.02 | −0.03 |
| 0.10 ..... | 11.31 | 0.31 | 0.03 | −0.22 | 0.07 | −0.03 | −0.05 |
| 0.15 ..... | 10.58 | 0.46 | 0.07 | −0.32 | 0.15 | −0.02 | −0.07 |
| 0.20 ..... | 9.92 | 0.58 | 0.13 | −0.41 | 0.25 | 0.00 | −0.08 |
| 0.25 ..... | 9.33 | 0.66 | 0.20 | −0.50 | 0.38 | 0.01 | −0.10 |
| 0.30 ..... | 8.80 | 0.76 | 0.32 | −0.57 | 0.52 | 0.02 | −0.11 |
| 0.35 ..... | 8.32 | 0.86 | 0.46 | −0.64 | 0.66 | 0.03 | −0.10 |
| 0.40 ..... | 7.88 | 1.00 | 0.60 | −0.70 | 0.78 | 0.04 | −0.09 |
| 0.45 ..... | 7.47 | 1.15 | 0.71 | −0.76 | 0.85 | 0.07 | −0.09 |
| 0.50 ..... | 7.10 | 1.32 | 0.79 | −0.81 | 0.90 | 0.11 | −0.08 |
| 0.55 ..... | 6.76 | 1.53 | 0.84 | −0.85 | 0.95 | 0.17 | −0.08 |
| 0.60 ..... | 6.45 | 1.78 | 0.88 | −0.89 | 1.03 | 0.27 | −0.07 |
| 0.65 ..... | 6.16 | 2.06 | 0.94 | −0.92 | 1.14 | 0.37 | −0.05 |
| 0.70 ..... | 5.89 | 2.33 | 1.01 | −0.96 | 1.29 | 0.47 | −0.02 |
| 0.75 ..... | 5.64 | 2.58 | 1.11 | −1.00 | 1.45 | 0.58 | 0.01 |
| 0.80 ..... | 5.40 | 2.80 | 1.26 | −1.03 | 1.66 | 0.66 | 0.06 |
| 0.85 ..... | 5.18 | 2.98 | 1.43 | −1.07 | 1.86 | 0.72 | 0.13 |
| 0.90 ..... | 4.98 | 3.15 | 1.60 | −1.10 | 2.07 | 0.76 | 0.21 |
| 0.95 ..... | 4.79 | 3.32 | 1.78 | −1.13 | 2.31 | 0.79 | 0.30 |
| 1.00 ..... | 4.61 | 3.49 | 1.99 | −1.17 | 2.54 | 0.82 | 0.39 |

TABLE 10E

$(e + k)$-CORRECTIONS FOR $(H_0, q_0, z_f) = (100, 0, \infty)$

| $z$ | Age (Gyr) | $K(B)$ | $k(V)$ | $k(K)$ | $k(g)$ | $k(r)$ | $k(i)$ |
|---|---|---|---|---|---|---|---|
| 0.00 ..... | 9.77 | 0.00 | 0.00 | 0.00 | 0.00 | 0.00 | 0.00 |
| 0.05 ..... | 9.30 | 0.15 | 0.03 | −0.10 | 0.04 | 0.00 | −0.01 |
| 0.10 ..... | 8.88 | 0.33 | 0.06 | −0.19 | 0.10 | 0.00 | −0.02 |
| 0.15 ..... | 8.49 | 0.49 | 0.11 | −0.27 | 0.19 | 0.02 | −0.02 |
| 0.20 ..... | 8.14 | 0.62 | 0.19 | −0.35 | 0.31 | 0.06 | −0.02 |
| 0.25 ..... | 7.81 | 0.74 | 0.28 | −0.42 | 0.45 | 0.09 | −0.02 |
| 0.30 ..... | 7.51 | 0.85 | 0.41 | −0.49 | 0.61 | 0.11 | −0.02 |
| 0.35 ..... | 7.23 | 0.97 | 0.56 | −0.54 | 0.76 | 0.13 | 0.00 |
| 0.40 ..... | 6.97 | 1.13 | 0.71 | −0.59 | 0.90 | 0.16 | 0.02 |
| 0.45 ..... | 6.73 | 1.31 | 0.85 | −0.64 | 1.00 | 0.20 | 0.05 |
| 0.50 ..... | 6.51 | 1.50 | 0.95 | −0.67 | 1.07 | 0.26 | 0.07 |
| 0.55 ..... | 6.30 | 1.74 | 1.02 | −0.69 | 1.15 | 0.34 | 0.09 |
| 0.60 ..... | 6.10 | 2.01 | 1.08 | −0.72 | 1.24 | 0.46 | 0.12 |
| 0.65 ..... | 5.91 | 2.29 | 1.15 | −0.74 | 1.37 | 0.57 | 0.15 |
| 0.70 ..... | 5.74 | 2.59 | 1.24 | −0.77 | 1.53 | 0.69 | 0.19 |
| 0.75 ..... | 5.58 | 2.85 | 1.36 | −0.79 | 1.71 | 0.81 | 0.23 |
| 0.80 ..... | 5.42 | 3.09 | 1.53 | −0.82 | 1.93 | 0.91 | 0.30 |
| 0.85 ..... | 5.27 | 3.30 | 1.72 | −0.84 | 2.15 | 0.99 | 0.38 |
| 0.90 ..... | 5.13 | 3.49 | 1.90 | −0.86 | 2.38 | 1.03 | 0.48 |
| 0.95 ..... | 5.00 | 3.68 | 2.10 | −0.89 | 2.63 | 1.08 | 0.58 |
| 1.00 ..... | 4.88 | 3.88 | 2.32 | −0.91 | 2.88 | 1.12 | 0.68 |

TABLE 10F

$(e+k)$-CORRECTIONS FOR $(H_0, q_0, z_f) = (100, 0.5, \infty)$

| $z$ | Age (Gyr) | $K(B)$ | $k(V)$ | $k(K)$ | $k(g)$ | $k(r)$ | $k(i)$ |
|---|---|---|---|---|---|---|---|
| 0.00 ..... | 6.52 | 0.00 | 0.00 | 0.00 | 0.00 | 0.00 | 0.00 |
| 0.05 ..... | 6.06 | 0.13 | 0.01 | −0.12 | 0.02 | −0.02 | −0.03 |
| 0.10 ..... | 5.65 | 0.26 | 0.01 | −0.23 | 0.05 | −0.04 | −0.06 |
| 0.15 ..... | 5.29 | 0.38 | 0.03 | −0.34 | 0.09 | −0.06 | −0.09 |
| 0.20 ..... | 4.96 | 0.48 | 0.07 | −0.43 | 0.18 | −0.05 | −0.12 |
| 0.25 ..... | 4.67 | 0.57 | 0.13 | −0.52 | 0.29 | −0.04 | −0.14 |
| 0.30 ..... | 4.40 | 0.66 | 0.23 | −0.60 | 0.42 | −0.04 | −0.15 |
| 0.35 ..... | 4.16 | 0.77 | 0.36 | −0.66 | 0.56 | −0.03 | −0.15 |
| 0.40 ..... | 3.94 | 0.91 | 0.49 | −0.72 | 0.67 | −0.02 | −0.14 |
| 0.45 ..... | 3.74 | 1.08 | 0.61 | −0.77 | 0.76 | 0.01 | −0.13 |
| 0.50 ..... | 3.55 | 1.25 | 0.70 | −0.81 | 0.83 | 0.06 | −0.12 |
| 0.55 ..... | 3.38 | 1.47 | 0.77 | −0.84 | 0.90 | 0.12 | −0.10 |
| 0.60 ..... | 3.22 | 1.72 | 0.83 | −0.87 | 0.99 | 0.22 | −0.09 |
| 0.65 ..... | 3.08 | 1.99 | 0.90 | −0.89 | 1.11 | 0.32 | −0.06 |
| 0.70 ..... | 2.94 | 2.27 | 0.99 | −0.92 | 1.26 | 0.44 | −0.03 |
| 0.75 ..... | 2.82 | 2.51 | 1.11 | −0.94 | 1.44 | 0.55 | 0.02 |
| 0.80 ..... | 2.70 | 2.73 | 1.27 | −0.96 | 1.65 | 0.66 | 0.08 |
| 0.85 ..... | 2.59 | 2.90 | 1.45 | −0.98 | 1.87 | 0.74 | 0.16 |
| 0.90 ..... | 2.49 | 3.07 | 1.63 | −1.00 | 2.10 | 0.80 | 0.25 |
| 0.95 ..... | 2.40 | 3.24 | 1.83 | −1.02 | 2.34 | 0.85 | 0.35 |
| 1.00 ..... | 2.31 | 3.41 | 2.05 | −1.04 | 2.58 | 0.90 | 0.45 |

with a spectrum corresponding to age $t(0)$, redshifted by an amount $z$.

Operationally, $m(z, t(z)) - m(z, t(0)) = e(z)$, where

$$e(z) = -2.5 \log \frac{\int \mathrm{SED}(\lambda, z, t(z)) S(\lambda) d\lambda}{\int \mathrm{SED}(\lambda, z, t(0)) S(\lambda) d\lambda}. \quad (26)$$

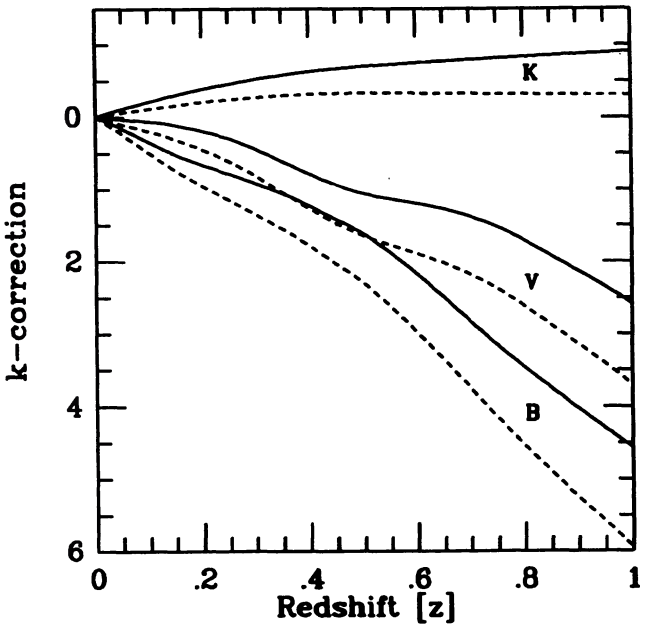


FIG. 32.—Evolutionary $(e+k)$-corrections in magnitudes for ETGs in the Johnson $B$, $V$, and $K$ bands (*solid lines*). An $(H_o, q_o, z_f) = (50, 0, \infty)$ universe is assumed. Also displayed for comparison are the curves for no evolution (i.e., $e$-term = 0; *dashed lines*).

Evolutionary corrections are systematically lower than the case of no evolution due to the brighter luminosity of ETGs at earlier epochs.

Both $k$- and $e$-corrections are necessary to consistently link distance modulus $(m - M)$ to luminosity distance $d_L$ for a galaxy at redshift $z$:

$$(m - M) = [m_{\mathrm{obs}} - k(z) - e(z)] - M = 5 \log d_L - 5 \quad (27)$$

with $M$ the absolute magnitude of a galaxy and $d_L$ is in parsecs.

The $e$-correction as a function of $z$ is not univocally determined, as the $k$-correction is. The reason is that it requires us to know the way galactic age changes with redshift, and this is a function of the cosmological model adopted (see Sandage 1988 for a nice review of this and other related aspects).

Attempting to cover a reasonably wide range of combinations of the leading cosmological parameters, we give in Tables 10A–10F a summary of the expected total $(e + k)$-correction for ETGs in six different models with $H_0 = 50$ and 100 km s$^{-1}$ Mpc$^{-1}$, and $q_0 = 0$ and $\frac{1}{2}$, assuming throughout a redshift for galaxy formation of $z_f = \infty$. For the $H_0 = 50$ models, the case of $z_f = 3$ has also been considered. In the tables, the $(e + k)$-correction is given for Johnson $B$, $V$, and $K$ bands, and for Gunn $g$, $r$, and $i$ bands (for the Gunn system see also Molinari, Buzzoni, & Chincarini 1990). An example of the derived $(e + k)$-function for the Johnson system in a $(H_0, q_0, z_f) = (50, 0, \infty)$ cosmology is shown in Figure 32. For comparison, the $k$-

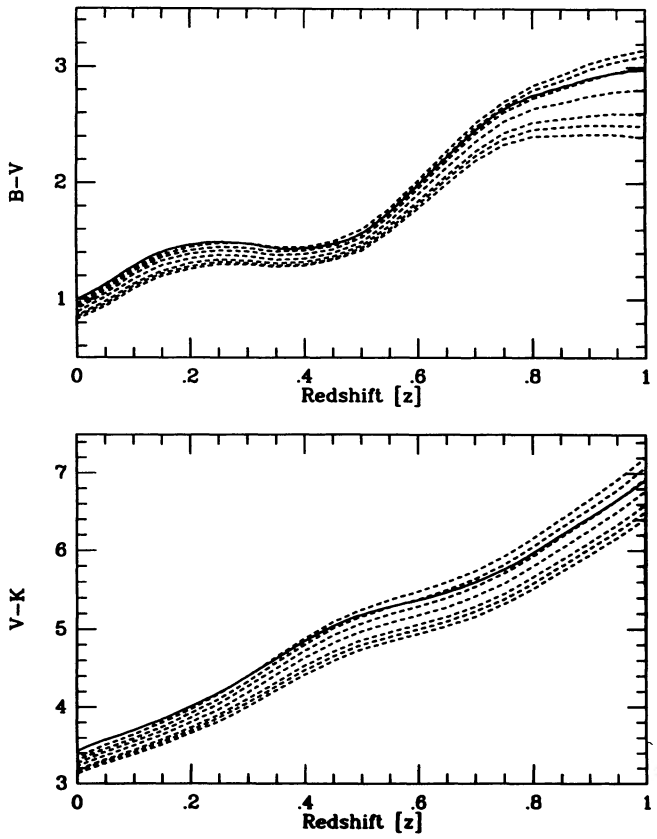


FIG. 33.—Expected color evolution of ETGs in an $(H_0, q_0, z_f) = (50, 0, \infty)$ universe. Each sheaf of dashed curves shows the apparent $B - V$ and $V - K$ colors at different redshifts for SSP models with fixed age $t = 4$, 5, 6, 8, 10, 12.5, and 15 Gyr (in the sense of redder colors in each sheaf). Solid curves are the expected evolutionary paths of galaxies crossing the dashed curves according to the age-redshift relationship given by the assumed cosmological model.

correction alone is singled out and reported in the figure, allowing us to appraise the amount of evolution.

The apparent color evolution in distant ellipticals can be evaluated with the help of Figure 33 (see also Molinari et al. 1990). Dashed lines in the figure are expected paths computed simply by redshifting SSP models with different ages. The advantage of this representation is that it is free from any assumption about cosmology. It is clear however that each curve should no longer be regarded *a rigori* as an evolutionary sequence, of course. Once a cosmological model is adopted, the real evolutionary path of the population will be a sort of envelope curve within the sheaf displayed, crossing younger ages with increasing $z$. As an example, this is shown in the figure (*solid line*) for a reference $(H_0, q_0, z_f) = (50, 0, \infty)$ cosmology that might be a somewhat relevant case, as the observation of ETGs in distant clusters leads us to think (Buzzoni et al. 1993).

Whatever the real cosmological model, it appears clear from the figure that most of the color change in ETGs with increasing $z$ is induced by the effect of the $k$-correction. Evolution plays in this case a minor role (in ETGs the rate of change in color is always less than the rate of change in luminosity). For comparison, in the previous reference cosmology we have that the blueing effect due to younger galaxies at $z = 1$ is only $\Delta(B - V) = 0.25$ mag, while it at most doubles by adopting $H_0 = 100$.

The entire list of persons to whom I am indebted to for so much precious advice, suggestions, and criticisms during the whole genesis of this work, started in 1989, would be too long to include.

I took most advantage of timely and fruitful discussions with Jim Rose. In the fatiguing controversy about M32, he is a valiant opponent in favor of the "young-stars" solution, and this gave me some supplementary reasons to better ground my differing point of view. The referee is acknowledged for wide competence in most of the problems faced in this work and for constructive comments that greatly encouraged me to clarify some important questions approached here. To Alvio Renzini, I give my greatest and friendly esteem for his innumerable advice, which contributed my scientific formation. Finally, it is my pleasure to acknowledge the Instituto Nacional de Astrofísica, Optica y Electrónica (INAOE) of Puebla for its warm hospitality during the final release of this paper.

This paper has received partial financial support from EEC contract ERB-CHRX-CT92-0033.

## REFERENCES

Aaronson, M., Frogel, J. A., & Persson, S. E. 1978, ApJ, 220, 442
Arimoto, N. 1988 in Towards Understanding Galaxies at Large Redshift, ed. R. G. Kron & A. Renzini (Dordrecht: Kluwer), 43
Arimoto, N., & Yoshii, Y. 1987, A&A, 173, 23
Baldwin, J. R., Danziger, I. J., Frogel, J. A., & Persson, S. E. 1973a, ApJ, 14, 1
Baldwin, J. R., Frogel, J. A., & Persson, S. E. 1973b, ApJ, 184, 427
Barnes, J. E. 1988, ApJ, 331, 699
———. 1989, Nature, 338, 123
Becker, S. A., & Iben, I., Jr. 1980, ApJ, 237, 111
Bell, R. A., & Briley, M. M. 1991, AJ, 102, 763
Bell, R. A., & Gustaffson, B. 1978, A&AS, 34, 229
Bell, R. A., & Tripicco, M. J. 1991, AJ, 102, 777
Bertelli, G., Chiosi, C., & Bertola, F. 1989, ApJ, 339, 889
Bertola, F., Capaccioli, M., & Oke, J. B. 1982, ApJ, 254, 494
Boulade, O., Rose, J. A., & Vigroux, L. 1988, AJ, 96, 1319
Bower, R. G., Lucey, J. R., & Ellis, R. S. 1992a, MNRAS, 254, 589
———. 1992b, MNRAS, 254, 601
Brocato, E., Matteucci, F., Mazzitelli, I., & Tornambè, A. 1990, ApJ, 349, 458
Brodie, J. P., & Huchra, J. P. 1990, ApJ, 362, 503
Bruzual, G. 1983, Rev. Mexicana. Astron. Astrof., 8, 63
Bruzual, G., & Charlot, S. 1993, ApJ, 405, 538
Burstein, D., Bertola, F., Buson, L., Faber, S. M., & Lauer, T. R. 1988a, ApJ, 328, 440
Burstein, D., Davies, R. L., Dressler, A., Faber, S. M., Lynden-Bell, D., Terlevich, R., & Wegner, G. 1988b, in Towards Understanding Galaxies at Large Redshift, ed. R. Kron & A. Renzini (Dordrecht: Kluwer), 17
Burstein, D., Faber, S. M., Gaskell, C. M., & Krumm, N. 1984, ApJ, 287, 586
Butcher, H., & Oemler, A., Jr. 1978, ApJ, 219, 18
Buzzoni, A. 1989, ApJS, 71, 817 (Paper I)
———. 1993, A&A 275, 433
Buzzoni, A., Chincarini, G., & Molinari, E. 1993, ApJ, 410, 499
Buzzoni, A., Gariboldi, G., & Mantegazza, L. 1992, AJ, 103, 1814
Buzzoni, A., Mantegazza, L., & Gariboldi, G. 1994, AJ, 107, 513
Caldwell, N. 1984, PASP, 96, 287
Canizares, C. R., Fabbiano, G., & Trinchieri, G. 1987, ApJ, 312, 503
Castellani, M., Limongi, M., & Tornambè, A. 1992, ApJ, 389, 227
Castellani, M., & Tornambè, A. 1991, ApJ, 381, 393
Ciardullo, R., & Demarque, P. 1977, Yale Trans., 35, 1
Ciotti, L., D'Ercole, A., Pellegrini, S., & Renzini, A. 1991, ApJ, 376, 380
Cohen, J. G., Frogel, J. A., & Persson, S. E. 1978, ApJ, 222, 165
Cowie, L. L., & Binney, J. 1977, ApJ, 215, 723
Davidge, T. J. 1990, AJ, 99, 561
Davidge, T. J., & Jones, J. H. 1992, AJ, 104, 1365
Davidge, T. J., & Nieto, J. L. 1992, ApJL, 391, L13
Davies, R. L., Burstein, D., Dressler, A., Faber, S. M., Lynden-Bell, D., Terlevich, R. J., & Wegner, G. 1987, ApJS, 64, 581
De Carvalho, R. R., & Djorgovski, S. 1989, ApJ, 341, L37
DePoy, D. L., Terndrup, D. M., Frogel, J. A., Atwood, B., & Blum, R. 1993, AJ, 105, 2121
Dressler, A. 1980, ApJ, 236, 351
Elston, R., & Da Silva, D. R. 1992, AJ, 104, 1360
Faber, S. M. 1972, A&A, 20, 361
———. 1973, ApJ, 179, 731
Faber, S. M., Friel, E. D., Burstein, D., & Gaskell, C. M. 1985, ApJS, 57, 711
Faber, S. M., & Jackson, R. E. 1976, ApJ, 204, 668
Faber, S. M., Wegner, G., Burstein, D., Davies, R. L., Dressler, A., Lynden-Bell, D., & Terlevich, R. J., 1989, ApJS, 69, 763
Ferrini, F. 1991, in Chemical and Dynamical Evolution of Galaxies, ed. F. Ferrini, F. Matteuci, & J. Franco (Pisa: ETS), 511
Ferrini, F., Palla, F., & Penco, U. 1990, A&A, 231, 391
Ferrini, F., & Poggianti, B. M. 1993, ApJ, 410, 44
Forman, W., Schwarz, J., Jones, J., Liller, W., & Fabian, A. C. 1979, ApJ, 234, L27
Freedman, W. 1989, AJ, 98, 1285
———. 1992, AJ, 104, 1349
Frogel, J. A., Persson, S. E., Aaronson, M., Becklin, E. E., Matthews, K., & Neugebauer, G. 1975, ApJ, 195, L15
Frogel, J. A., Persson, S. E., Aaronson, M., & Matthews, K. 1978, ApJ, 220, 75
Frogel, J. A., Persson, S. E., & Cohen, J. G. 1980, ApJ, 240, 785
Frogel, J. A., & Whitford, A. E. 1987, ApJ, 320, 199
Fusi Pecci, F., & Renzini, A. 1976, A&A, 46, 447
Gingold, R. A. 1973, ApJ, 204, 116
Golay, M. 1974, Introduction to Astronomical Photometry (Dordrecht: Reidel)
Gorgas, J., Efstathiou, G., & Aragon Salamanca, A. 1990, MNRAS, 245, 217
Gorgas, J., Faber, S. M., Burstein, D., Jesus Gonzalez, J., Courteau, S., & Prosser, C. 1993, ApJS, 86, 153
Governato, F., Bhatia, R., & Chincarini, G. 1991, ApJ, 371, L15

Governato, F., Reduzzi, L., & Rampazzo, R. 1993, MNRAS, 261, 379
Green, E., Demarque, P., & King, C. R. 1987, The Revised Yale Isochrones and Luminosity Functions (New Haven: Yale Univ. Press)
Greggio, L., & Renzini, A. 1990, ApJ, 364, 35
Guiderdoni, B., & Rocca-Volmerange, B. 1987, A&A, 186, 1
Gunn, J. E., Stryker, L. L., & Tinsley, B. M. 1981, ApJ, 249, 48
Hamilton, D. 1985, ApJ, 297, 371
Hardy, E., Couture, J., Couture, C., & Joncas, G. 1994, AJ, 107, 195
Hejlesen, P. M., Jørgensen, H. E., Otzen Petersen, J., & Rømcke, L. 1972 in IAU Colloq. 17, Stellar Ages, ed. C. Cayrel de Strobel & A. M. Delplace (Paris: Meudon Obs.)
Iben, I., Jr, & Renzini, A. 1983, ARA&A, 21, 271
Johnson, H. L. 1966, ARA&A, 4, 193
Kurucz, R. 1979, ApJS, 40, 1
———. 1992, in The Stellar Populations of Galaxies, ed. B. Barbuy & A. Renzini (Dordrecht: Kluwer), 225
Leach, R. W. 1979, Ph.D. thesis, Harvard Univ.
Lebofsky, M. J. 1981, ApJ, 245, L59
Lilly, S. J., & Longair, M. S. 1984, MNRAS, 211, 833
Malagnini, M. L., Morossi, C., Buser, R., & Parthasarathy, M. 1992, A&A, 261, 558
Matteucci, F., & Brocato, E. 1990, ApJ, 365, 539
Mengel, J. G., Sweigart, A. V., Demarque, P., & Gross, P. G. 1979, ApJS, 40, 733
Michard, R. 1980, A&A, 91, 122
Molinari, E., Buzzoni, A., & Chincarini, G. 1990, MNRAS, 246, 576
Nørgaard-Nielsen, H. U., & Kjærgaard, P. 1981, A&A, 93, 290
O'Connell, R. W. 1976, ApJ, 206, 370
———. 1980, ApJ, 236, 430
———. 1982, ApJ, 257, 89
———. 1983, ApJ, 267, 80
———. 1986, in Stellar Populations, ed. C. A. Norman, A. Renzini, & M. Tosi (Cambridge: Cambridge Univ. Press), 167
O'Connell, R. W., et al. 1992, ApJ, 395, L45
Oemler, A., Jr. 1974, ApJ, 194, 1
Persson, S. E., Frogel, J. A., & Aaronson, M. 1979, ApJS, 39, 61
Pickles, A. J. 1985, ApJ, 296, 340
———. 1989, in The Epoch of Galaxy Formation, ed. C. S. Frenk et al. (Dordrecht: Kluwer), 191
Rana, N. C. 1987, A&A, 184, 104
Recillas-Cruz, E., Carrasco, L., Serrano, A., & Cruz-Gonzalez, I. 1990, A&A, 229, 64
———. 1991, A&A, 249, 312
Reimers, D. 1975, Mem. Soc. Roy. Sci. Liège, 6th Ser., 8, 369
Renzini, A. 1986, in Stellar Populations, ed. C. A. Norman, A. Renzini, & M. Tosi (Cambridge: Cambridge Univ. Press), 213
———. 1988 in Evolutionary Phenomena in Galaxies, ed. J. Beckman (Cambridge: Cambridge Univ. Press), 422
———. 1993, in IAU Symp. 153, Galactic Bulges, ed. H. Dejonghe & H. Habing (Dordrecht: Kluwer),
Renzini, A., & Buzzoni, A. 1986, in Spectral Evolution of Galaxies, ed. C. Chiosi & A. Renzini (Dordrecht: Reidel), 195
Rich, R. M., & Mould, J. R. 1991, AJ, 101, 1286
Rich, R. M., Mould, J. R., & Graham, J. R. 1993, AJ, 106, 2252
Rose, J. A. 1984, AJ, 89, 1238
———. 1985a, AJ, 90, 787
———. 1985b, AJ, 90, 803
———. 1985c, AJ, 90, 1927
———. 1994, AJ, 107, 206
Rose, J. A., & Tripicco, M. J. 1984, ApJ, 285, 55
Saito, M. 1979, PASJ, 31, 181
Salsa, M. 1993, master thesis, Univ. Milan
Sandage, A. 1988, ARA&A, 26, 561
Sandage, A., & Hardy, E. 1973, ApJ, 183, 743
Sandage, A., & Tammann, G. 1981, A Revised Shapley-Ames Catalog of Bright Galaxies (Washington, DC: Carnegie Inst. Washington)
Sanders, R. H. 1980, ApJ, 242, 931
Scalo, J. M. 1986, Fund. Cosmic Phys., 11, 1
Schaller, G., Schaerer, D., Meynet, G., & Maeder, A. 1992, A&AS, 96, 269
Schechter, P. 1980, AJ, 85, 801
Schechter, P., & Gunn, J. E. 1979, ApJ, 229, 472
Schweizer, L. Y. 1987, ApJS, 64, 427
Sharov, A. S., & Lyutyi, V. M. 1983, Soviet Astron., 27, 1
Spinrad, H., & Taylor, B. J. 1969, ApJ, 157, 1279
———. 1971, ApJS, 22, 445
Stiavelli, M., Londrillo, P., & Messina, A. 1991, MNRAS, 251, 57p
Tinsley, B. M. 1973, ApJ, 186, 35
———. 1978, ApJ, 222, 14
Tinsley, B. M., & Gunn, J. E. 1976, ApJ, 203, 52
Toomre, A. 1977, in The Evolution of Galaxies and Stellar Populations, ed. B. M. Tinsley & R. B. Larson (New Haven: Yale Univ. Press), 401
Trinchieri, G., Fabbiano, G., & Canizares, C. R., 1986, ApJ, 310, 637
Tripicco, M. J., & Bell, R. A. 1990, AJ, 99, 691
van Buren, D. 1983, BAAS, 15, 923
Vandenberg, D. A. 1985, ApJS, 58, 711
Vandenberg, D. A., & Laskarides, P. G. 1987, ApJS, 64, 103
Visvanathan, N., & Sandage, A. 1978, ApJ, 216, 214
Volkov, E. V. 1990, Astrophysics, 32, 80
Wang, B. 1991a, ApJ, 374, 456
———. 1991b, ApJ, 383, L37
White, S. D. M. 1979, MNRAS, 189, 831
Whitford, A. E. 1975, in Stars and Stellar Systems (Chicago: Univ. Chicago Press)
Whitmore, B. C. 1990, in STScI Symposium Ser., 4, Clusters of Galaxies, ed. W. R. Oegerle, M. J. Fitchett, & L. Danley (Cambridge: Cambridge Univ. Press), 139
Worthey, G. 1992, Ph.D. thesis, Univ. California, Santa Cruz
Worthey, G., Faber, S. M., & Gonzalez, J. 1992, ApJ, 398, 69
Wyse, R. F. G. 1985, ApJ, 299, 593
Yoshii, Y., & Takahara, F. 1988, ApJ, 326, 1
Zinn, R. 1980, ApJS, 42, 19